DOSIMETRIC CHARACTERISTICS OF BORATE BASED THERMOLUMINESCENT MATERIALS

By
O. ANNALAKSHMI
(Enrollment No: PHYS02200704007)

Indira Gandhi Centre for Atomic Research
Kalpakkam – 603102
Tamil Nadu, India

A thesis submitted to the
Board of Studies in Physical Sciences
In partial fulfillment of requirements
For the Degree of

DOCTOR OF PHILOSOPHY

of

HOMI BHABHA NATIONAL INSTITUTE

Mumbai

August, 2013

Homi Bhabha National Institute

Recommendations of the Viva Voce Board

As members of the Viva Voce Board, we certify that we have read the dissertation prepared by **Ms. O. Annalakshmi** entitled **"Dosimetric Characteristics of borate based thermoluminescent materials"** and recommend that it may be accepted as fulfilling the dissertation requirement for the Degree of Doctor of Philosophy.

____ **Date:**

Chairman – C. S. Sundar

____ **Date:**

Convener/Guide – G. Amarendra

____ **Date:**

External Examiner

____ **Date:**

Member – B. Venkatraman

____ **Date:**

Member – N. Subramanian

Final approval and acceptance of this dissertation is contingent upon the candidate's submission of the final copies of the dissertation to HBNI.

Date:

Place:

CERTIFICATE

I hereby certify that I have read this dissertation prepared under my direction and recommend that it may be accepted as fulfilling the dissertation requirement.

Date: **(G. Amarendra)**

Place: **Thesis Supervisor**

STATEMENT BY AUTHOR

This dissertation has been submitted in partial fulfillment of requirements for an advanced degree at Homi Bhabha National Institute (HBNI) and is deposited in the Library to be made available to borrowers under rules of the HBNI.

Brief quotations from this dissertation are allowable without special permission, provided that accurate acknowledgement of source is made. Requests for permission for extended quotation from or reproduction of this manuscript in whole or in part may be granted by the Competent Authority of HBNI when in his or her judgement the proposed use of the material is in the interests of scholarship. In all other instances, however, permission must be obtained from the author.

(O. Annalakshmi)

DECLARATION

I, hereby declare that the investigation presented in the thesis has been carried out by me. The work is original and has not been submitted earlier as a whole or in part for a degree / diploma at this or any other Institution / University.

(O. Annalakshmi)

To my little one……

S. Swetha

ACKNOWLEDGEMENTS

I sincerely thank my guide Dr. G. Amarendra, Head, MPD, MSG for his valuable guidance and suggestions for completion of my thesis work in time. I consider myself very fortunate for working with a very considerate and encouraging person like him, who cared so much about my work and who responded to any queries promptly.

I whole heartedly thank Dr. M.T. Jose, Head, RSS/RSD for his help throughout the course of this work. His encouragement, help, moral support and technical discussions during preparation of the manuscript and thesis made me feel that I was not isolated in my research.

I am thankful to Dr. U. Madhusoodanan for his active involvement during the course of the thesis work. I thank Dr. B. Venkatraman, Head, RSD & AD, RSEG for his support and encouragement. I am thankful to Shri. S.A.V. Satyamurthy, Director, EIRSG, Dr. P. Chellapandi, Director, RDG/former Director Safety Group, for the support.

I am extremely grateful to my husband Dr. S.V.M. Saytanarayana, who was a constant source of support (emotional and moral). He has taught me ‘how to learn physics’ right from the initial days of my research career.

Help and assistance from Prof. J. Subramaniam, Dr. Phanikumar and Ms. J. Sridevi from CLRI, Chennai, Dr. J. Lakshmana Rao from Sri Venkateswara Univeristy, Tirupati for the EPR measurements is gratefully acknowledged. I am thankful for the help rendered by Dr. S.R. Anishia, of Annamalai University. I am also thankful to Dr. V.V. Ravikanthkumar and Mr. B. Shanmugavelu from Department of Physics, Pondicherry University for the SEM measurements and Prof. N. Satyanarayana of the same department for valuable discussion on EPR. The help rendered by Ms. S. Kalavathi, MSG for providing the XRD data is greatly acknowledged. I am also thankful to Shri. P. Ilayaraja, SRF, RSD for carrying out the IR measurements.

Special thanks are due to Dr. R. Indira, former Head, RSD for giving permission to work in Luminescence lab and to Dr. V. Meenakshisundaram, former Head, RSS for giving permission to do the research work.

I am also thankful to my doctoral committee members Dr. C.S. Sundar, Director MSG, IGCAR, Dr. N. Subramanian Head, XCGS, CMPD, IGCAR for their creative suggestions for the successful completion of the thesis work.

I am thankful to Dr. P.R. Vasudeva Rao, Director, IGCAR, Shri. S.C. Chetal and Dr. Baldev Raj former Directors of IGCAR for allowing me to use the facilities for the research work. I also thank my colleagues Dr. V. Subramanian, Smt. C.P. Jayasree, Smt. Sreeletha Choudhary and Ms. E. Yasodha of TLD lab for their support.

I acknowledge Mr. Haribabu and Mr. Varghese Anto Chirayath for their help and discussions. I also thank Ms. Zareena Hamza for the kind friendship and concern on my work. Special thanks to my friends Ms. M. Margret, Ms. Priyada, Ms. M. Manohari, Ms. N. Chitra, Ms. Thilagam, Mr. E. Alaguraja, Mr. A. Arul Anantha Kumar, Mr. Yadagiri, Ms. P. Usha, Ms. I. Vijayalakshmi, Ms. D. Bakkiam, Mr. R. Ramar, Mr. Ajay Rawat, Mr. Soubatra Sen, Ms. O. Chellamal Ms. M.M. Shanthi and others who were concerned about my thesis.

My heartfelt thanks to my parents, mother-in-law, brothers, brothers-in-law and sisters-in-law for their support. I am indebted to my three year old daughter for her mature forbearance of the deprival of mother's love during difficult times all along the thesis work.

It is indeed a pleasure to thank all my colleagues of Radiological Safety Division who directly or indirectly helped me during the completion of the thesis work. Finally, I thank all friends in Kalpakkam, Chennai, Pondicherry, Nagercoil and in other parts of the country for their continuous interest in my work and welfare.

(O. Annalakshmi)

Contents

Chapter 1 Overview of luminescence properties of borates ....1 - 25

Chapter 2 Synthesis and structural characterization .... 26 - 37

Chapter 4 Kinetic parameters from TL glow curves .... 74 - 99

Chapter 5 EPR – TL correlation ....100 – 120

CHAPTER - 1

OVERVIEW OF LUMINESCENCE PROPERTIES OF BORATES

Chapter – 1

Overview of luminescence properties of borates

1.0 Preamble

Studies on thermoluminescence dosimetric properties of borate based phosphor materials are presented in this thesis. This chapter begins with a brief description of the concept of thermoluninescence (TL). Applications of TL for radiation dosimetry are discussed. In order to place the present work in context, a brief review of the status and current understanding on the borate based phosphor materials for radiation dosimetry applications is presented. The chapter is concluded with description of the motivation for choosing borate based phosphors for investigation and scope of the work reported in the thesis.

1.1 Luminescence: General concept

Luminescence refers to emission of radiation in visible or near visible region subsequent to absorption of energy by a substance (excitation). Based on the characteristic time scale (τ) between the excitation and emission of radiation, luminescence can be broadly classified into two types, viz., flourescence and phosphorescence. The time scales involved in flourescence are very small of the order of 10^{-8} s, which is almost same as relaxation time of an isolated gaseous ion, whereas for phosphorescence it is in milliseconds. In the case of phosphorescence, the emission occurs even after the excitation has ceased and is also termed as afterglow. The increase in decay time for phosphorescence is because the transition leading to emission of light proceeds via a metastable state. The source of excitation is used as a prefix to luminescence for further classification of luminescence such as photoluminescence if the source of excitation is electromagnetic radiation and chemiluminescence if the source of excitation is chemical reactions and so on.

Thermoluminescence (TL) differs from other luminescent phenomena in the sense that the prefix is not a source of excitation, but is a source of stimulation. Explicitly, TL is also referred to as radiothermostimulated luminescence, where the source of excitation is ionizing radiation and thermal energy is used to stimulate the emission. During irradiation, material absorbs energy from ionizing radiation and the energy absorbed during excitation is stored either by electron-hole pair production, exciton creation, and/or by direct displacement damage, followed by charge localization (trapping) at defects present in the host lattice. On heating the material, the stored energy is released in the form of luminescence as the sample temperature is increased. This luminescence originates from electron-hole recombination or vacancy-interstitial recombination. In both cases, electrons undergo de-excitation from metastable excited states to the ground state, thereby restoring equilibrium. The process is initiated when phonon coupling between the trapped electron and the lattice transfers an amount of thermal energy to the electron. The probability per second that the amount of energy is sufficient enough to release the trapped electron from its localized state (i.e. to overcome the energy barrier E and move to the conduction band) is given by

$$p(T) = s(T)exp[-E/kT] \tag{1.1}$$

where, $s(T)$ is frequency factor and is related to the local lattice vibrational frequency and the entropy change associated with the charge release. As the temperature increases and reaches the level just high enough for the electron to cross the barrier, the electron will be released into conduction band and will then be free either to get retrapped or to recombine with trapped holes. The recombination process may result in the emission of phonons (non-radiative recombination) or photons (radiative recombination). It is the latter that is monitored when recording TL emission. Thus, the system returns to equilibrium with a portion of the excess energy emitted as light.

A schematic description of thermoluminescence is presented in fig. 1.1. The occurrence of TL following an initial excitation is a ‘one shot’ effect. Cooling the sample and re-heating it normally does not result in TL emission.

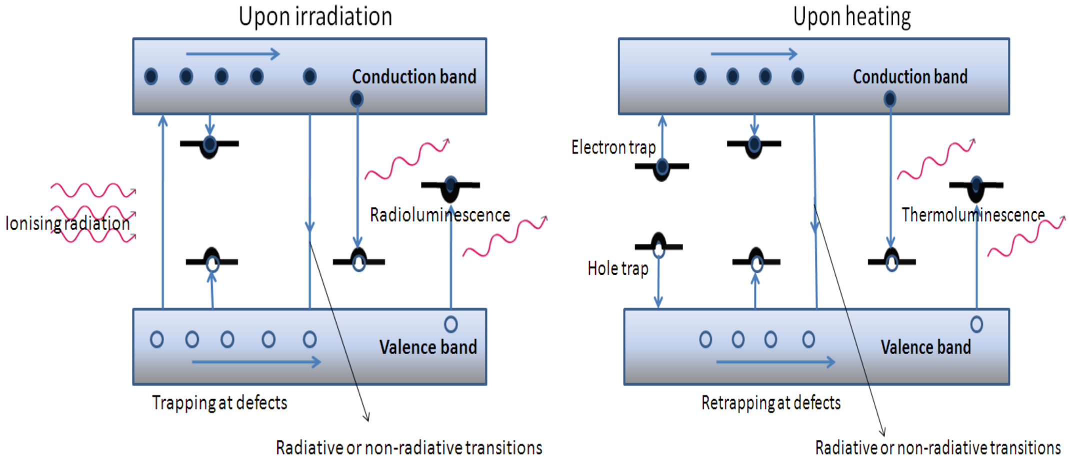

Fig. 1.1 Illustration of a simple model for thermoluminescence

For recording TL, the material exposed to ionizing radiation is heated at constant rate. The intensity of emitted light, referred to as TL intensity is a function of temperature (time), the resulting curve is termed as glow curve. A typical glow curve consists of one or more isolated/overlapping peaks. Glow curve also depends on the light sensitive detector used to record spectrum and its spectral characteristics. A peak in the glow curve, preferably isolated or well resolved is considered as a dosimetric peak. In TL dosimetry, the TL intensity of the dosimetric peak is directly proportional to the absorbed dose. Thus, by a suitable calibration of dosimeter, unknown doses absorbed by the material can be estimated by measuring TL.

1.2 Dosimetric characteristics of TL Phosphors

For several decades, thermoluminescence detectors (TLDs) have been widely used in medical, personnel and environmental dosimetry. In order to use a phosphor for dosimetric application it should qualify the following important properties.

1.2.1 Linear Dose response: This is one of the most desirable properties for a phosphor to qualify as a TL dosimeter. That is the phosphor should exhibit a linear relationship between TL output (either in terms of the area under the peak or peak height) and absorbed dose (D). TL output as a function of absorbed dose is known as dose response curve, which linear only over a range of doses. The linear dose response is quantified in terms of dose response function (or supralinearity index) $\mathrm{f(D)}$, which is defined as [1],

$$\mathrm{f(D)} = \frac{[\mathrm{S(D)} - \mathrm{S_0}]/\mathrm{D}}{[\mathrm{S(D_L)} - \mathrm{S_0}]/\mathrm{D_L}} \qquad (1.2)$$

where $\mathrm{S_0}$ is the intercept on the TL axis of the extrapolation of the linear region of the dose response curve and $\mathrm{S(D)}$ and $\mathrm{S(D_L)}$ are the TL intensities at doses D and D_L respectively. The dose D_L is in the region where the response is linear. For a phosphor to be an ideal dosimeter, $\mathrm{f(D)} = 1$ from 0 Gy dose level to several MGy dose levels. But in practical cases, $\mathrm{f(D)} = 1$ is observed only in a very narrow range in most of the TL phosphors. Supralinearity and sublinearity are terms used to describe nonlinear dose response corresponding to $\mathrm{f(D)} > 1$ and $\mathrm{f(D)} < 1$ respectively. The dose response function, $\mathrm{f(D)}$, depends on dose, dose rate [2], thermal history of the phosphor, type (Linear Energy Transfer) [3] and energy of the radiation field in which the phosphor is irradiated as well as the heating procedure during measurement.

1.2.2 Sensitivity: Sensitivity of any TL phosphor in general is the TL signal strength per unit absorbed dose. This absolute definition of sensitivity is practically inadequate because the TL signal depends on many instrumental parameters used in the TL readout system, heating rate used, and method of measurement (peak height or area under the peak) and so on. Hence, in order to overcome these experimental difficulties, one normally defines what is called as the relative sensitivity by comparing the TL signal of the phosphor of interest with that of the standard phosphor (normally TLD-100 or $CaSO_4$:Dy are used as standard) given by,

$$R(D) = \frac{S(D)_{test\,phosphor}}{S(D)_{standard\,phosphor}} \tag{1.3}$$

Where $S(D)_{test\,phosphor}$ and $S(D)_{standard\,phosphor}$ are the strength of TL signals at dose D of the phosphor which is under test and the standard phosphor measured using the same measurement system. This relative sensitivity also depends on dose, dose rate, Linear Energy Transfer (LET), and heating rate.

1.2.3 Fading: Fading is a loss of TL signal with time. It may be caused either due to thermally or optically stimulated release of the electrons or a combination of both. High thermal fading is observed when the glow curve contains low temperature peaks. If the trap depth *E* is too small then severe fading of the signal will occur, both during irradiation and between irradiation and readout. Phosphors, which are to be used for dosimetry purposes should possess a glow curve with a dosimetric peak in the range 200°C - 250°C. Usually in this temperature range the trap depth is larger and no appreciable trap emptying can take place. Unwanted fading of the TL signal can also occur by optical excitation of the charge carriers from the trap. Absorption of photons of energy ≥ optical trap depth will result in a release of trapped charge and a corresponding reduction in the TL signal. In TL signal optical fading is caused by the exposure to UV light [4].

1.2.4 Other Desirable Characteristics of TL Phosphors: The other important properties that a phosphor should posses for dosimetric applications are,

- Synthesis of phosphor materials should be easy, simple, inexpensive, scalable to bulk production and involve no chemicals that are toxic.
- Phosphors must exhibit simple glow curve structure with a single or a well resolved dosimetric peak.
- Chemical stability and inertness to extreme climatic conditions such as temperature and humidity.
- TL emission spectrum should be suitable for the detector system. Phosphors must have their characteristic light emission lying in the high efficiency region (300-500 nm) of standard photomultiplier tube.
- Phosphor should have a reasonably flat energy response, that is the TL output should be same over a range of energies of absorbed radiation.
- Negligible or low non-radiative induced signal from the phosphor material.
- Preferably near tissue equivalence.
- Simple annealing procedure for reuse and no loss of sensitivity with reuse and repeated annealing.
- Should have a very good shelf life. Its sensitivity should not show any decrease if the phosphor is stored without using for long duration.
- Should not be affected by any external influence such as mechanical, electrical or any other type.
- It should be possible to make dosimeter of any form, size and shape from the phosphor without any change in its sensitivity or other dosimetric characteristics

1.3. Phosphor Materials for TL Dosimetry

Approximately over two thirds of the known natural minerals are known to exhibit thermoluminescence. There are some natural minerals like CaF_2 which are considered to be the most efficient TL materials. The first official report on the discovery of thermoluminescence was presented by Robert Boyle on October 28, 1663 to the royal Society of London, describing TL as a ‘glimmering light’ [5] which was observed from heating diamond in dark. The first controlled and extensive investigation of TL in natural and synthetic materials was carried out by Wiedmann et al [6], Urbach [7] Randall and Wilkins [8] who recorded TL glow curves of several materials and investigated their trap parameters such as activation energies and frequency factors. Daniels et.al [9] has suggested the application of thermoluminescence in areas like geological stratigraphy, geological age determination and radiation dosimetry. Radiation dosimetry applications of TL, include measurement of an exposure of 60 R by internal ingestion of LiF by a cancer patient treated with ^{131}I in the early 1950s. Field test using LiF pellets were also carried out in 1952 by placing it at different stations monitoring radiation from atomic bomb explosions and to measure exposures varying from few thousand to a few Roentgens. The earlier attempts for radiation dosimetry using TL focused mainly on LiF but its complex glow curve structure and thermal annealing procedure were not very encouraging [10]. Later several new materials like Al_2O_3 [11] and $CaSO_4$:Mn [12] were studied for dosimetric applications. They were not successful because of lesser TL efficiency and poor post irradiation stability. The use of TL for dosimetric applications have once again started following the development of sealed CaF_2:Mn dosimeters for personnel monitoring [13] which had better TL efficiency and simple distribution of trap centers [14]. Some of the important TL materials that have been developed over the years are (i) Borates - $Li_2B_4O_7$:Mn [15], $Li_2B_4O_7$:Cu [16], LiB_3O_5 [17], SrB_4O_7 [18], $LiSrBO_3$:RE [19], $LiCaBO_3$:RE [20], $NaSr_4(BO_3)_3$:RE [21], $KSr_4(BO_3)_3$:RE [22], $LiKB_4O_7$ [23], $LiBa_2B_5O_{10}$:RE [24], $NaSrBO_3$ [25], MgB_4O_7:Dy/Tm [26], BaB_4O_7 [27] and SrB_6O_{10}:Tb [28], (ii) Sulphates - $CaSO_4$:Dy/Tm [29], $SrSO_4$:Tb [30],

$BaSO_4$:Eu [31], (iii) Fluorides - LiF:Mg,Cu,P [32], LiF:Mg,Ti [33], CaF_2:Dy [34], CaF_2:Tm [35], BaF_2:Dy [36], MgF_2:RE [37], (iv) Oxides - BeO [38,39], Al_2O_3:Si,Ti [40], Al_2O_3:C [41] and (v) Silicates - Mg_2SiO_4:Tb [42]. Since the application of thermoluminescence is diverse, such as radiation dosimetry, archaeology, geology, medicine, solid state physics, biology and organic chemistry, development of new phosphors or improving the characteristics of existing phosphors has been a topic of continuous research. Some of the phosphor materials developed over many decades and their dosimetric properties are summarized in table 1.1.

1.4 Luminescence properties of borates - General

Borate based phosphor materials like lithium tetraborate and magnesium tetraborate are nearly tissue equivalent. These materials were investigated extensively for their applications in personnel dosimetry. Lithium tetraborate doped with manganese was the first reported TL dosimeter material based on borates [43]. However, this material had a relatively lesser sensitivity, which is attributed to the incompatibility of red emission (600 nm) of this material with the spectral response of the photomultiplier tubes. The sensitivity was improved 10 times by the use of copper as the dopant which shifted the emission wavelength from red region to ultraviolet region (360 nm) [44]. Following these, several studies were carried out to improve the TL properties of borates either by changing the preparation technique, or by the use of different modifiers and or activators. These studies involved preparation of phosphor materials in all the three forms, namely, single crystals [45], polycrystalline powders [46] and glasses [47]. With regard to modifiers, several alkali/alkaline metals were used as modifiers to strengthen the relative stability of borate glass [48,49]. With regard to activators, a variety of dopants and co-dopants either transition metals [46,50] or rare earths [51,52] were added to the host in order to enhance the luminescence. This enhancement is attributed to the amendment of electron traps and/or trap centers.

Table 1.1 Dosimetric characteristics of some common TL Phosphors

Sl.No.	Material	Z_{eff}	Glow peak temperature	TL emission wavelength	Fading	Sensitivity	Linearity range	Annealing
1	LiF:Mg,Ti [33]	8.2	200˚C	400 nm	5% in 3 months	1	20 µGy to 10 Gy	400˚C, 1 h + 80˚C, 24 h
2	LiF:Mg, Cu, P [32]	8.2	210˚C	400 nm	5% in 3 months	25	0.2 µGy to 10 Gy	400˚C, 1 h + 80˚C, 24 h
3	$Li_2B_4O_7$:Cu [16]	7.4	178˚C	368 nm	11% in 3 months	2	10^{-3} Gy to 10^{3} Gy	300˚C, 30 min
4	$Li_2B_4O_7$:Cu,In [53]	7.4	210˚C	368 nm	6% in 3 months	0.7	10^{-4} Gy to 10^{3} Gy	300˚C, 15 min
5	$Li_2B_4O_7$:Cu,In, Ag [53]	7.4	190˚C	368 nm	10% in 3 months	2	10^{-4} Gy to 10^{3} Gy	300˚C, 15 min
6	$Li_2B_4O_7$:Cu,Ag,P [54]	7.4	185 - 190˚C	370 nm	<10% in 3 months	5	10^{-3} Gy to 10^{3} Gy	650˚C, 15 min
7	$Li_2B_4O_7$:Mn [15]	7.4	220˚C	605 nm	4% in 1 month	5	0.1 mGy to 3 Gy	400˚C, 30 min
8	LiB_3O_5:Al [17]	7.34	218˚C	520 nm	<5% in 1 month	0.5	0.015 Gy to 10^{3} Gy	400˚C, 30 min
9	$CaSO_4$:Dy [29]	15.3	220 - 240˚C	480, 570 nm	1% in 2 months	40	2 µGy to 10 Gy	300˚C, 30 min
10	$CaSO_4$:Tm [55]	15.3	220˚C	450 nm	1 - 2% in 2 months	40	2 µGy to 10 Gy	300˚C, 30 min
11	$CaSO_4$:Tm/Dy, Ag [56]	15.3	350 - 370˚C	445, 480, 570 nm	<1% in 1 months	40	2 µGy to 10 Gy	400˚C, 1 h
12	CaF_2:Dy [34]	16.3	240˚C	480, 570 nm	5% in 2 months	50	10 µGy to 10 Gy	500˚C, 1 h

Sl.No.	Material	Z_{eff}	Glow peak temperature	TL emission wavelength	Fading	Sensitivity	Linearity range	Annealing
13	CaF_2:Mn [57]	16.3	280˚C	500 nm	16% in 2 weeks	10	10 µGy to 10 Gy	500˚C, 1 h
14	$BaSO_4$:Eu [31]	46.9	230˚C	380 nm	40% in 40 days	100	0.5 mGy to 10 Gy	400˚C, 30 min
15	$SrSO_4$:Eu [58]	30.3	210˚C	380 nm	15% in 30 days	>40	Upto 10^{-2} Gy	400˚C, 30 min
16	Mg_2SiO_4:Tb [42]	11	200˚C	540 nm	Very less	>40	10 µGy to 1 Gy	400˚C, 30 min
17	BeO [38,39]	7.1	180 - 200˚C	330 - 340 nm	10% in 3 months	1	10 µGy to 10 mGy	300˚C, 30 min
18	Al_2O_3:C [41]	10.2	180˚C	420 nm	21% in 3 months	40 - 60	0.1 µGy to 10 Gy	400˚C, 30 min
19	$LiCaBO_3$:Tm [20]	18.6	233˚C	455 nm	15% in 1 month	3	1 Gy to 10^3 Gy	500˚C, 1 h
20	$LiMgBO_3$:Tb [59]	10.2	250˚C	544 nm	negligible	4	mGy to 10^3 Gy	500˚C, 1 h
21	MgB_4O_7:Dy,Na [60]	8.55	190˚C	480, 570 nm	8% in 3 month	6	10^{-4} Gy to 40 Gy	400˚C, 1 h
22	ZnB_2O_4:Dy [61]	22.5	200˚C	480, 570 nm	-	-	1 Gy to 100 Gy	-
23	SrB_6O_{10}:Tb [28]	31.8	210˚C	542 nm	-	-	50 Gy to 200 Gy	-
24	BaB_4O_7:Dy [27]	52.1	345˚C	480, 570 nm	-	-	1 Gy to 100 Gy	-
25	BaB_4O_7:Ce [27]	52.1	250˚C	-	-	1.8	1 Gy to 100 Gy	-

In the recent times, interest has been focused on the thermoluminescence of borate glasses due to their outstanding features such as easiness of handling and preparing, good host for several dopants, low cost and thermal stability. On the other hand, the hygroscopic nature of pure borate glasses is still a disadvantage, which affects directly the reproducibility and fading properties.

Lithium potassium borate glasses doped with Copper and magnesium resulted in a single isolated TL glow peak around 220 - 240°C. The optimum condition for annealing to erase the effect of previous irradiations is reported to be 400°C for 30 m which is encouraging. Also the TL sensitivity is around 3 times that of TLD-100 [62]. SrB_4O_7 doped with rare earth cations are particularly advantageous due to their high mechanical strength, optical properties and non-hygroscopicity. These properties are relevant when the material is thought to be subjected to repetitive use. Dy-doped Strontium tetraborates are promising as TL dosimeters due to the high efficiency shown, in comparison with the commercial phosphor TLD-700 [63]. Cerium doped barium tetraborate phosphor synthesized by melting method was reported to have a TL sensitivity of 1.8 times that of TLD-100 [27]. Another class of borates which are of relevance is the copper doped alkali borates. In this class of borates it is observed that the emission is high if copper entered the lattice as Cu^+ rather than Cu^{2+} [64]. Recently rare earth doped mixed borates based on alkaline earth metal borates are being studied for dosimetric applications due to their high sensitivity and low fading characteristics [20].

1.5 Literature on Phosphors Studied – A Review

Four families of borate based phosphors are studied in the work reported in the thesis, namely, lithium tetraborate (LTB), magnesium tetraborate (MTB), zinc metaborate (ZMB) and cadmium tetraborate (CTB). The literature existing on each of these borate phosphors is reviewed in this section.

1.5.1 Lithium tetraborate based phosphors

1.5.1.1 Synthesis: In order to use a particular material for dosimetric applications, one of the important requirements will be the ease of synthesis of the material in bulk quantities. With respect to this criteria, borate based phosphors can be synthesized very easily and there are a variety of techniques by which these phosphors were synthesized. Lithium tetraborate (LTB) doped with manganese was the first TL material investigated for dosimetric applications [15]. This material was synthesized by melting method where the required raw materials was heated to a temperature greater than the melting point and then rapidly cooled to room temperature. The resultant glassy material was then crystallized by subsequent heating and used for dosimetric applications. This technique was used by several others to develop doped LTB phosphors [65,66].

Single crystals of LTB were first produced by Garret et al. [67] for use in infrared transmission studies. Later to study the structural properties and to understand the mechanism of LTB phosphors, single crystals of LTB phosphors were synthesized by several groups. Adamiv etal [68] has developed single crystals of undoped, Cu and Ag doped LTB phosphors by the simple Czochralski technique from congruent melt in air atmosphere and studied the structure using synchrotron radiation. Thermoluminescence dosimetric characteristics of Mn doped LTB single crystals grown by Czochralski method have been studied by Ignatovych [69] and that of Ag doped LTB single crystals was studied by Holovey et al [70].

Polycrystalline powder samples of doped LTB phosphors were synthesized by sintering method for the first time in the year 1980 [16]. Later this technique has been used [71,72,73] to develop LTB phosphors and their dosimetric characteristics were studied. The sintering method will be simple compared to the melting method because it is a one step process and it does not in general require the Pt crucibles. Rare earth doped LTB phosphors were synthesized [74] but because of the poor sensitivity to low doses it was not continued further.

1.5.1.2 Dosimetric properties (Sensitivity, Fading and dose response): LTB was proposed to be a candidate for medical therapy dosimetry way back in 1967 by Schulman et al. [15]. This is because the effective atomic number (Z_{eff}) of LTB phosphor is 7.3 which is almost same as that of human tissue. Dopants like Copper [16], Silver [75], Manganese [76], Indium [77], magnesium [78] etc., have been tried in LTB phosphor to improve the dosimetric properties. When LTB was doped with Cu, the resultant phosphor showed a unique and extremely useful TL feature of perfect linearity in its TL response with dose upto 10^3 Gy followed by sublinear behaviour without any supralinearity [79]. The emission wavelength of LTB:Cu was around 360 nm which matches with the spectral emission of most of the commercially available photomultiplier tubes. A combination of copper, silver and phosphorus [80] or copper and indium [53] as dopants in LTB phosphor were also studied. LTB:Mn was reported to have a sensitivity 595 times less [65] than that of commercial LiF (TLD-100 from Harshaw make). LTB:Cu phosphor synthesized by Prokic [53] showed a TL sensitivity almost equal to that of LiF (Harshaw make). Later sintered LTB co-doped with several dopants such as Cu, In; Cu, In, Ag; Mg, Cu, P have been studied in order to produce TL materials with good dosimetric characteristics [53,54]. It has been reported that the TL intensity of the dosimetric peak has increased twice when LTB:Cu was co-doped with In [54]. The thermoluminescence dosimetric properties of LTB:Mn, LTB:Cu, LTB:Cu,Ag have been reported by Driscoll et al.

[81] and the results show that LTB:Cu is advantageous when one wants to measure doses below 20 μGy though it suffers from fading upon exposure to light. LTB based phosphors are highly sensitive to light. Exposure to direct sunlight causes considerable optical fading and it has been reported [54] that the intensity drops by a factor of almost 5 upon exposure to sunlight for 3 h. Exposure to room light results in a fading of around 10% in 6 h. Spectral characteristics of Mn doped LTB single crystals and glasses have been studied and was found that Mn is present in Mn^{2+} state, in the case of single crystals and Mn^{3+} state, in the case of LTB:Mn glasses. The response of Cu doped and undoped LTB phosphors in a mixed field of gamma and thermal neutrons was studied by Fernandes et al. [82] and was found that undoped LTB phosphor is about 5 times less sensitive to thermal neutrons compared to TLD-100 and 5 times more sensitive compared to LTB:Cu. The low gamma sensitivity combined with the high relative thermal neutron sensitivity suggest that LTB and LTB:Cu pairs can be used for mixed dosimetry [82]. The kinetic trapping parameters of doped and undoped LTB phosphors have been determined by the standard methods by several groups [83,84].

1.5.1.3 Mechanism of TL in LTB phosphors: Brant et al [85] have identified the electron and hole traps in silver doped LTB phosphors using EPR and ENDOR techniques. The hole traps are identified as substitutional Ag^+ ions which form paramagnetic Ag^{2+} ions and the electron traps are identified as interstial Ag^+ ions and form defects that have the unpaired spin shared by the interstitial ion and a neighboring substitutional ion. The mechanism of TL in LTB:A, (A=Cu, Ag) single crystals shows that, the electron formed upon irradiation is captured quickly by A^+ ion resulting in the formation of A^0 center and the hole precipitates near the boron-oxygen complex [68]. Upon heating the released electron and hole results in the formation of a self trapped exciton (STE) and the radiative annihilation of the STE results in TL.

1.5.2 Magnesium tetraborate based phosphors:The use of magnesim borate as TL material has been investigated by several researchers. The preparation of polycrystalline magnesium borate doped with dysprosium has been reported for the first time in 1974 [86]. This phosphor become important because of the near tissue equivalence ($Z_{eff} = 8.5$) compared to that of tissue which is 7.4. Since then, there have been continuous efforts in improving the dosimetric properties of magnesium borate based phosphors. Dy/Tm activated magnesium tetraborate along with a sensitizer was developed in the year 1980 [26]. This material has a TL sensitivity which is almost 7 times that of TLD-100. This co-activator did not affect the spectral distribution of the phosphor but only enhanced the relative emission efficiency. This material has been used in large scale personnel TL dosimetry in Yugoslavia [87]. Magnesium tetraborate can be used for photon, beta and neutron dosimetry [88]. The chemical composition of the material permits the construction of an albedo neutron dosimeter. The sensitivity of the phosphor depends on the quality of the chemicals (raw materials) used for the synthesis. It has been reported that trace amount of impurities like copper, nickel, iron, potassium, manganese, calcium etc., cause a substantial reduction of the intensity of the main dosimetric peak [88]. The dosimetric glow peak of Dy/Tm along with the senistizers was around 200˚C. The sensitivity of the phosphor is not the same for in all the reports. Manganese doped magnesium tetraborate was developed by Prokic [89]. Though this phosphor showed a dosimetric peak around 270˚C, the sensitivity of the phosphor varied based on the instrument used for measurement. This is because the relative intensities of the maxima of the TL emission spectra changes with the chemical form of the dopant. It is reported that the

TL sensitivity vary from 6 to 12 times [89] compared to TLD-100 for the 2000 TL Analyser and the Alnor TLD reader.

The linearity range of magnesium tetra borate phosphor is not uniform in all the existing reports. Furretta [90] has reported that the response of MgB_4O_7:Dy,Na is linear from 100 μGy to 7 Gy and the sensitivity is almost twice as that of TLD-100. But he has observed a shift in peak temperature upon storage and a strong fading. When anlaysed with glow curve deconvolution it is seen that the trap depth and also the order kinetics vary in the same pattern as the peak temperature. Based on the analysis of trap depth and the order of kinetics, it was found that the TL emission in magnesium borate is due to the complex trap structure resulting in a continuous distribution of traps. If this material has to be used for dosimetry applications, accurate calibration must be introduced and should be taken into account while dose evaluation. The glow peak structure of MgB_4O_7:Dy was also studied by Souza et. al [91] and it was reported that atleast a combination of 11 peaks of first order kinetics is necessary to describe the glow curve behaviour. In another report on Tm doped magnesium tetraborate synthesized by sintering method at 900°C, it is found that the dose response is linear from 50 Gy to 6 kGy [92] and 30% fading of signal in 45 days. In recent times due to the increased use of ionizing radiation in medical field both for radiodiagnostic and therapeutic purposes, strict quality control is required to avoid unnecessary irradiations to the healthy tissues. This has led to the use of tissue equivalent or nearly tissue equivalent dosimeters for dosimetric applications. This has once again awakened the development of MgB_4O_7 based phosphors. Cano et. al [93] has reported that the MgB_4O_7:Dy,Na synthesized by them has a dose linearity from 0.2 mGy to 50 Gy and the lower limit of detection is ten times lower than that of TLD-100, which makes the material ideal for environmental and clinical dosimetry.

The mechanism of TL in Tm doped magnesium tetraborate phosphor has been studied by EPR technique [92]. They have identified the formation of BO_3^{2-}, a hole trapped radical and O_2^- an electron trapped radical. The temperature dependence of EPR signals revealed the thermal destruction of BO_3^{2-} around 197°C. On heating thermally released hole from BO_3^{2-} radical recombines with an electron at O_2^- and the recombination energy excites Tm^{2+} ion. Deexcitation of Tm^{2+} results in TL

1.5.3 Zinc metaborate and Cadmium tetraborate based phosphors: TL phosphors ZnB_2O_4 and CdB_4O_7 have not been studied in detail for dosimetric purposes. Polycrystalline powder samples of Terbium and Dysprosium doped ZnB_2O_4 phosphor has been synthesized by solid state technique and their photoluminescence and thermoluminescence dosimetry properties have been reported by Li et al [61,94]. According to them, the PL and TL emission in this phosphor were characteristic of the rare earth dopant. The TL glow peak was reported to be broad spreading between 135°C and 240°C. They have also reported that the phosphor has a linear response to Co-60 gamma rays in the dose range from 1 to 100 Gy suitable for clinical dosimetry. Nil Kucuk et al [95] has reported the thermoluminescence dosimetric properties of beta irradiated Lanthanum doped ZnB_2O_4 phosphor synthesized by nitric acid method. They have observed that the shape of the TL glow peaks is independent of the concentration of the dopant but the main glow peak shifted slightly to high temperature with increasing dopant concentration. The dose response is observed to be linear for beta dose in the range 143 mGy to 60 Gy. The mimimum measurable dose (MMD) was reported to vary with the concentration of the dopant and is found to be 4 mGy for 10% La doped ZnB_2O_4. The TL mechanism in this phosphor is not yet clearly understood. Dittmann et al. [96] has reported that Mn activated $Cd_2B_2O_5$ exhibited TL emission in the red region (630 nm) after excitation with cathode rays and UV radiation in the wavelength region between 248 nm and 312 nm. They have also reported that for a given excitation wavelength, the luminescence output depends on the temperature.

1.6 Motivation for the present work

Borate based phosphors are gaining more importance because of the ease of synthesis in bulk quantites, simple glow curve structure, increased neutron and gamma sensitivity, near tissue equivalence in some cases and simple thermal treatment procedure.

The aim of the present work was to be able to propose a borate based TL phosphor for each of the dosimetric application such as clinical or personnel or environmental monitoring and study these materials in terms of their structural, morphological properties, dosimetric characteristics, analysis of kinetic parameters and mechanism of TL emission.

In the present work, two borate based phosphors, namely, lithium tetraborate and magnesium tetraborate are investigated as candidates for clinical as well as personnel dosimetry applications because of their near tissue equivalence (LTB: 7.3 and MTB:8.5). Lithium tetraborate and magnesium teraborate are well studied in the literature. However, some of the TL characteristic properties such as temperature of the dosimetric peak of Mn doped lithium tetraborate, fading and hygroscopic nature of both lithium and magnesium tetraborate have been improved in the present work. This is achieved by preparing the material using solid state sintering method and using different initial materials for synthesis. Zinc metaborate and cadmium tetraborate are investigated for environmental dosimtery applications. Among these borates, cadmium borate has been prepared and studied for the first time and detailed rare earth doped studies of zinc borate have also been studied for the first time.

Further, the studies on mechanism of TL in these phosphors have been very few. The TL mechanism may depend on the preparation method since the defect centers can be different in different methods. A systematic and detailed EPR studies have been carried out to understand the TL mechanism by analyzing EPR – TL correlations for chosen phosphors from each of the four classes of borates.

1.7 Scope of the thesis

Ideally, the dose absorbed by the phosphor to be used in personnel dosimetry should correspond approximately to that absorbed by the human tissue in the same radiation field over a wide range of photon energies. This implies that effective atomic number of the phosphor should be close to that of the human tissue (7.4). Conventional high sensitive phosphors such as calcium fluoride and calcium sulfate though have a high sensitivity the effective atomic numbers are high. At photon energies below 100 KeV, the response of these phosphors for a given absorbed dose of radiation becomes significantly greater than that of the tissue. The lack of tissue equivalence may be compensated by suitable filtering the low energy photons which reduces sensitivity of the phosphor and the precision of the absorbed dose assessment. TL materials with reasonable tissue equivalence such as lithium fluoride do not have high enough sensitivity for assessment of absorbed dose for low dose measurement. In addition lithium fluoride based phosphors have complex glow curve structure and require complicated thermal treatment for re-use.

This thesis presents dosimetric studies of borate based phosphors. Four borate based phosphors, viz., lithium tetraborate, magnesium tetraborate, zinc meta borate and cadmium tetraborate have been synthesized and characterized. The synthesis method used to prepare borate phosphors is solid state sintering method, which is easy, fast and can be employed to prepare materials in bulk quantities. It is demonstrated that the materials prepared with not very high purity chemicals also give rise to good dosimetric characteristics and hence preparation is inexpensive. $Li_2B_4O_7$:Mn prepared using solid state sintering method exhibits a dosimetric peak at 280˚C, which is highest temperature for this material studied in the literature. The high temperature glow curve results in no fading in one month. Further, $MnCO_3$ used as an initial material for Mn doping in the present study resulted in the material that is less hygroscopic. In the reported literature, $MnCl_2$ or manganese acetate was used for Mn doping. MTB doped with Gd exhibits TL peak at highest temperature 250˚C compared all other dopants studied in the literature. Further co-doping of monovalent metals resulted in the increase of TL sensitivity, highest being observed for Li. Among different rare earth doped zinc meta borate phosphors studied, maximum TL sensitivity is observed for Tm doped zinc meta borate. Cadmium tetraborate exhibits a dosimetric peak at 185˚C with its sensitivity twice that of TLD 100 (Harshaw make). Zinc borate and cadmium borate exhibit good storage stability and are suitable for environmental dosimetry applications.

In the present work, LTB doped with Cu with several co-dopants and LTB doped with Mn have been synthesized using solid state sintering method. LTB doped with Cu has a dosimetric peak in the range 190 - 200°C and is largely independent of dopants and co-dopants. The TL intensity was found to be high for LTB doped with copper, silver and phosphorus. However, LTB:Mn synthesized using solid state sintering method has a high temperature glow peak and as a result has the benefit of less fading. Among many MTB phosphors synthesized with different dopants and co-dopants, MTB doped with Gd exhibits dosimetric peak at highest temperature. Among monovalent co-dopants along with Gd, Li has maximum TL sensitivity. Hence detailed studies on LTB: Mn and MTB: Gd, Li are reported in the thesis.

Similarly, among phosphors synthesized based zinc and cadmium borates, studies of zinc meta borate doped with Tm and undoped cadmium tetraborate are presented in the thesis.

The thesis is organized as follows. Synthesis procedure, structural and morphological characterization of phosphors studied using XRD, FTIR and SEM are discussed in chapter 2. Detailed dosimetric characterization of phosphors prepared forms the content of chapter 3. Estimation of kinetic parameters using different methods for the materials under study is presented in chapter 4. Chapter 5 consists of results of EPR measurements and analysis to understand the mechanism of TL. Summary, principal conclusions and scope for the future work are discussed in chapter 6.

1.8 References

---

[1]. Chen R. and McKeever S.W.S., Radiat. Meas. **23** (1994) 667

[2]. Goldstein N. Health Phys. **22** (1972) 90

[3]. Mische E.F. and McKeever S.W.S., Radiat. Prot. Dosim., **29** (1989) 159

[4]. Reuven Chen and Stephen W. S. Mckeever, (1997), World Scientific Publishing Co. Pvt. Ltd, Singapore

[5]. Becker K., CRC Press, Inc., Cranwood Parkway, Cleveleand, Ohio 44128, U.S.A. (1973)

[6]. Wiedemann E. and Schmidt G.C., Ann. Phys. Chem. Neue Folge, **54** (1895) 604

[7]. Urbach F., Sitzungsber. Akad. Wiss. Wien Math. Naturwiss. Kl. Abt. 2A, **139** (1930) 349

[8]. Randall J.J. and Wilkins M.H.F., Proc. R. Soc. London Ser. A. **A184** (1945) 366

[9]. Daniels F., Boyd C.A. and Saunders D.F., Science **117** (1953) 343

[10]. Kelly S.P. and Clemmons J.J., J. Phys. Chem. **23** (1958) 586

[11]. Daniels F. and Rieman W.P., Final Report Project No. 4-12-80-001, U.S. Army Procurement Agency, Washington D.C., 1954

[12]. Kossel W., Mayer U. and Wolf H.C., Naturwissenchaften, **41** (1954) 209

[13]. Schulman J.H., Attix, F.H., West E.J. and Ginther R.J., Proc. Symp. Personnel Dosimetry Techniques, OECD/ENEA, Paris, (1963) 319

[14]. Ginther R.J. and Kirk R.D., J. Electrochem. Soc., **104** (1957) 365

[15]. Schulman J. H., Kirk R.D. and West E.J., USAEC Symposium series 650637, Luminescence dosimetry, (1967) 113

[16]. Takenaga Mutsuo, Yamamoto Osamu and Yamashita Tadaoki, Nucl. Instrum. Methods, **175** (1980) 77

[17]. Zeynep Ozdemir., Gulhan Ozbayoglu., Aysen Yilmaz., J. Mater. Sci., **42** (2007) 8501

[18]. Santiago, M., Grasseli, C., Caselli, E., Lester, M., Lavat, A., Spano, F., Phys. Status Solidi A, **185** (2001) 285

[19]. Jiang, L.H., Zhang, Y.L., Li, C.Y., Hao, J.Q., Su, Q., Applied Radiation and Isotopes, **68** (2010) 196

[20]. Anishia S.R., Jose M.T., Annalakshmi O., Ponnusamy V. and Ramasamy V., J. lumin. **130** (2010) 1834

[21]. Jiang Lihong, Zhang Yanli., Li Chengyu., Pang Ran., Shi Lili., Zhang Su., Hao Jingquan., Su Qiang., J. Rare Earths, **27** (2009) 320

[22]. Jiang, L.H., Zhang, Y.L., Li, C.Y., Hao, J.Q., Su, Q., J. Alloys Compd., **482** (2009) 313

[23]. Adamiv, V. T., Antonyal, O. T., Burak, Ya. V., Teslyuk, I. M., J. Cryst. Growth, **289** (2008)157

[24]. Liyan Liu., Yanli Zhang., Jingquan Hao., Chengyu Li., Shubin Wang., Qiang Su., J. Phys. Chem. Solids, **68** (2007) 1745

[25]. Wu. L., Chen, X.L., Zhang, Y., Kong, Y.F., Xu, J.J., Xu, Y.P., J. Solid State Chem., **179** (2006) 1219

[26]. Prokic M., Nucl. Instrum. Methods, **175** (1980) 83

[27] Necmeddin Yazici, A., Mehmet Dogan., Emif jadafar, V., Huseyin Toktamis. Nucl. Instrum. Methods Phys. Res., Sect. B, **246** (2006) 402.

[28]. Liu Lyan., Jingquan., Li Chengyu., Tang Qiang., Zhang Chunxiang., Su Qiang., Wang Shubin, J. Rare Earths, **24** (2006) 276

[29]. Yamashita T., Nada N, Onishi H and Kitamura S., Health Phys. **21** (1971) 295

[30]. Dixon R.L. and Ekstrand K.E., Proc. 4th Int. Conf. Luminescence Dosimetry, Institute of Nuclear Physics, Krakow, (1974) 481

[31]. Gonzalez, P.R., Furetta, C., Calvo, B.E., Gaso, M.I., Cruz-Zaragoza, E., Nucl. Instrum. Methods Phys. Res., Sect. B, **260** (2007) 685

[32]. Nakajima T., Murayama Y., Matsuzawa T. and Koyano A., Nucl. Instrum. Methods **157** (1978)155

[33]. Fairchild R.G., Mattern P.L., and Lengweiler K., J. Appl. Phys., **49** (1978) 4523

[34]. Binder W., Disterhoft S. and Cameron J.R. Proc. 2nd Int. conf. on Luminescence Dosimetry, Gatlinburg, **CONF 680920** (1968) 43

[35]. Burgkhardt B., Singh D., and Piesch E., Nucl. Instrum. Methods, **141** (1977) 363

[36]. Lucas A.C., and Kapsar B.M., Proc. 4th Int. Conf. Luminescence Dosimetry, Institute of Nuclear Physics, Krakow, (1974) 507

[37]. Nagpal J.S., Kathuria V.K., and Bapat V. N., Int. J. Appl. Radiat. Isot. **32** (1981)147

[38]. Tochilin E., Goldstein N., and Miller W.G., Health Phys., **16** (1969) 1

[39]. Crase K.W., and Gammage R.B., Health Phys. **29** (1975) 189

[40]. Mehta S.K., and Sengupta S., Health phys. **31** (1976) 176

[41]. Akselrod M S, Kortov V S and Gorelova E A, Rad. Prot. Dosim. **33** (1990) 119

[42]. Nakajima T., Health Phys. **23** (1972) 133

[43]. Schulman, J. H., Kirk, R. D. and West, E. J. Proceedings of the International Conference on Luminescence Dosimetery, Stanford University. **CONF-650637**, (1967)113.

[44]. Takenaga, M., Yamamoto, O. and Yamashita, T., Nucl. Instrum. Methods **175** (1980) 77

[45]. Xiong, Z., Ding, P., Tang, Q., Chen, J. and Shi, W., Adv. Mat. Res. **160** (2011) 252.

[46]. Sangeeta, C. K. and Sabharwal, S. C. J. Lumin. **109** (2004) 69

[47]. Venkateswara Rao, G., Reddy, P. Y. and Veeraiah, N., Mater. Lett. **57** (2002) 403.

[48]. Manam, J. and Sharma, S. K. Nucl. Instrum. Methods B **2** (2004) 314.

[49]. Takenaga, M., Yamamoto, O. and Yamashita, T., Health Phys., **44** (1983) 387.

[50]. Prokic M., Nucl. Technol.,**100** (2002) 265.

[51]. Li, J., Hao, J. Q., Li, C. Y., Zhang, C. X., Tang, Q., Zhang, Y. L., Su, Q. and Wang, S. B. Radiat. Meas. **39** (2005) 229.

[52]. Madhukumar, K., Varma, H. K., Komath, M., Elias, T. S., Padmanbhan, V. and Nair, C. M. K. Bull. Mater. Sci. **30** (2007) 527.

[53]. Ignatovych M., Holovey V., Vidoczy T., Baranyai P., and Kelemen A, Radiat. Phys. Chem. **76** (2007) 1527

[54]. Holovey V.M., Sidey V.I., Lyamayev V.I., and Puga P.P., J. Lumin., **126** (2007) 408

[55]. Madhusoodanan U, Jose M.T , Tomita A, Hoffmann W and Lakshmanan A.R, J. *Lumin.*, **82** (1999) 221

[56].Madhusoodanan U, Jose M.T , Tomita A and Lakshmanan A.R, J. Lumin., **87–89** (2000) 1300

[57]. Gorbics S.G., Attix F.H. and Kerris K., Health Phys. **25** (1973) 499

[58]. Dixon R.L. and Ekstrand K.E., Proc. 4th Int. conf. Luminescence dosimetry, Institute of Nuclear Sciences, Krakow, (1974) 481

[59]. Anishia S.R., Jose M.T. , Annalakshmi O., Ramasamy V., J. Lumin., **131** (2011) 2492

[60]. Furetta C., Prokic M., Salamon R. and Kitis G., Appl. Radiat. Isotopes, **52** (2000) 243.

[61]. Li J., Zhang C.X., Tang Q., Zhang Y.L., Hao J.Q., Su Q. and Wang S.B., J. phys. Cem. solids, **68** (2007) 143

[62].Yasser Saleh Mustafa Alajerami, Suhairul Hashim, Ahmad Termizi Ramli, Muneer Aziz Saleh and Taiman Kadni, Radiat. Prot. Dosim., **155** (2013) 1

[63]. Santiago M., Marcazzó J., Grasselli C., Lavatc A., Molina P., Spano F., Caselli E., Radiat. Meas., **46** (2011) 1488.

[64] . Santiago M., Lester M., Caselli E., Lavat A., Ges A., Spano F. and Kessler C., J. Mater. Sci. Lett., **17** (1998) 1293

[65]. Abubakar R., Untung S. and Oberhofer M., Radiat. Prot. Dosim., **33** (1990) 95

[66]. Bhuwan Chandra and Bhatt R.C., Nuclear Instrum. Methods, **184** (1980) 557

[67]. Garrett J.D., Natrajan-Iyere M., and Greedan, J. Cryst. Growth, **41** (1977) 225

[68]. Adamiv V. T., Antonyak O.T., Ya.V. Burak, Pidzyrailo M.S.,and Teslyuk I.M., Funct. Mat., **12** (2005) 278

[69]. Ignatovych M., Holovey V., Watterich A, Vidoczy T, Baranyai P., Kelemen A., and Chuiko C, Radiat. Meas., **38** (2004) 567

[70]. Holovey V.M., Sidey V.I., Lyamayev V.I., and Puga P.P., J. Lumin., **126** (2007) 408

[71]. El-Faramawy N.A., El-Kameesy S.U., El-Aframy A. and Metwally G., Radiat. Phys. Chem., **58** (2000) 9

[72]. Furetta C., Prokic M., Salamon R., Prokic V. and Kitis G., Nucl. Instrum. Methods Phys. Res. Sect. A, **456** (2001) 411

[73]. Huy B.T., Quang V.X., and Chau H.T. B., J. lumin. **128** (2008) 1601

[74]. Rzyski B.M. and Morato S.P., Nucl. Instrum methods, **175** (1980) 62

[75]. Hooshang Mohammadi and Paul L. Ziemer, Nucl. Instrum. methods, **155** (1978) 503

[76]. Ignatovych M., Holovey V., Vidoczy T., Baranyai P., and Kelemen A, Radiat. Phys. Chem. **76** (2007) 1527

[77]. Prokic M, Radiat. Meas. **33** (2001) 393

[78]. Kang Soo Park, Ahn J.K., Kim D.J., Kim H.K., Hwang Y. H., Kim D.S., Park M.H., Yumi Park, Jin-Joo Yoon, Jae-Young Leem, J. cryst. growth, **249** (2003) 483

[79]. Srivastava J.K., and Supe S.J, J.Phys. D:Appl. Phys. **22** (1989) 1537

[80]. Can N, KAralli T., Townshend P.D. and Yildiz F., J.Phys.D: Appl. Phys. **39** (2006) 2038

[81]. Driscoll C.M.H, Fisher E.S., Furetta C., and Padovani R., Radiat. Prot. Dosim., **6** (1983) 305

[82]. Fernandes A.C., Osvay M., Santos J.P., Holovey V., Ignatovych M., Radiat. Meas. **43** (2008) 476

[83]. Kitis G., Furetta C., Prokic M and Prokic V., J.Phys. D: Appl. Phys. **33** (2000) 1252

[84]. Manam J., and Sharma S.K., Radiat. Eff. Defects solids, **163** (2008) 813

[85]. Brant A.T., Kananan B.E., Murari M.K., McClory J.W., Petrosky J.C., Adamiv V.T., Ya V. Burak, Dowben P.A., and Halliburton L.E., J. Appl. Phys, **110** (2011) 093719

[86]. Kazankaya V. A., Kuzmin V.V., Minaeva E.E., Sokolov A.D., Proc. 4th Int. Conf. Luminescence Dosimetry, Kracow, Poland, 1974, 581.

[87]. Prokic M., Health Phys. **42** (1982) 849

[88]. Prokic M., Radiat. Prot. Dosim. **17** (1986) 393

[89]. Prokic M., Radiat. Prot. Dosim., **47** (1993) 191

[90]. Furetta C., Kitis G., Weng P.S., and Chu T.C., Nucl. Instrum. Methods Phys. Res., Sect. A **420** (1999) 441

[91] Souza J.H., Ferrari V.A. and de Freitas L.C., Radiat. Prot. Dosim., **47** (1993) 239

[92] Porwal N.K., Kadam R.M., Seshagiri T.K., Natarajan V., Dhohale A.R. and Page A.G., Radiat. Meas. **40** (2005) 69

[93]. Cano A., Gonzalez P.R. and Furetta C., Mod. Phys. Lett. B, **22** (2008) 1997

[94]. LI Juan, ZHANG Chunxiang, TANG Qiang, HAO Jingquan, ZHANG Yanli, SU Qiang and WANG Shubin, J. rare earths, **26** (2008) 203.

[95]. Nil Kucuk, Ilker Kucuk Merve Cakir and Sule Kaya Keles, J. lumin. **139** (2013) 84

[96]. Dittman R, Hahn D. and Muller U., J. Lumin. **3** (1970), 230

CHAPTER - 2

SYNTHESIS AND STRUCTURAL CHARACTERIZATION

Chapter – 2

Synthesis and Structural Characterization

2.0 Preamble

This chapter presents a description of the synthesis of borate based TL phosphors by simple solid state sintering. The raw materials used in the synthesis of the phosphors and the steps followed during solid state sintering are described schematically. The characterization of the phosphors by XRD, FTIR and SEM is presented. The effective atomic number of the phosphors is also given.

2.1 Introduction

Development of tissue equivalent TL materials suitable for clinical dosimetry applications and phosphors with combined neutron and gamma sensitivities has attracted considerable interest. In this regard, TL phosphors based on borates play an important role because of their near tissue equivalent absorption coefficient and neutron sensitivity due to high thermal neutron absorption cross-section of ^{10}B [1,2]. TL characteristics of the mixed borate $LiCaBO_3$ (LCB) doped with rare earth elements and lithium magnesium borates have also been studied recently because of their neutron sensitivity and relatively lesser effective atomic number [3,4] and their feasibility in radiation dosimetry applications have been demonstrated.

Synthesis of borate based compounds is quite difficult. Based on the preparation technique borate compounds may form crystalline as well as glassy phase. For obtaining efficient luminescent materials crystalline forms are required. Also the TL properties of the phosphor depend on the starting materials used for the synthesis of phosphors [5]. There are several other methods used for the synthesis of borate based phosphors like the melting method [6], combustion method [7], growing of single crystals [8], Sol-gel method [9], hydrothermal synthesis [10] etc. All the phosphors used in the present study were synthesized by solid state sintering technique because it is a simple method for the synthesis of bulk amount in less time which lowers the preparation cost.

2.2 Synthesis of borate based phosphors

All the borate based phosphors used in the present study were synthesized by wet chemical mixing followed by simple solid state sintering at high temperature slightly lower than the melting point of the end product. The chemicals (raw materials) used in the synthesis, are low cost local chemicals of AR grade purity. The starting materials (chemicals) used for the synthesis of the different borate phosphors is shown in Table 2.1.

Table 2.1 Raw materials used in the synthesis of different borate based phosphors

Phosphor	Raw materials	Temperature (°C)	No. of hours (h)
$Li_2B_4O_7$:Mn	Li_2CO_3	750	3
	H_3BO_3		
	$MnCO_3$		
MgB_4O_7:Gd,Li	$MgCO_3$	900	5
	H_3BO_3		
	Gd_2O_3		
	Li_2CO_3		
ZnB_2O_4:Tm	$ZnCO_3$	875	5
	H_3BO_3		
	Tm_2O_3		
CdB_4O_7	$CdCO_3$	850	4
	H_3BO_3		

Only phase purity and reproducibility of the properties for different batches becomes important for dosimetry applications. The various steps involved in the synthesis by solid state route are shown in fig. 2.1.

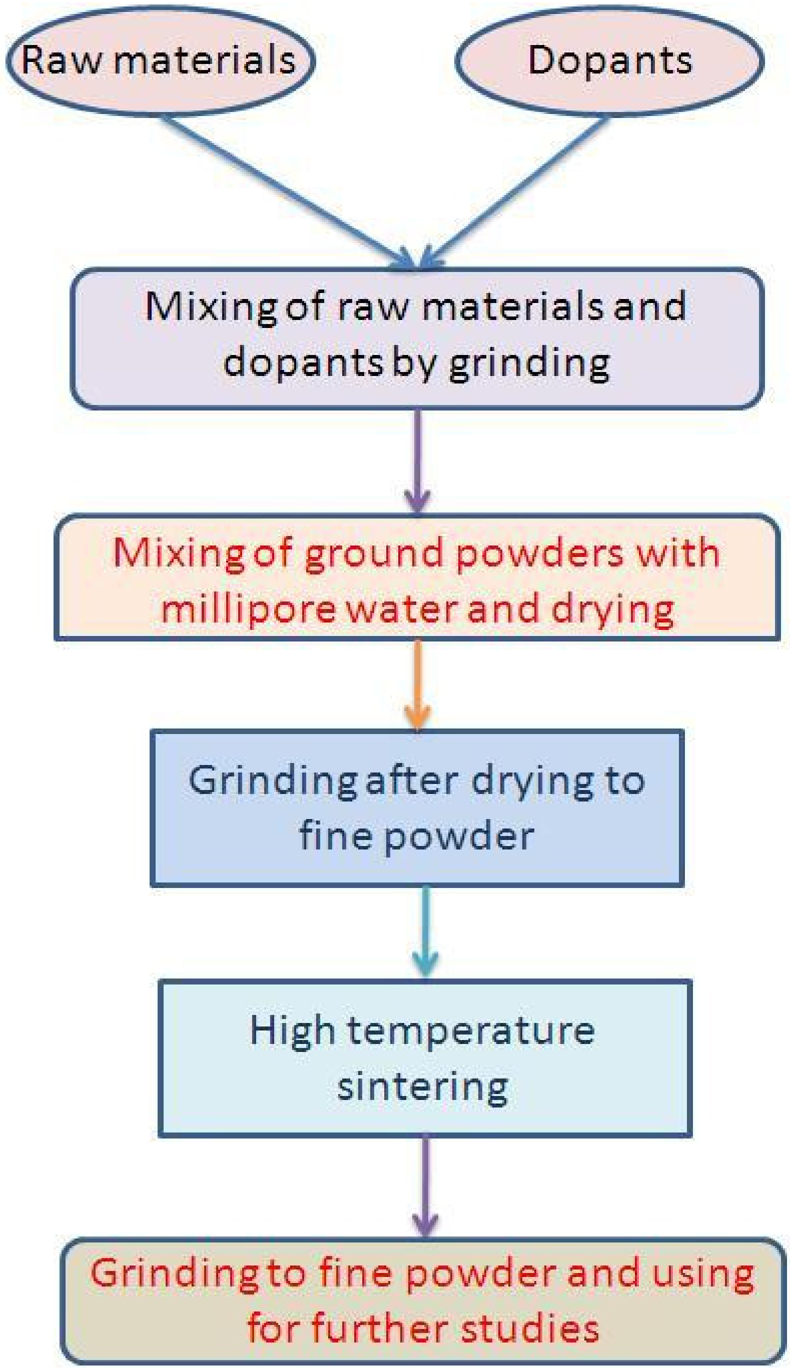

Fig. 2.1 Schematic representation of the steps involved in the solid state sintering technique used for the synthesis of borates.

The raw materials needed for the synthesis of these phosphors are weighed in the appropriate stoichiometric ratio, and are mixed together by dry grinding using a mortar and pestle. Once when the raw materials are mixed thoroughly, it is transferred to a silica crucible and a small amount of millipore water is added to the mixture to form slurry (paste). This ensures uniform mixing of dopant in the mixture. The slurry is then dried by heating around 100°C. After drying once again it is ground using a mortar and pestle and then transferred to an alumina crucible and sintered in a furnace at high temperature in air atmosphere. Sintering temperature is maintained slightly lower than the melting points of the respective phosphors. After maintaining the sample at this high temperature for a few hours (Table 2.1) the furnace is switched off. Once the temperature reaches around 500°C (by natural cooling), the sample is removed from the furnace and suddenly cooled to room temperature. It is then ground into fine powder and used for further characterization.

2.3 X-ray diffraction (XRD) pattern

X-ray diffraction pattern of the phosphors synthesized were recorded using STOE diffractometer using Cu-kα radiation of wavelength 1.54060 Å. The diffraction patterns obtained were compared with that of reported ones (JCPDS files) and the phases were identified. The X-ray diffraction pattern of LTB:Mn phosphor is shown in fig. 2.2.

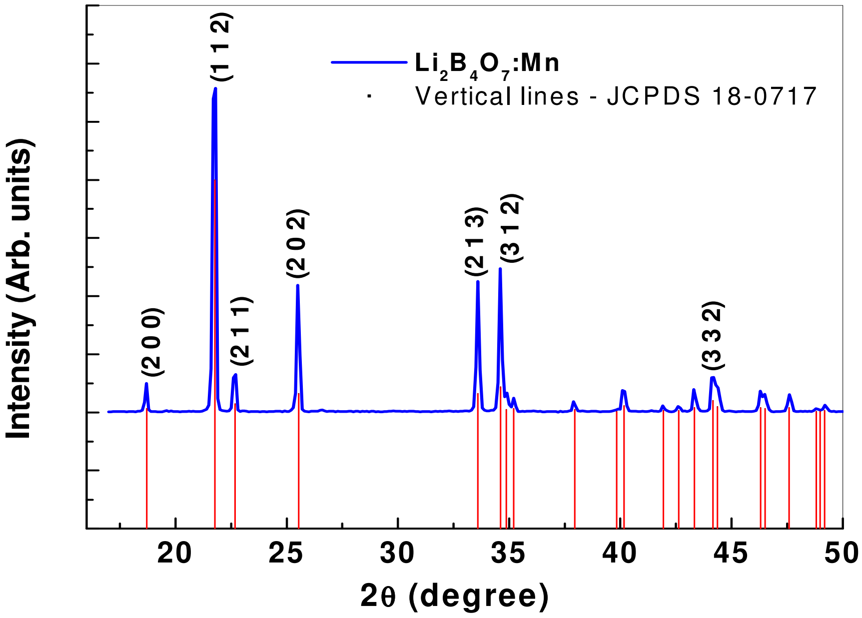

Fig. 2.2 XRD pattern of $Li_2B_4O_7$:Mn

The peaks observed in the diffraction pattern are indexed as per the JCPDS database 18-0717. It has a tetragonal (body centered) crystal structure with lattice parameters a = b = 9.477 Å and c = 10.286 Å. The space group is $I4_1cd$. Fig. 2.3 shows the X-ray diffraction pattern of MTB:Gd,Li phosphor synthesized by solid state sintering technique.

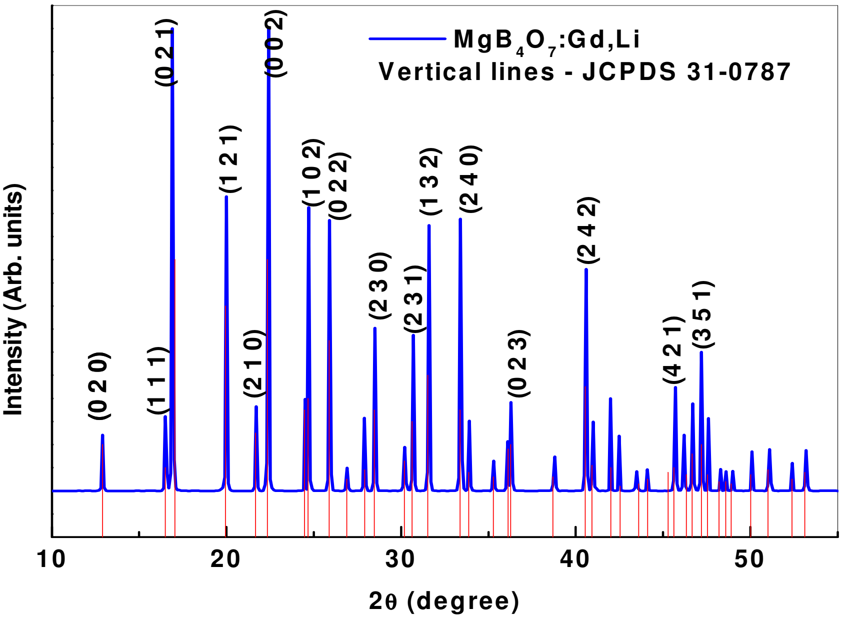

Fig. 2.3 XRD pattern of MgB_4O_7:Gd,Li

The crystal structure was identified as orthorhombic and the peaks observed in the diffraction pattern were indexed based on the JCPDS database 31-0787. The lattice parameters are a=8.596 Å, b=13.72 Å, c=7.956 Å and the space group is Pbca.

Similarly the diffraction patterns of Zinc borate and cadmium borate are shown in Figs. 2.4 and 2.5 respectively. For indexing the peaks of the diffraction pattern, the JCPDS data files 39-1126 and 30-0204 were used respectively. Zinc borate has crystallized into a body centered cubic structure with lattice parameter a=7.473 Å and space group $Im\bar{3}m$ whereas cadmium tetra borate has crystallized into an orthorhombic structure with a=8.704 Å, b=14.17 Å, c=8.229 Å and space group Pbca.

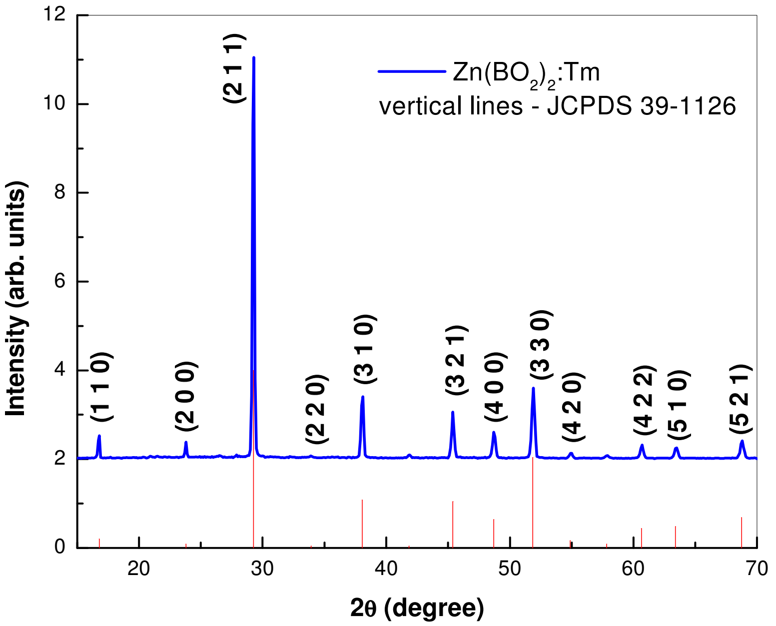

Fig. 2.4 XRD pattern of ZnB_2O_4:Tm

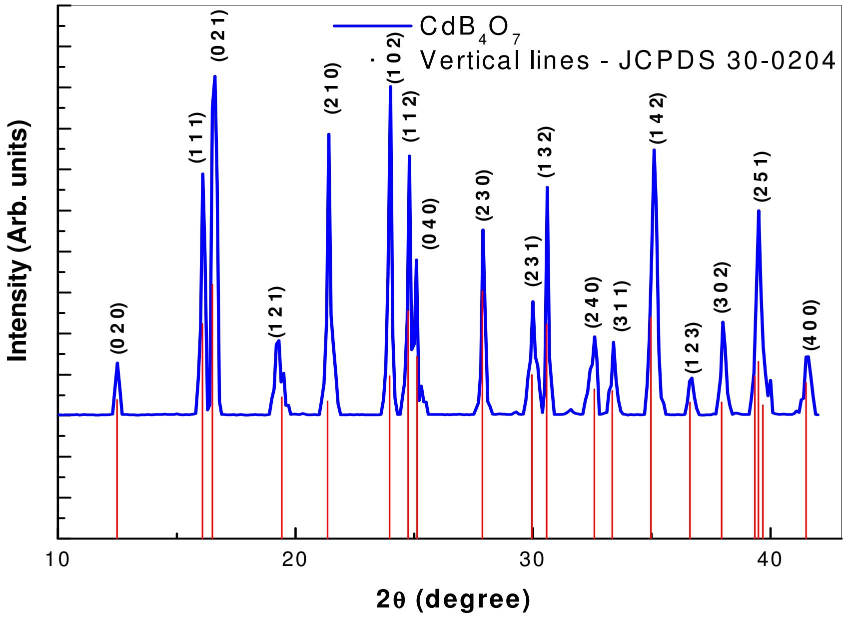

Fig. 2.5 XRD pattern of CdB_4O_7

2.4 Infra red spectra

IR spectra of the synthesized phosphors were recorded using FTIR spectrometer (ABB make, model MB3000) which uses ceramic material as an IR source. The detector used is DTGS (deuterated triglycine sulphate) with Horizon MB Software.

Spectral measurements were carried out with 16 cm^{-1} resolution using 32 scans in the range between 500 cm^{-1} to 4000 cm^{-1} i.e. in the mid-infrared region. The finely ground phosphor is mixed with KBr and the sample is usually ground with an agate mortar and pestle and made into a clear transparent disc. IR measurements were carried out in the transmission mode. In the present study, infrared radiation from the source is allowed to pass through the sample and the portion of the beam that is transmitted, i.e. not absorbed by the sample is recorded. The IR spectrum of LTB:Mn phosphor is shown in Fig. 2.6.

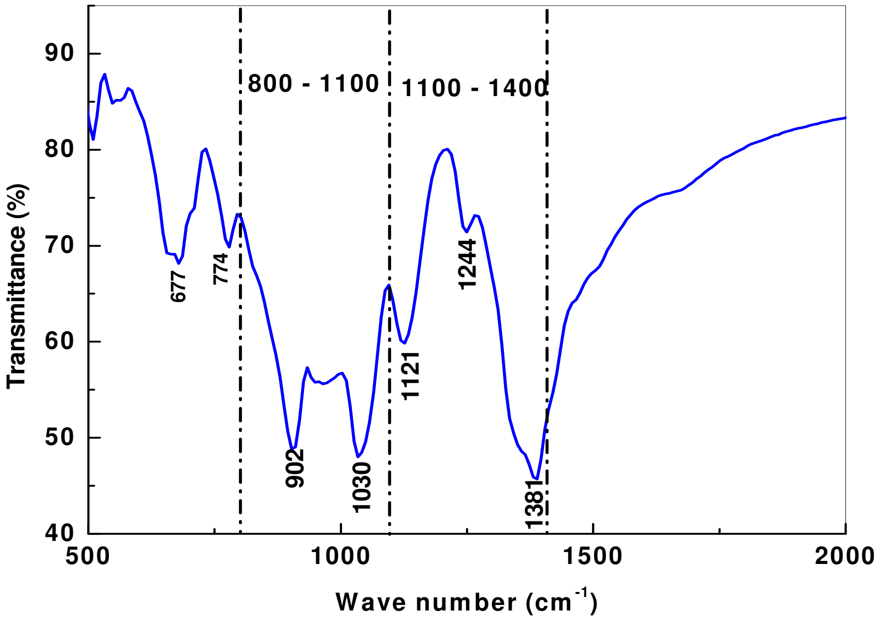

Fig. 2.6 FTIR spectra of lithium tetraborate doped with Mn

The spectrum shows evidence for the presence of both 3 and 4 fold co-ordinated boron atom. The bands in the region 800 – 1100 cm^{-1} are indicative of 4 fold co-ordination and correspond to the B-O stretching modes of tetrahedral BO_4 units. The bands between 1100 – 1400 cm^{-1} are indicative of 3 fold co-ordination and corresponds to the B-O vibrational modes of trigonal BO_3 units [11]. The bands at 677 cm^{-1} and 774 cm^{-1} indicates the presence of ^{11}B in the compound. The strong absorption band near 1381 cm^{-1} and 1244 cm^{-1} corresponds to the symmetric stretching vibration of trigonal BO_3 units [12].

The FTIR spectra of Zinc metaborate is shown in Fig. 2.7. Zinc metaborate contains four formula units in its structural formula.

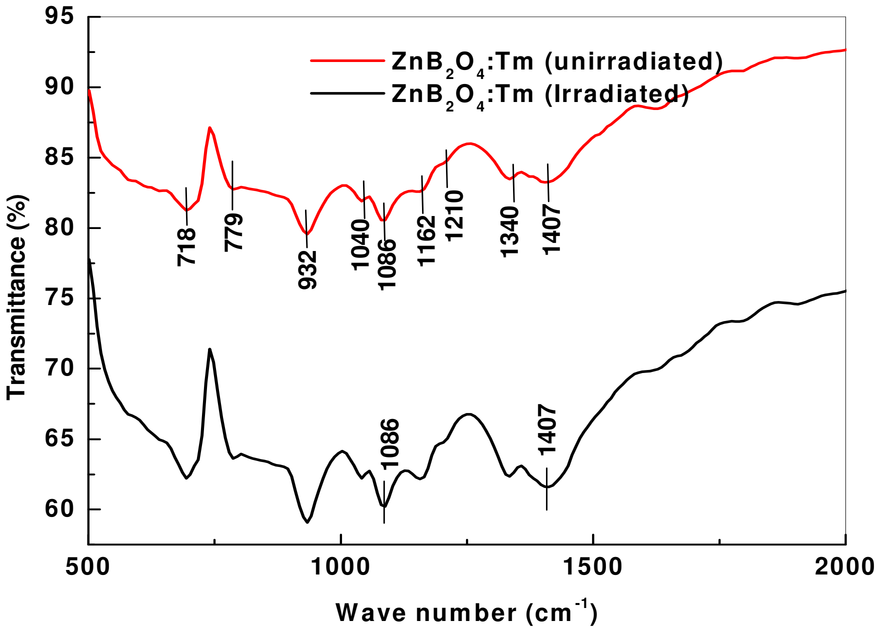

Fig. 2.7 FTIR spectra of unirradiated and irradiated ZnB_2O_4*:Tm phosphors*

This compound is very different compared to the other borates studied. This compound is formed of mainly tetrahedral boron atoms and the tetrahedras are coupled at certain corners to form the complex 3 dimensional array [12,13] whereas the other borates studied are made of both tetrahedral and trigonal arrangements of the borate functional group. In the tetrahedra, one oxygen atom is connected to a zinc atom and the other 3 atoms are shared by 3 different tetrahedra. Though all B-O bonds are similar, the oxygen coupled with zinc is unique and hence the symmetry can be considered as trigonal instead of tetrahedral co-ordination. Hence the basic unit can be visualized as containing a central atom (Boron) bonded to two different kinds of atoms viz., oxygen bound to zinc and the other three oxygen atoms connected into the network. The presence of strong fundamental absorption in the region 800 cm^{-1} to 1100 cm^{-1} suggests that boron is co-ordinated tetrahedrally. The absorption at 1086 cm^{-1} corresponds to the fundamental absorption due to the asymmetric stretching vibration of tetrahedrally co-ordinated boron. The absorption at 1407 cm^{-1} corresponds to the asymmetric stretching vibration of B-O bond in BO_3 units. In the case of gamma irradiated phosphor, due to B-O bond breakage in the tetrahedra, there is a formation of of BO_3 radicals. The increase in the absorption at 1407 cm^{-1} gives the evidence for the asymmetric stretching vibration of B-O bond in BO_3 units.

The IR spectra of unirradiated magnesium tetraborate and cadmium tetraborate phosphor are shown in Fig. 2.8.

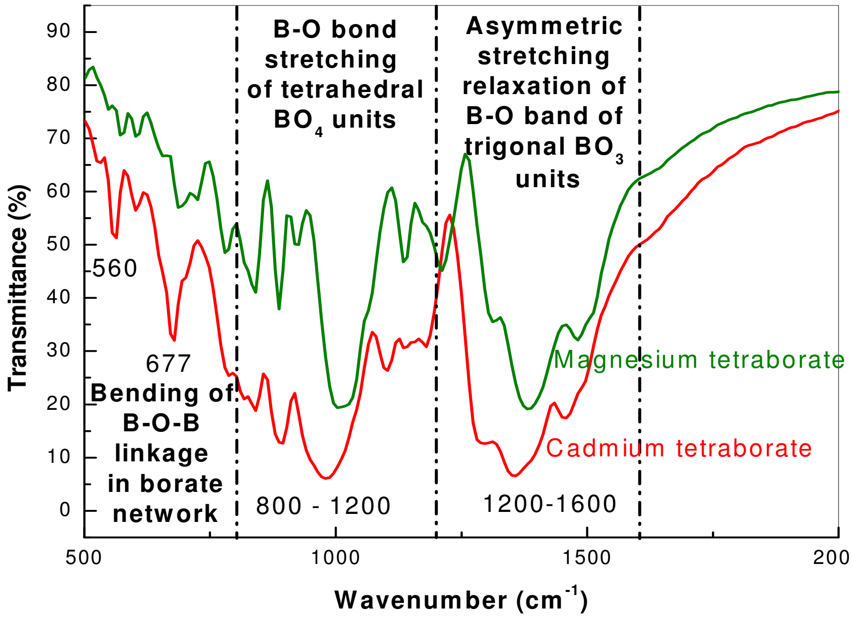

Fig. 2.8 FTIR spectra of MTB:Gd,Li and CdB_4O_7

From the IR spectrum it is clear that the compound is formed out both BO_3 and BO_4 networks. The absorption bands in the region 1200 to 1600 cm^{-1} corresponds to the stretching of B-O bonds of trigonal BO_3 units and the bands in the region, 800 to 1200 cm^{-1} corresponds to the B-O bond stretching of tetrahedral BO_4 units. The bands below 800 cm^{-1} corresponds to the B-O-B bending vibrations of borate networks.

2.5 Scanning electron microscope

The surface morphology of the synthesized phosphors was examined using Scanning Electron microscope (SEM) Hitachi make (S-3400N model, Tokyo, Japan). Figures 2.9 shows the SEM micrographs of the borate based TL phosphors studied. The SEM images show that the particles are of non-uniform size and shape and mostly found in agglomerated form.

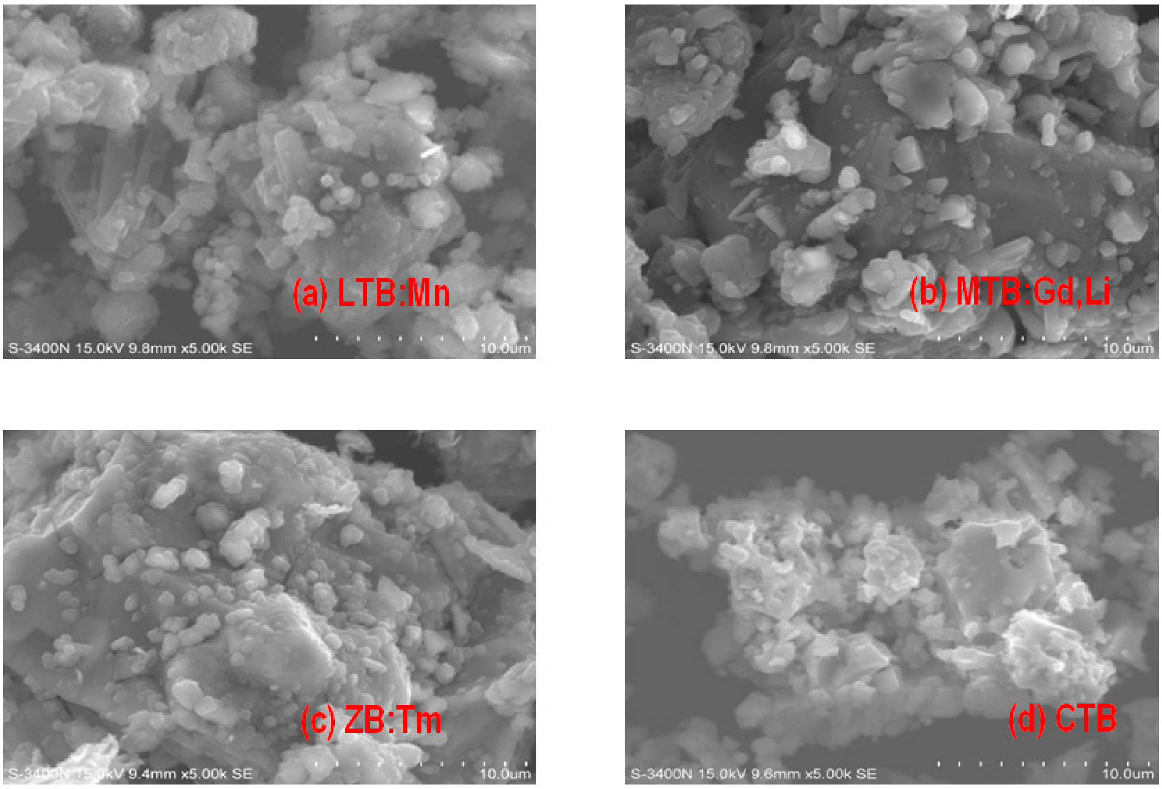

Fig.2.9 SEM micrographs of the synthesized borate phosphors

2.6 Effective atomic number

The response of a TL phosphor to ionizing radiations (in particular X and Gamma rays) depends on the atomic number of the constituents. Hence, it is necessary to determine the effective atomic number *(Z_{eff})* of the phosphor apriori to know the response of the phosphor to radiations of different energy. One method to determine the *Z_{eff}* is to obtatin the fractional number of electrons of each element constituting the phosphor [14]. Based on this Z_{eff} is given by, $Z_{eff} = \sqrt[2.94]{\sum_i a_i Z_i^{2.94}}$ where $a_i = \frac{n_i(Z_i)}{\sum_i n_i(Z_i)}$, $n_i = N_A Z_i$, where a_i corresponds to the fractional contents of electrons in elements with atomic number Z_i, n_i is the number of electrons in one mole and N_A is the Avagadro number. The effective atomic number calculated for the phosphors is shown in table 2.2.

Table 2.2 Effective atomic number of borate based TL phosphors

Sl. No.	Phosphor	Effective atomic number
1	$Li_2B_4O_7$	7.25
2	MgB_4O_7	8.37
3	ZnB_2O_4	22.45
4	CdB_4O_7	34.83
5	Tissue	7.4

From the table 2.2 it is clear that both lithium tetraborate and magnesium tetraborate phosphors are nearly tissue equivalent whereas, zinc metaborate and cadmium tetraborate have a higher effective atomic number compared to tissue. Higher atomic number materials generally result in high sensitivity to gamma radiation but needs suitable filters to compensate for over response at lower energy radiation, when used for personnel monitoring.

2.7 Conclusions

Single phase polycrystalline powder samples of LTB:Mn; MTB:Gd,Li; ZMB:Tm and CTB thermoluminescent phosphors were synthesized by simple solid state sintering technique. The raw materials used for the synthesis of these phosphors were of local AR grade chemicals. The X-ray diffraction patterns of the synthesized phosphors were recorded and the peaks observed in the diffraction pattern were indexed using the standard JCPDS data. The vibrational modes of the borate network in these phosphors have been identified using IR studies. It was found that these borates are made of both trigonal BO_3 and tetrahedral BO_4 units.

2.8 References

---

[1]. Huy, B.T., Quang, V.X., Chau, H.T.B., J. Lumin., **128** (2008) 1601

[2]. Tolga Depci., Gulhan Ozbayoglu., Aysen Yilmaz., Necmeddin Yazici, A., Nucl. Instrum. Methods Phys. Res. B, **266** (2008) 755.

[3]. Anishia S.R., Jose M.T., Annalakshmi O., Ponnusamy V. and Ramasamy V., J. Lumin., **130** (2010) 1834.

[4]. Anishia S.R., Jose M.T., Annalakshmi O. and Ramasamy V., J. Lumin., **131** (2011) 2492

[5]. Prokic M., Radiat. Prot. Dosim., **100** (2002), 265

[6]. Kar S., Sunil Verma, Bartwal K.S., Journal of alloys and compounds, **495** (2010) 288

[7].Thakare S.S., Omanwar S.K., Moharil S.V., Dhopte S.M., Muthal P.L., and Kondawar V.K., Opt. Mater., **29** (2007) 1731

[8]. Magdalyna Ignatovych, Mauro Fasoli, and Andras Kelemen, Radiat. Phy. Chem. **81** (2012) 1528

[9]. Santiago M., Marcazzo J., Grasselli C., Lavat A., Molina P., Spano F., and Caselli E., Radiat. Meas. **46** (2011) 1488

[10]. Byrappa K. and K.V. K. Shekar, Mat. Res. Bull., **28** (1993) 709

[11]. Weir C.E. and Schroeder R.A., Journal of research of the National Bureau of Standards – A. Physics and Chemistry, **68A** (1964) 465

[12]. Chandikiram Gautam, Avadesh Kumar Yadav and Arbind Kumar Singh, ISRN Ceramics, **2012** (2012) 428491-(1-17)

[13]. Krogh-Moe J., Z. Krist. **117** (1962) 166

[14]. Gonzalez P.R., Furetta C., Calvo B.E., Gaso M.I., Cruz Zaragoza E., Nucl. Instrum. Methods in Phys. Res. Sect., B **260** (2007) 685

CHAPTER - 3

DOSIMETRIC CHARACTERISTICS

Chapter – 3

Dosimetric characteristics

3.0 Preamble

Thermoluminescence dosimetry is the widely used means of dosimetric measurements especially for personnel monitoring of radiation workers. The materials used for personnel monitoring should meet several requirements like high sensitivity, low fading, linear response over a wide range of dose and no energy dependence. A single material may not satisfy all the requirements for personnel dosimetry. The field evolves by the development of new materials or improving the characteristics of existing phosphors by using different synthesis technique or by changing the dopants. This chapter presents important dosimetric characteristics of borate based phosphors developed for dosimetric applications.

3.1 Introduction

Thermoluminescence is exhibited by most of the inorganic compounds. However, to use a phosphor for dosimetric applications, it should qualify some properties which limit the choice to only a handful of materials. Some of the most desirable properties that qualify a phosphor for dosimetric applications are,

- A high concentration of electrons and/or hole traps and a high efficiency in the recombination process resulting in intense light emission upon heating (high sensitivity).
- A sufficient storage stability resulting in comparatively less fading due to undesirable factors like temperature, humidity, light etc. This can be achieved if the glow peak of the phosphor lies between 180˚C and 300˚C. Glow peaks with higher temperature will have the infrared contribution resulting in the

interference with the measurement of low doses and thereby reducing the accuracy.

- The wavelength of the emitted light should match the spectral sensitivity of the detector system used and it should have poor interference with the incandescent or IR emission from the surroundings or the heated phosphor.
- Trap distribution should not complicate the evaluation process by the presence of additional rapidly fading low temperature peaks or high temperature peaks which will be difficult to anneal and give rise to retrapping process.
- The phosphor should have good resistance against environmental factors like light, humidity, common fumes and gases.
- It should have low photon energy response and linear response over a wide range of doses.
- The phosphor should be nontoxic and should not deteriorate upon storage and it should also be synthesized easily with reproducible properties.

The following sections of this chapter present important dosimetric characteristics like TL glow curve, TL emission wavelength and gamma dose response of the synthesized borate based TL phosphors viz., LTB:Mn, MTB:Gd,Li, ZMB:Tm and CTB. Glow curve variation with dopant concentration was studied and the optimum concentration was determined for each of the borates. Also the other dosimetric parameters like reusability, storage stability, light sensitivity, reproducibility in synthesis etc. are also studied and presented in this chapter.

3.2 Experimental details

All TL measurements used in this study were carried out using RISO TL/OSL reader model DA-20 [1]. Powder samples (~10 mg) are loaded onto an exchangeable sample carousel that can accommodate up to 48 samples. The sample carousel is placed in the sample chamber which can be programmed to be individually heated to any temperature between room temperature and 700°C at constant heating rates from 0.1 to 10°C/s, to be individually irradiated (using inbuilt beta source) and to be optically stimulated by various light sources in situ. The sample carousel rests on a motor driven turntable, which enables rotation of the sample carousel. Rotation is computer controlled and position holes drilled through the carousel in close proximity to the sample positions enable the system to keep track of the position of the carousel using optoelectronics. The sample is lifted through slots in the sample carousel into the measurement position by a lift, which also functions as heating element. The heating strip can be cooled by a nitrogen flow, which also protects the heating system from oxidation at high temperatures. The emitted luminescence is measured by the light detection system comprising of a Photomultiplier tube (bialkali EMI 9235QB PMT) which has maximum detection efficiency between 200 and 400 nm. A weak reference light source (known as the blue “calibration LED”) is incorporated in the reader and is used for routine check of the detection system.

Photoluminescence measurements were carried out by using a JOBIN YVON-Spex Spectrofluorometer [2] (Fluorolog version-3; model FL 3-11) which has a 450 W high-pressure xenon lamp as a light source for excitation, monochromators for dispersing the excitation and emission light and help to select required wavelength, a photomultiplier tube for the detection of light. The TL emission wavelength of the phosphors were recorded using a TL reader (TL-1007) coupled to the Flurolog-3 spectrometer with a bifurcated and randomized optic fiber bundle (model 1950-1M Jobin Yvon) of 1 m which provides high transmission of the light from sample to the emission spectrometer. The samples can be heated to different temperatures isothermally and the wavelength of the emitted light can be recorded.

3.3 Lithium tetra borate ($Li_2B_4O_7$) based phosphors

Lithium tetraborate is one of the TL phosphors which have been studied for a long time since its first introduction due to its tissue equivalence. Lithium tetraborate doped with copper is reported to have a better sensitivity among other dopants studied. LTB:Cu with several co-dopants have been synthesized by solid state sintering technique and their TL glow curves were recorded. It is found that the dosimetric peak occurs around 190 - 200°C and is largely independent of dopants and co-dopants. The TL intensity was found to be high for LTB doped with copper, silver and phosphorus. But LTB:Mn synthesized using solid state sintering method has a high temperature glow peak and hence has the benefit of less fading. Hence a detailed investigation has been carried out on this material with reference to increasing the TL intensity, PL spectrum, dose response, reusability and storage stability.

3.3.1 TL Glow curve of LTB:Mn: The TL glow curves of lithium tetra borate doped with manganese synthesized under different atmospheres while sintering and recorded with a heating rate of 10°C/s after gamma irradiation of 2.14 Gy is shown in Fig. 3.1.

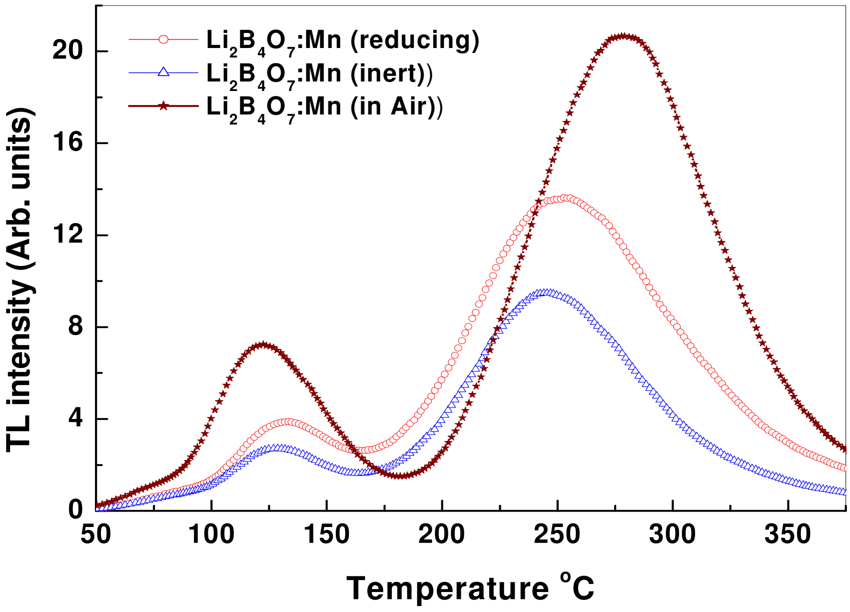

Fig. 3.1 TL glow curves of gamma irradiated (2.14 Gy) LTB:Mn synthesized under different conditions. (heating rate used 10°C/s)

Reducing atmosphere was created using carbon monoxide (CO) by inverted crucible technique and for inert atmosphere nitrogen gas is flushed while sintering. The glow peak temperature as well as the peak height varied with the nature of the atmosphere in which the sample was synthesized. The TL glow curve composed of a dominant TL peak around 250°C and a small peak around 120°C. This is in contrary with the results reported in literature [3] where the main dosimetric peak was observed to be around 210°C for the Mn doped LTB for the same heating rate. The low temperature peak however fades within 24 h of storage.

The phosphor sintered in air atmosphere has a higher TL intensity and the dosimetric peak is also at a slightly higher temperature of 270°C compared to the phosphor sintered in reducing atmosphere. This is consistent with the work of Holovey *et al* [4] who studied the influence of different annealing conditions on the luminescent properties of $Li_2B_4O_7$:Mn single crystals. They have reported that annealing of the LTB:Mn single crystals in the reducing environment results in a sharp drop in intensity for both TL peaks, displacement of the peak maxima towards lower temperatures, and intensity redistribution in favor of the low temperature peak. In this work, detailed dosimetric investigations are carried out on phosphor synthesized in air atmosphere.

3.3.2 Glow curve variation with dopant (Mn) concentration: The Mn concentration is known to have considerable influence on the achievable TL intensity and hence, the variation of TL intensity with manganese concentration was studied from 0.15 mol% to 0.75 mol%. No change in the shape of the TL glow curve was observed with Mn concentration but there was a shift in the glow peak temperature with Mn concentration. For undoped LTB the glow peak temperature is around 210°C. As the Mn concentration increases, the glow peak shifts to higher temperature up to around

270°C for optimum Mn concentration and then glow peak temperature decreases with increasing Mn concentration. As can be seen, the TL intensity was found to vary with Mn concentration. Figure 3.2 shows the variation of the TL intensity as a function of Mn concentration.

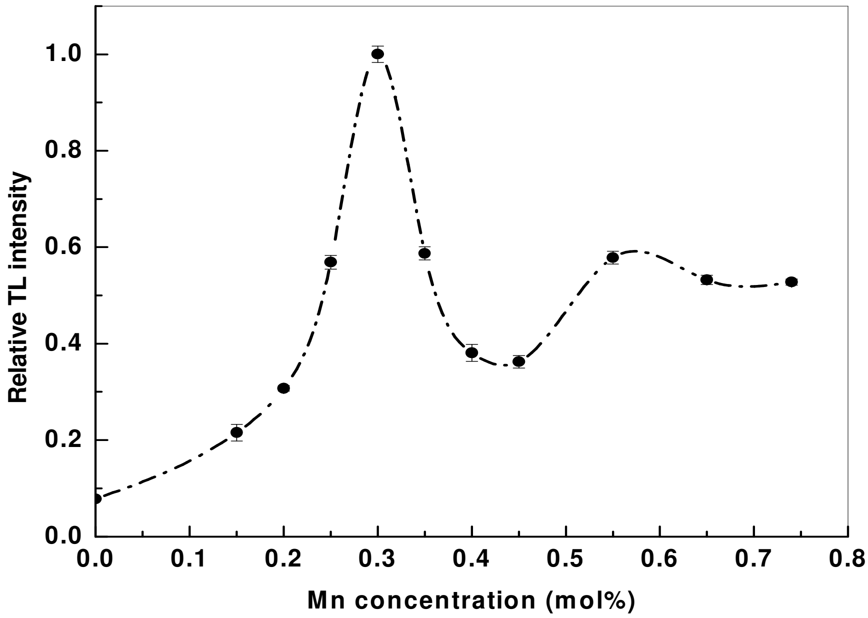

Fig. 3.2 Variation of TL intensity with Mn concentration in LTB phosphor. The dashed line through the data points is a guide to the eye. The error bars in the figure are the standard deviation of the 5 measurements carried to generate a single data point.

Holovey et al.[5] studied dopant concentration dependence of TL in LTB:Mn single crystals. The glow curve shape changes significantly with increase of Mn concentration, but all the curves demonstrate two well separated broad peaks, the first lying between 25 and 150°C range and second, within 150-280°C. The maximum intensity for the high temperature TL peak was observed with single crystal sample for an optimal concentration of Mn [5]. These single crystals have quiet different glow curve shapes at various dopant concentrations but in the case of polycrystalline samples synthesized by solid state sintering no major change in glow curves shape is observed as a function of dopant concentration. However, position and intensity of high temperature peak varied with Mn concentration. In the present study, the optimum TL intensity was obtained for a dopant concentration of 0.3 mol%. Hence, for all subsequent studies this sample having optimal Mn concentration of 0.3 mol% was used. Another review by Horowitz [6] reported that in LTB:Mn material, increase of Mn concentration reduces the temperature of low temperature peak and increases the temperature of the dosimetry peak. But in the case of the polycrystalline phosphor synthesized by us, we have observed a systematic increase/decrease of both low temperature and high temperature dosimetric peak. This shows that the trap centers responsible for both glow peaks may be possibly the same.

3.3.3 TL emission spectra: The knowledge of TL emission wavelength is useful in identifying the emission center and also to check the spectral mismatch with the detector system. Hence TL emission spectra were recorded for gamma irradiated LTB phosphors with different dopants (Cu doped and Mn doped). The TL emission spectra of LTB:Mn phosphor along with one Cu doped LTB phosphor is shown in Fig. 3.3. It was found that for all phosphors with Cu as one of dopant the TL emission is around 365 - 370 nm which is characteristic of copper. This emission around 365 nm matches well with the spectral sensitivity of common photo multiplier tubes (PMTs) and hence these phosphors have a relatively higher sensitivity than Mn doped LTB phosphors. This emission at 365 nm may be attributed to the metal centered transitions $3d^9 \leftarrow 3d^9 4s$ of the Cu^+ ions which can act as direct recombination centers [7].

For the case of undoped LTB phosphor, the TL emission is around 360 nm which is characteristic of host lattice. LTB doped with Ag alone resulted in a TL emission around 285 nm, however when Ag is used as a codopant with copper in LTB lattice, this emission at 285 nm is masked and the emission corresponding to Cu is more pronounced. This shows that addition of silver increases the concentration of traps responsible for TL. But in the case of Mn doped LTB, the emission is around 580 nm which is characteristic of Mn^{2+} emission [8].

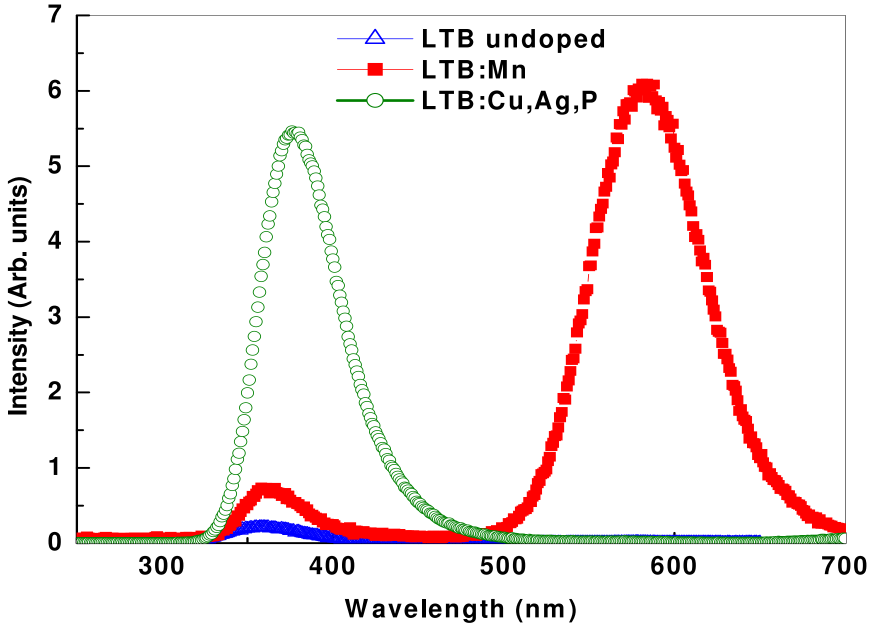

Fig. 3.3 TL emission spectra of LTB phosphors. (Dose 10 Gy)

In the case of the phosphors developed by solid state sintering, a variation in the temperature of the glow peak with Mn concentration variation was observed, but there is no change in the emission spectra with concentration variation. The host emission at around 360 nm is not exactly matching with excitation peaks of Mn^{2+} at 336 and 395 nm but it partly overlaps with 395 nm broad peak. Hence the emission at 580 nm which is related to 395 nm excitation is only seen in TL emission spectra. An orange fluorescence is associated with Mn in many systems but this fluorescence is dependent on manganese concentration and the local environment in the crystal. In fact, if Mn substitutes for Li in LTB phosphor its coordination will be a distorted tetrahedron. It is possible that the peak emission for this phosphor may vary slightly from batch to batch due to changes in Mn distribution and overall stoichiometry [9]. The Mn^{2+} emission from LTB:Mn can be understood in two ways. One is by the oxidation – reduction of dopant ion upon irradiation and heating respectively. The other choice for the Mn^{2+} emission is by the release of recombination energy from the dopant ions from nearby recombination centers via non radiative transfer. Studies on single crystals has revealed the oxidation – reduction mechanism in LTB:Mn[7,10]. In the polycrystalline powder samples developed by solid state sintering, no evidence for the conversion of Mn^{2+} to Mn^{3+} was observed.

3.3.4 Photoluminescence spectra: The photoluminescence excitation and emission spectra of un-irradiated LTB:Mn is shown in Fig. 3.4.

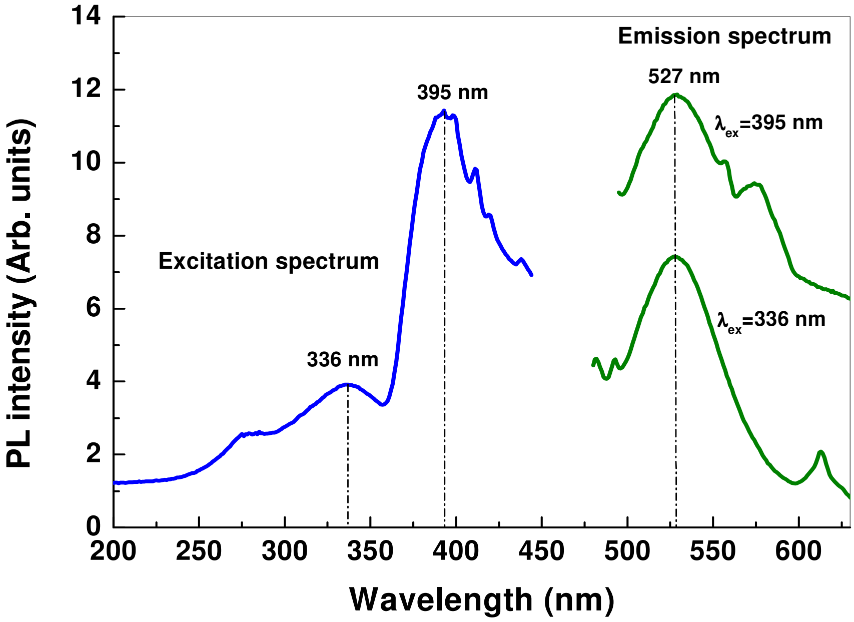

Fig. 3.4 Photoluminescence spectra of LTB:Mn. Excitation spectra were recorded by fixing the emission wavelength at 527 nm.

Excitation spectrum has two peaks at 336 and 395 nm corresponding to the 527 nm emission. Two emission spectra are recorded for excitations at 336 and 395 nm separately. Both the excitations produced broad emission peak at 527 nm but 395 nm excitation showed a minor peak around 580 nm also. These emission wavelengths are characteristic of Mn^{2+} ions in tetrahedral coordination (527 nm) and octahedral co-ordination (580 nm) [11]. The spectral position of the emission band can give information about the site symmetry of the Mn^{2+} ion. Based on ‘‘coordination number’’ concept, tetrahedrally coordinated Mn^{2+} ions emit yellow–green luminescence (band is near to 500 nm), while the octahedrally coordinated ones have luminescence in orange–red near 600 nm. Thus, from both the TL emission spectra and PL spectra it may be understood that Mn is present in both tetrahedral and octahedral co-ordination in the phosphors synthesized by solid state route. Those Mn ions which are present in octahedral co-ordination take part in TL emission process and those which are co-ordinated tetrahedrally are responsible for the photoluminescence emission.

3.2.5 Dose response: The gamma dose response was studied by irradiating the phosphors to gamma radiation from two different sources viz., Cs-137 and Co-60 for lower and higher doses respectively. The dose response studies were carried out only for Mn doped phosphor with dopant concentration showing the maximum TL intensity and having a higher glow peak temperature. In the case of LTB phosphors, dose response was studied for LTB:Mn (0.3 mol%) phosphor. The TL glow curves of the phosphor recorded for some representative doses are shown in Fig. 3.5 (intensities are not in same scale for comparison). It is observed that the temperature of the dosimetric peak shifts with dose to higher temperature up to a maximum of around 280°C and then back to lower temperature which is characteristic of non first order kinetics [12]. This is similar to what is reported for $CaSO_4$:Dy [13].The TL sensitivity of the phosphor is expressed in terms of the glow curve area per unit weight of the phosphor and per unit dose of radiation and is compared with that of LiF:Mg,Ti (TLD-100 Harshaw make). It is found that the sensitivity of LTB:Mn is 0.9 times that of TLD-100. TL intensity (area under the glow peak) vs absorbed dose for gamma rays of LTB:Mn phosphor is shown in Fig. 3.6.

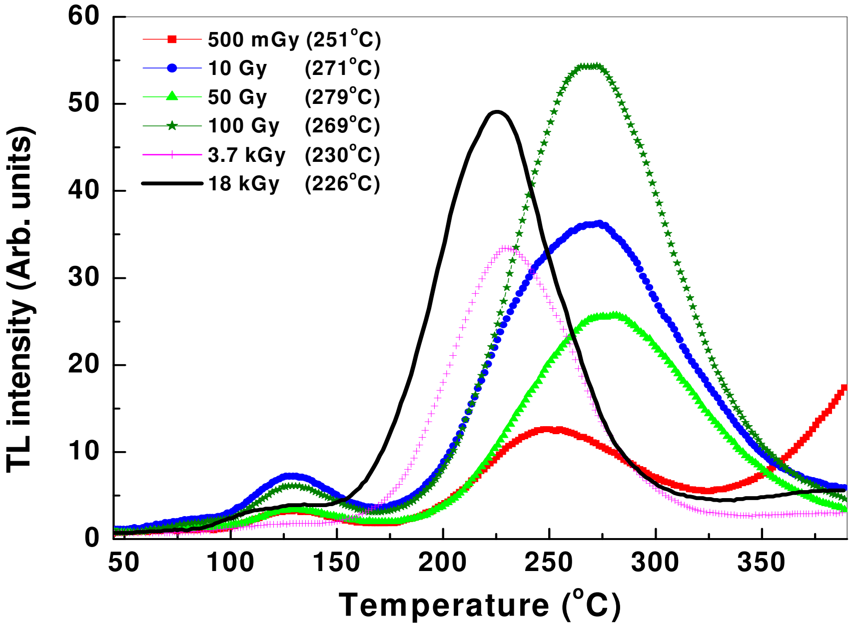

Fig 3.5. TL glow curves of LTB:Mn with gamma dose obtained with a heating rate of 5°C/s.

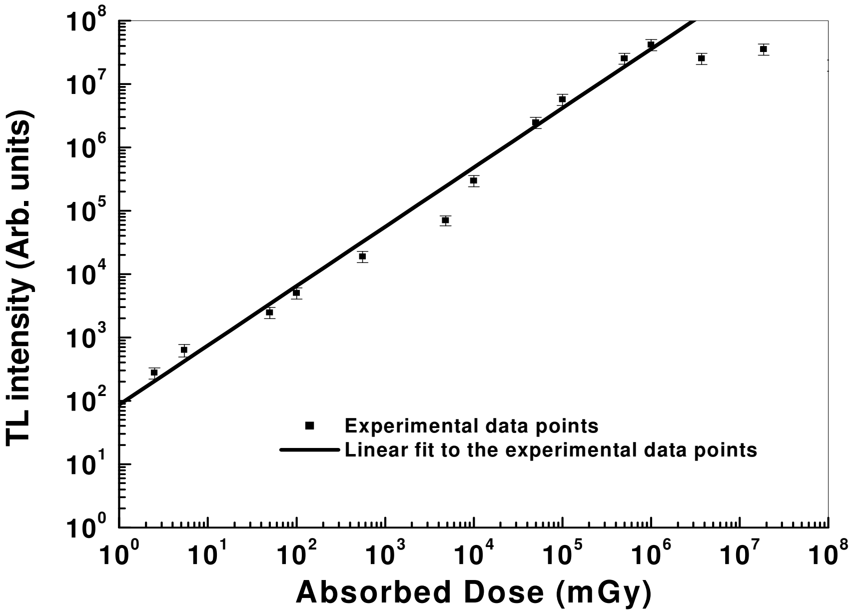

Fig. 3.6 Dose response of LTB:Mn phosphor. The straight line shows the linear fit to the data points. The slope of the straight line is close to unity.

The results show that the response of the phosphor appears to be linear 1 mGy to 10 Gy followed by a supralinearity till the saturation dose of 10^3 Gy. Langmead and Walls [14] reported the gamma response of 0.15 mass% Mn doped lithium borate powder to doses up to 10 Gy that was determined using a ^{137}Cs source and then repeated using ^{6o}Co γ-rays. Both sets of measurements produced virtually the same result, namely a linear TL response with dose up to about 0.5 Gy with a supralinear response above this dose level. This threshold is lower than that reported by others who have found thresholds of 3 and 30 Gy with lithium tetraborate produced elsewhere [14]. The Mn doping level may be a deciding factor on the threshold dose for supralinearity in LTB:Mn. For example, Pradhan et al. [15] observed a linear dose response up to 10^5 Gy for the high temperature glow peak in LTB: Mn,Si at Mn doping level 0.3 wt% rather than the usual 0.1 wt%.

3.4 Magnesium tetra borate (MgB_4O_7) based phosphors

Magnesium tetraborate phosphors doped with different rare earth dopants were synthesized by the simple solid state sintering. The synthesized phosphors were irradiated to a gamma dose using Co-60 gamma irradiation and the TL glow curves were recorded with a heating rate of 5°C/s. The TL glow peak of undoped MTB phosphor is around 210°C and that with different RE dopants except Gadolinium is around 190 - 225°C. For the case of gadolinium doped MTB phosphor, the glow peak is around 250°C. Hence, detailed dosimetric studies were carried out for MTB:Gd phosphor.

3.4.1 TL glow curve of MTB:Gd: The TL glow curves of gamma irradiated (2.14 Gy) magnesium tetraborate (MTB) doped with gadolinium and recorded with a heating rate of 5°C/s is shown in Fig. 3.7. Since Gd doped MTB phosphor showed TL peak at comparatively higher temperature around 250°C, detailed dosimetric studies were carried out in MTB:Gd. But the TL intensity was only 1/6th and 1/3rd of that doped with Dy and Tm (synthesized under the same conditions) respectively. No change in the shape or the dosimetric peak temperature of the glow curve was observed with dopant concentration variation but the intensity alone varied.

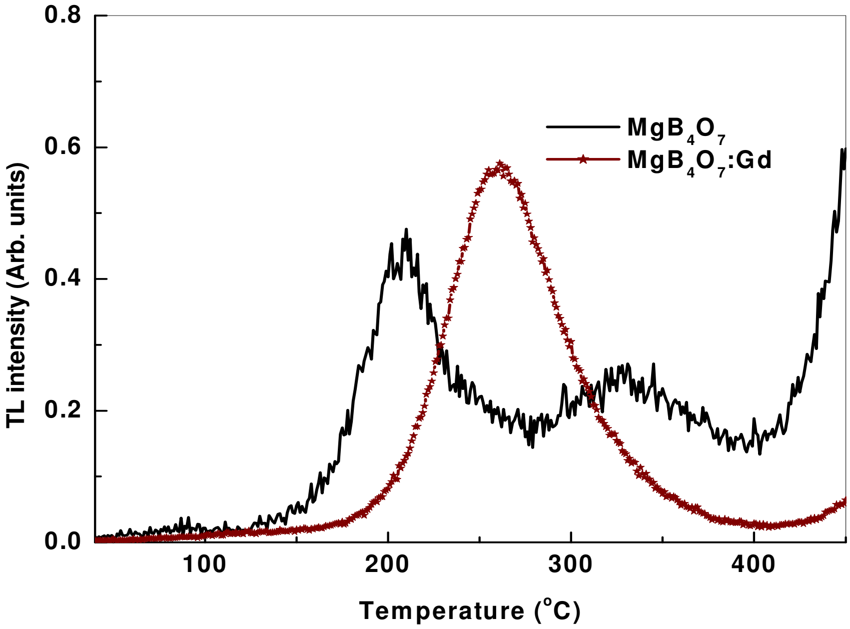

Fig. 3.7 TL glow curves of gamma irradiated (2.14 Gy) MTB:Gd phosphors. The data points of MTB are scaled up for better visibility.

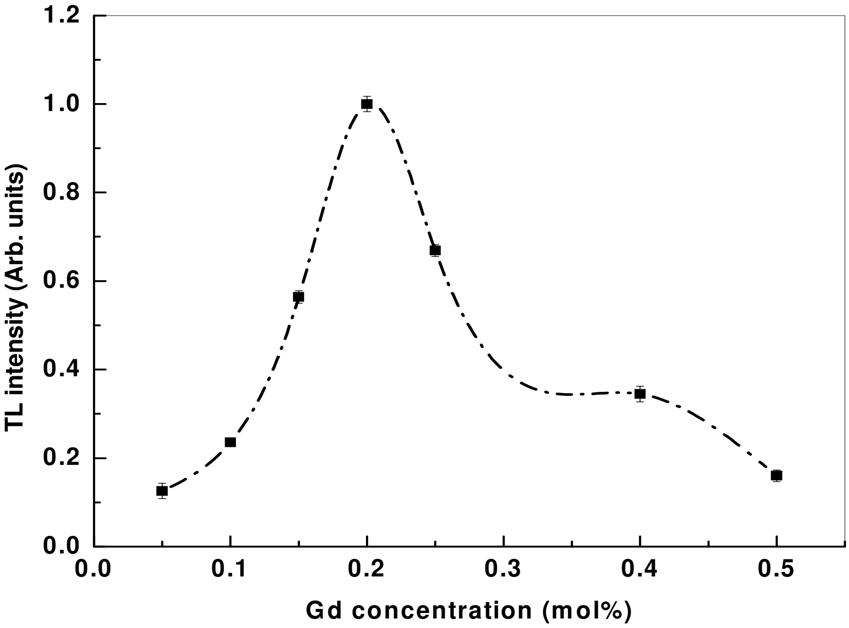

Fig.3.8 Variation of TL intensity with Gd concentration variation. The dotted line through the data points is a guide to the eye. The error bar is of the size of the data markers.(Dose delivered – 2 Gy, heating rate 5°C/s)

The TL intensity increases with dopant concentration variation upto a concentration of 0.2 mol% beyond which the TL intensity decreased due to concentration quenching. This can be viewed clearly from Fig. 3.8 which is a plot of dopant concentration versus TL intensity.

3.4.2 Effect of monovalent dopants: It is known from literature [16] that addition of monovalent dopants to RE doped TL phosphors increases the sensitivity. Hence the effect of monovalent dopants were studied in the RE doped magnesium tetraborate phosphors. It was observed that the TL intensity increased nearly 5 – 6 times upon doping MTB:Dy/Tm with monovalent dopants like Lithium. Similarly codoping monovalent dopants like Li, Na and silver with Gd, the TL peak intensity was found to enhance without change in peak temperature. Fig. 3.9 shows the TL glow curves of MTB:Gd codoped with monovalent dopants.

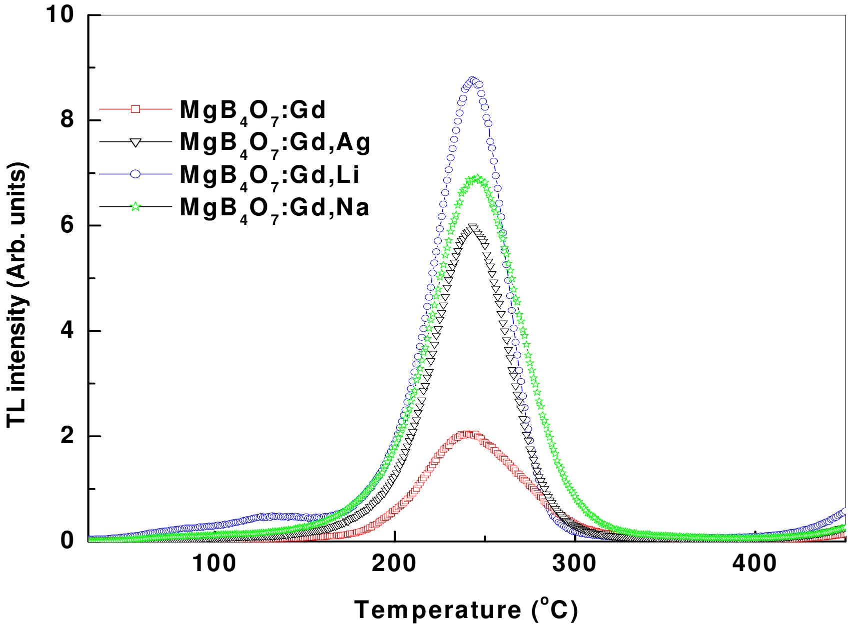

Fig. 3.9 Effect of monovalent dopants on the TL glow curves of gamma irradiated (2 Gy, heating rate 5°C/s) MTB:Gd phosphor

The increase was found to be more in the case of Li compared to other monovalent dopants. This increase in TL intensity is due to increase in the dissolution of dopants in the host lattice. Hence the effect of different concentration of monovalent dopant (Li) on the TL sensitivity of Gd doped MgB_4O_7 was studied. Fig.3.10 shows the effect of doping Li on the TL of MgB_4O_7:Gd. The TL intensity was found to be maximum for concentration of 0.3 mol% Li without change in the glow peak temperature. The TL sensitivity of MTB:Gd,Li is 5 times more than that of MTB:Gd for optimum concentrations of Gd and Li. Hence detailed dosimetric studies were carried out for MTB:Gd,Li (0.2, 0.3 mol%). The phosphors doped with Ag and Na showed slight coloration upon irradiation and readout and hence are not considered for further studies.

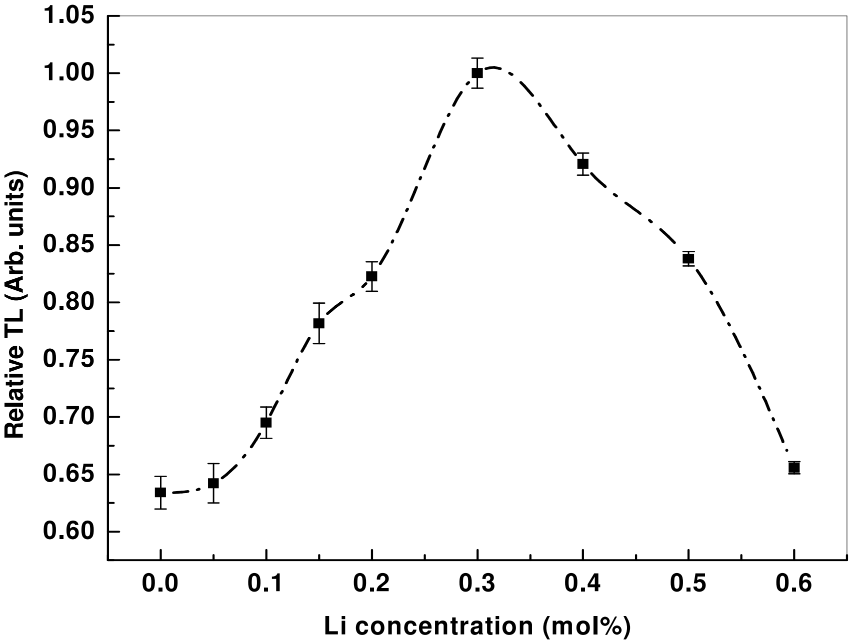

Fig. 3.10 TL sensitivity variation with Li concentration in MTB:Gd (0.2 mol%). The dotted line through the data points is a guide to the eye. (Dose delivered – 2 Gy, heating rate – 5°C/s)

3.4.3 TL and PL emission spectra of MTB:Gd: The TL emission spectra of undoped MTB, MTB:Gd and MTB:Gd codoped with monovalent dopants irradiated to a gamma dose of 21.4 Gy are shown in Fig.3.11. The TL emission is around 550 nm (greenish yellow) in all the cases, which shows that the emission is characteristic of host lattice and not of the dopants. The photoluminescence spectra (excitation and emission spectra) of Gd doped MTB phosphors are shown in Fig. 3.12. On excitation of the phosphor with 275 nm the emission characteristic of Gadolinium (Gd^{3+}) at 314 nm was observed.

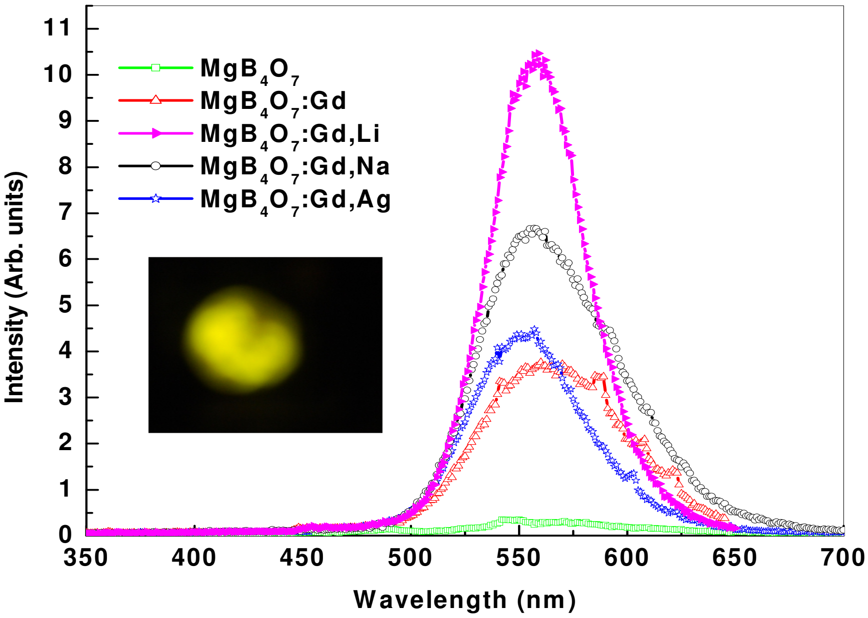

Fig. 3.11 TL emission spectra of gamma irradiated MTB:Gd and MTB:Gd with monovalent dopants. The inset shows the color of the light emitted.

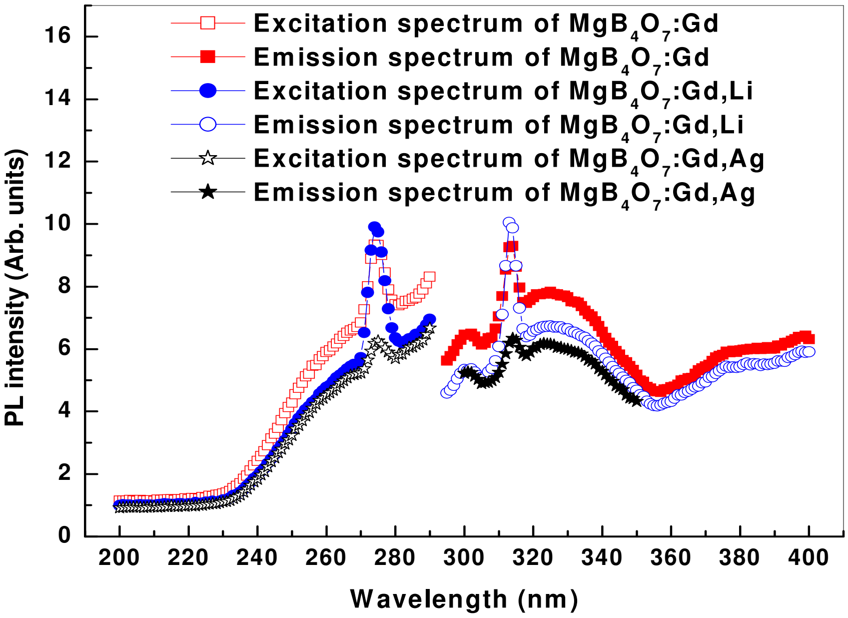

Fig.3.12 Excitation and emission spectra of MTB.

3.4.4 *Dose response:* Dose response studies were carried out for MTB:Gd,Li (0.2, 0.3 mol%) phosphors which has a relatively higher glow peak temperature and high intensity among all the Gd doped phosphors. Fig. 3.13 shows the TL glow curves of MTB:Gd,Li for different doses (Intensities are not to scale for comparison). The sensitivity of MTB:Gd,Li is compared with that of the standard TL phosphor. For this both MTB:Gd,Li and the standard phosphor TLD-100 (Harshaw make) were irradiated to the same dose and the area under the dosimetric peak is measured in both the phosphors. The TL sensitivity expressed in TL/mg/mGy was then estimated and the sensitivity is almost 5 times that of standard TLD-100. The response of the phosphor is studied in the dose range of 1 mGy to 10^3 Gy to study the range of linearity of the response. Fig. 3.14 shows the dose response curve for MTB:Gd,Li. This range is very much suitable for clinical and environmental dosimetry.

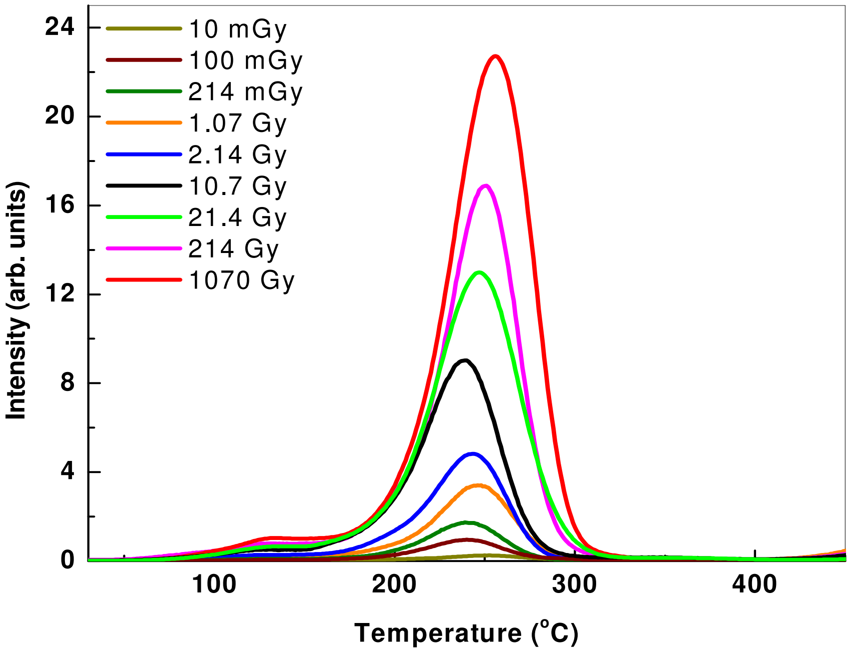

Fig. 3.13 TL glow curves of gamma irradiated MTB:Gd,Li(0.2, 0.3 mol%)

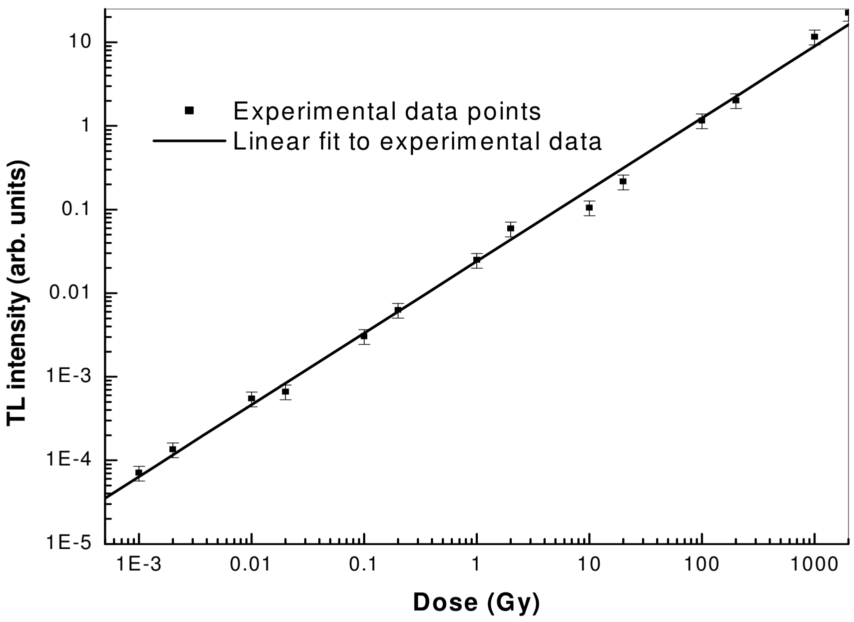

Fig. 3.14 Dose response of MTB:Gd,Li. The errors in the measurements are of the size of the markers used to represent data points. The straight line corresponds to the linear fit to the data points. The slope of the line is close to unity.

3.5 Zinc metaborate (ZnB_2O_4) based phosphors

Zinc metaborate (ZMB) TL phosphors doped with different rare earth elements were synthesized by simple solid state sintering technique. The TL glow curves of the synthesized phosphors were recorded after gamma irradiation at a heating rate of 5°C/s.

3.5.1 TL Glow curve with different dopants: TL glow curves of different RE doped Zinc metaborate (ZMB) along with Mn doped ZMB is shown in Fig. 3.15. From the figure it is clear that all RE doped ZMB phosphors have a similar glow curve structure with two glow peaks one at around 165°C (peak 1) and the other at around 300°C (peak 2) whereas Mn doped ZMB also has two glow peaks but peak 2 appears at around 250°C. Of the two peaks, peak 2 which is at a high temperature can be considered to be the dosimetric peak. The intensity of peak 2 is less than that of peak 1 in the case of Mn doped phosphor and hence, is not considered for detailed studies. Among the different RE doped ZMB phosphors, the intensity of peak 2 is higher for Tm doped phosphor and hence, detailed dosimetric characterization was carried out for this phosphor. The TL glow curves of undoped ZMB and Tm doped ZMB along with the standard $CaSO_4$:Dy (synthesized by co-precipitation technique) irradiated to the same gamma dose (3 Gy) and recorded with a heating rate of 5 °C/s is shown in Fig. 3.16.

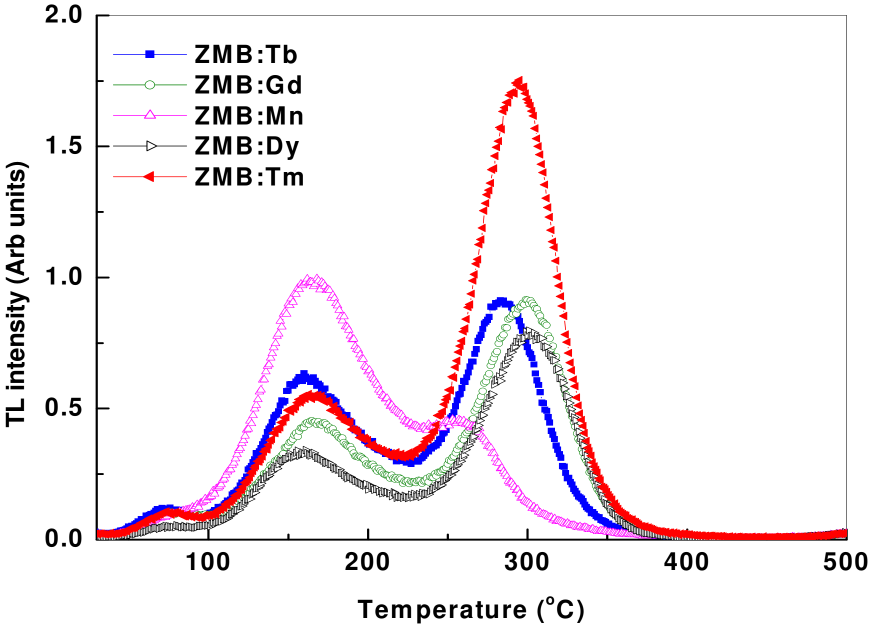

Fig. 3.15 TL glow curves of RE doped ZMB along with Mn doped ZMB phosphor (dose delivered – 2.14 Gy, heating rate 5°C/s)

Here $CaSO_4$:Dy was chosen as a standard to compare the sensitivity because of the higher effective atomic number of ZMB phosphor. From the figure it is clear that, in undoped ZMB, the TL intensity is very less compared to the Tm doped ZMB. This shows that the addition of thulium has increased the concentration of the traps responsible for TL. Comparing the TL intensities (height of peak 2) of ZMB and $CaSO_4$:Dy, it can be seen from the figure that the peak height of ZMB:Tm is 0.6 times that of $CaSO_4$:Dy. But from the glow curve structure one can observe that $CaSO_4$:Dy has very broad peak with overlapping satellite peaks on both sides of the dosimetric peak whereas for ZMB, the glow peaks are well separated and hence, it is easier to isolate a single peak for dosimetric applications.

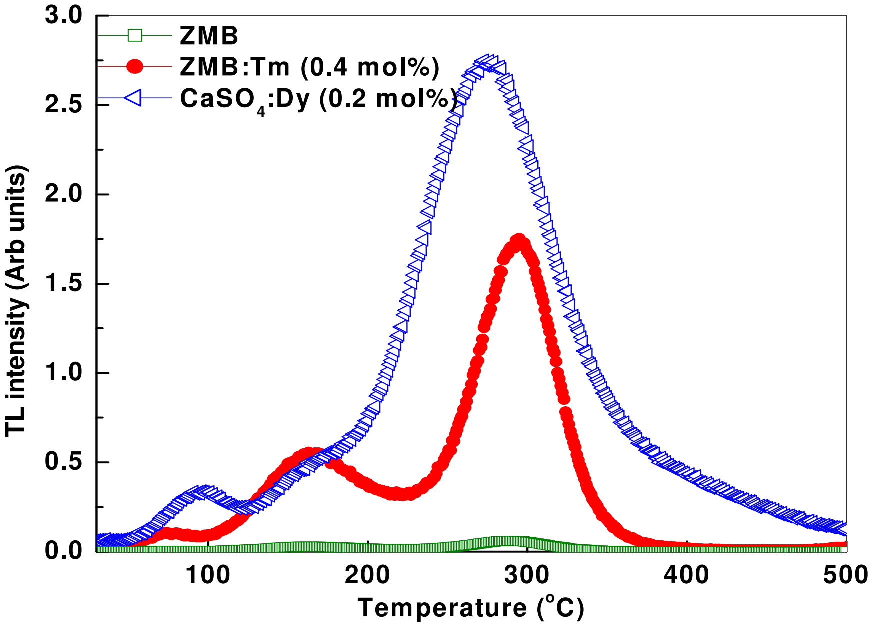

Fig. 3.16 TL glow curves of undoped and Tm doped ZMB in comparison with CaSO$_4$:Dy (dose 3 Gy, heating rate 5°C/s)

3.5.2 Glow curve variation with concentration of dopant (Tm): The TL intensity was found to vary with the concentration of dopant added in all RE doped phosphors.The variation of TL intensity with Tm concentration is shown in Fig. 3.17.

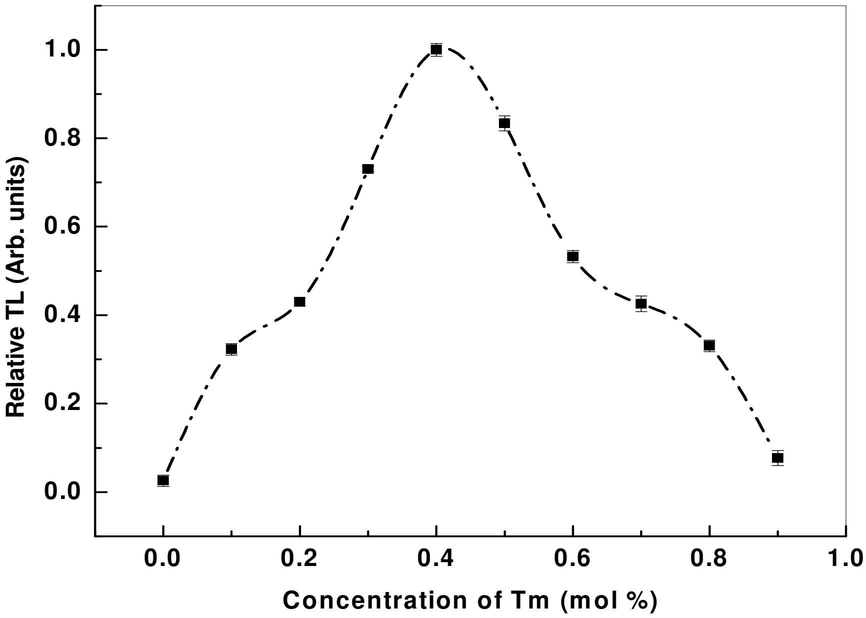

Fig. 3.17 Variation of TL intensity with dopant (Tm) concentration in ZMB phosphors. The dotted line through the data points is a guide to the eye. The error bars are the standard deviations of the different measurements against each data points.

Only the intensity of the glow peaks varied with Tm concentration, but the glow peak structure remained the same. The glow peak intensity is found to increase upto a dopant concentration of 0.4 mol% beyond which there is a decrease corresponding to concentration quenching as shown in Fig. 3.17. Hence, sample with 0.4 mol% of thulium was used for further dosimetric characterization.

3.5.3 TL and PL emission spectra: TL emission spectra recorded for gamma irradiated (6 Gy) undoped and Tm doped ZMB phosphor is shown in Fig. 3.18.

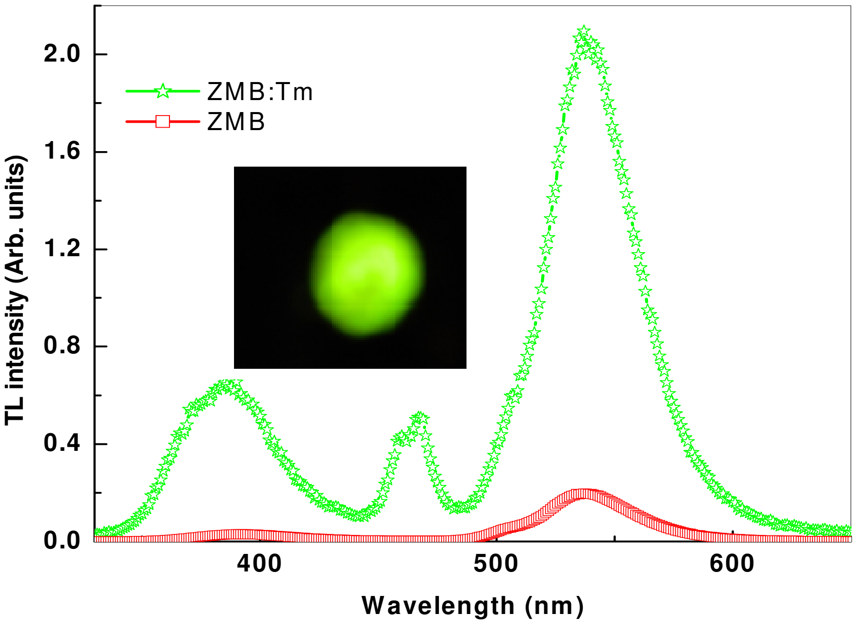

Fig. 3.18 TL emission spectra of gamma irradiated (6 Gy) Tm doped Zinc meta borate. The inset shows the color of the light emitted.

The TL emission centers correspond to two wavelength regions one around 390 nm and the other around 535 nm in undoped and Tm doped ZMB phosphors are characteristic of the host lattice and not of the dopant. The increase in intensity of TL with the addition of dopant shows that the dopant, though directly do not act as the recombination center, helps in increasing the concentration of defect centers (traps) responsible for TL.

The emission at 535 nm (green emission) corresponds to the oxygen vacancy related defect centers [17,18].The photoluminescence excitation and emission spectra of ZMB:Tm phosphor are shown in Fig. 3.19. Both the excitation and emission spectra are characteristic of the rare earth dopant thulium. In the case of TL emission spectra the emission is characteristic of host lattice for all RE dopants but for Tb.

3.5.4 Dose response: In the case of zinc borate, the phosphor ZMB:Tm (0.4 M%) was used for studying the dose response. The phosphor was irradiated to different doses of gamma radiation using Co-60 and Cs-137 sources.

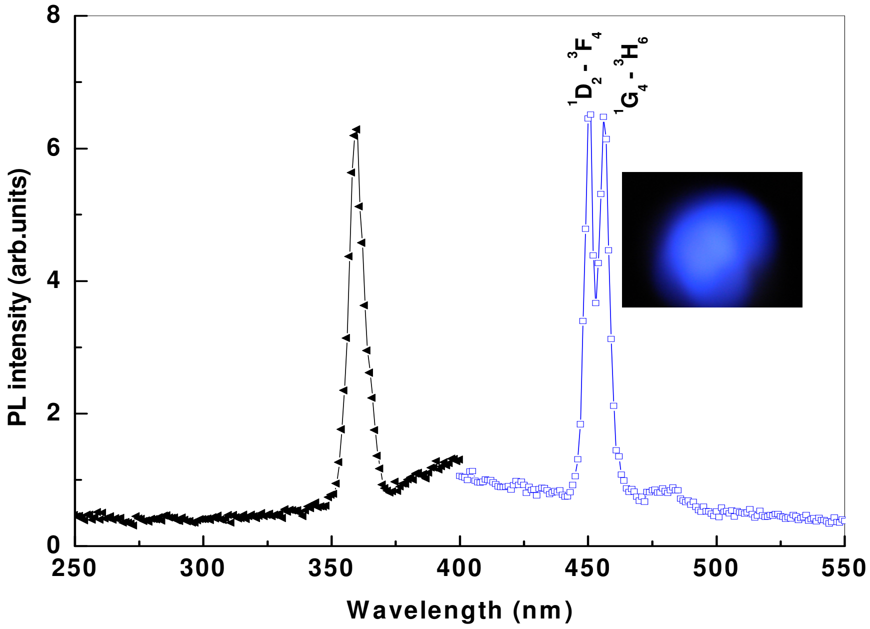

Fig. 3.19 PL excitation and emission spectra of Tm doped Zinc borate phosphors. The inset shows the color of the emission spectra.

The irradiated phosphors were heated linearly at a heating rate of 5°C/s and the area under the dosimetric peak (peak 2) was considered to determine the sensitivity. The sensitivity was found to be around 25 times that of TLD-100. The variation of TL glow curves with dose is shown in Fig. 3.20. The peak structure remains the same for all dose ranges from 10 mGy to 10^3 Gy. The dosimetric peak position varies slightly with dose which is a characteristic of non-first order kinetics. The photon dose response curve for ZMB:Tm is shown in Fig. 3.21. It shows that the response is linear over a wide range from 0.1 mGy to 10^3 Gy. This range is suitable for routine personnel dosimetry applications.

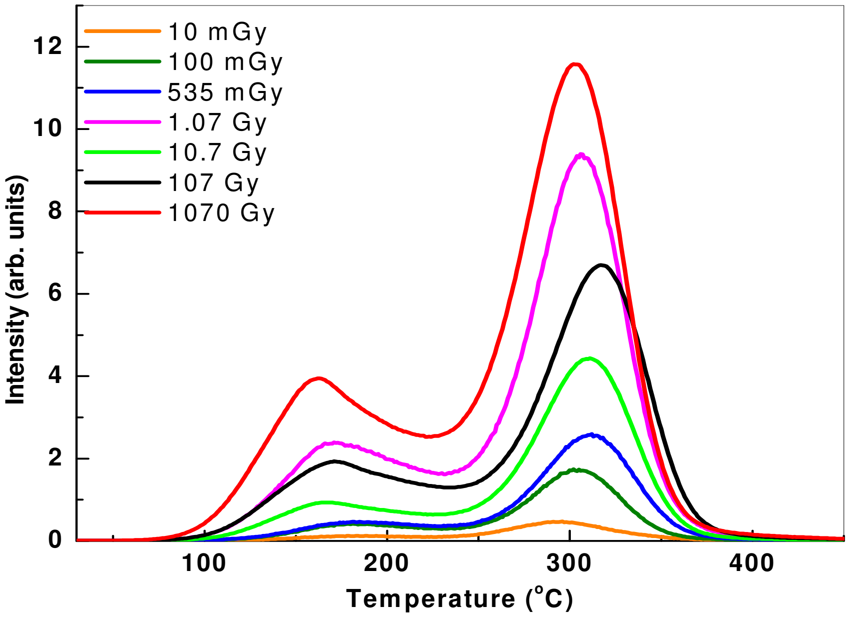

Fig. 3.20 Variation of TL glow curves with gamma dose. (heating rate 5 °C/s). The phosphors were irradiated to different doses and all measurements were carried out at the same time by adjusting the filters.

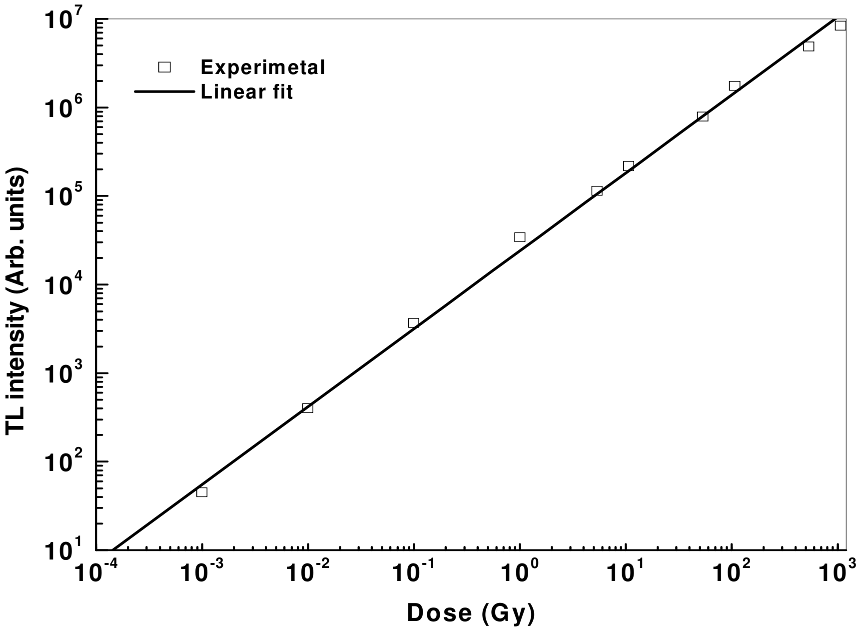

Fig. 3.21 Gamma dose response of ZMB:Tm phosphor. The error bar is of the size of the marker. (heating rate 5°C/s).The straight line is the linear fit to the data points. The slope of the line is close to unity.

3.6 Cadmium tetraborate (CdB_4O_7) based phosphors

3.6.1 TL glow curve: The TL glow curves of the cadmium tetraborate phosphor recorded after gamma irradiation is shown in Fig. 3.22.

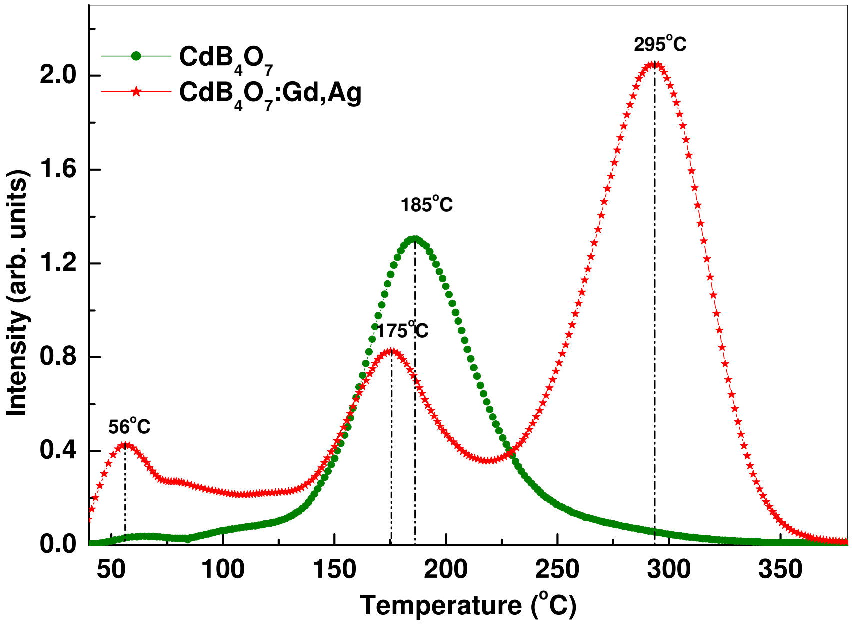

Fig. 3.22 TL glow curve of Cadmium tetraborate phosphors. (Dose delivered – 1 Gy, heating rate – 5 °C/s)

It is observed that, undoped cadmium borates CdB_4O_7 have a single peak around 185°C whereas for CdB_4O_7 doped with Gd and Ag, a new intense high temperature peak was observed around 295°C. The γ- ray sensitivity of the undoped phosphor is found to be twice of TLD-100 (Harshaw make). The phosphors doped with Gd and Ag showed coloration upon irradiation and/or storage due to the oxidation of Ag and hence detailed investigations have not been considered in the thesis.

3.6.2 TL and PL emission spectra: TL emission spectra of cadmium borate phosphors were recorded after irradiating the phosphors to a dose of 10 Gy with Co-60 gamma source. The emission occurred at a wavelength of about 515 nm (green emission) for cadmium tetraborate. When cadmium tetraborate was doped with Gd and Ag, the emission was around 515 nm which is characteristic of the host lattice only and not of the dopants. Fig.3.23 shows the TL emission spectra of the cadmium borate phosphors, while Fig. 3.24 shows the PL excitation and emission spectra of cadmium tetraborate. When UV light of wavelength 258 nm was shined on CTB phosphor an intense red emission was observed as shown in the inset of Fig. 3.24.

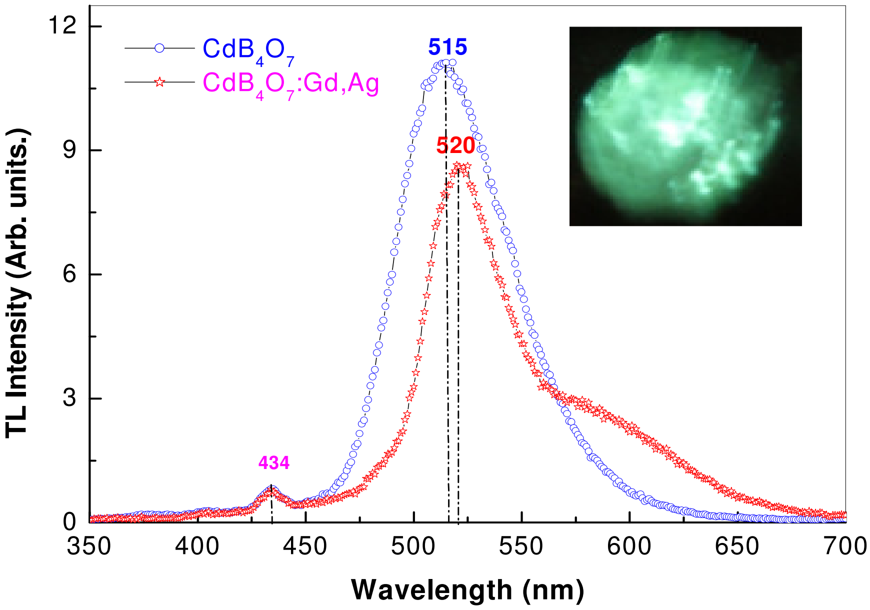

Fig. 3.23 TL emission spectra of Cadmium borate phosphors. The inset shows the color of the light emitted. (Dose 10 Gy)

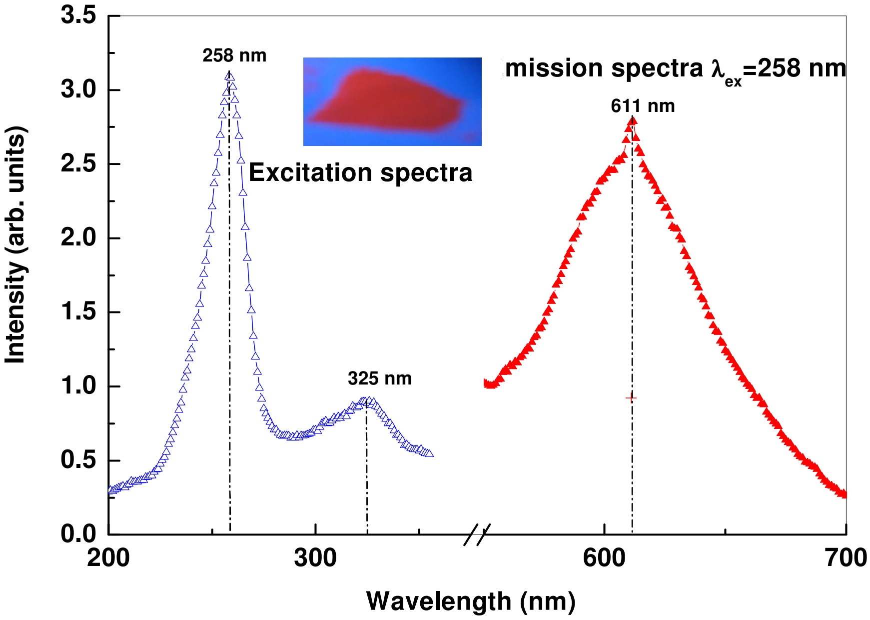

Fig. 3.24 PL excitation and emission spectra of CTB. The inset shows the color of the emission when the phosphor is shnined with UV light of wavelength 256 nm.

3.6.3 Dose response: In the case of cadmium borate, the dose response was studied for undoped cadmium tetra borate. This is because, doped cadmium borate (doped with Gd and Ag) showed coloration upon irradiation and read out. But undoped cadmium borate did not show any coloration upon irradiation or read out. To study the dose response, the phosphor was irradiated to different doses of gamma radiation using Co-60 and Cs-137 sources. The irradiated phosphors were heated linearly at a heating rate of 5°C/s and the area under the dosimetric peak was considered to determine the sensitivity. The sensitivity was found to be around 2 times that of TLD-100. The photon dose response curve for cadmium tetraborate phosphor is shown in Fig. 3.25. It is found that the response is linear from 0.1 mGy to 10^3 mGy beyond which saturation sets in.

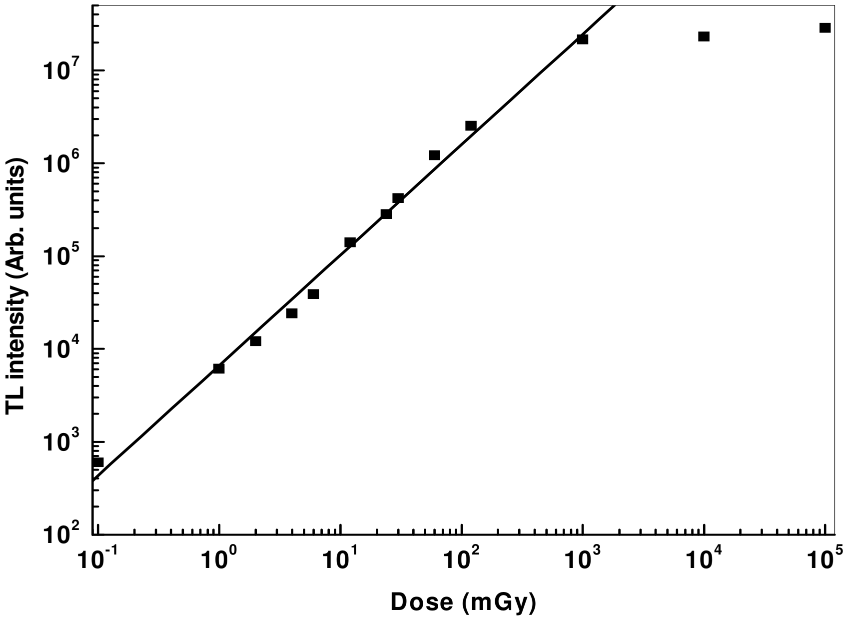

Fig.3.25 Photon dose response curve for cadmium tetraborate. The slope of the straight line fit to the data is close to unity.

The comparison of important TL characteristics of borate based phosphors synthesized by solid state sintering along with standard phosphors $CaSO_4$:Dy (Co-precipitation technique) and TLD-100 (Harshaw make) is shown in table 3.1.

Table 3.1: Important TL characteristics of borate based phosphors

Sl. No.	Material	Effective atomic number	Dosimetric peak temperature (°C)	TL emission wavelength (nm)	Dose linearity	Min. detection threshold (µGy)
1	$Li_2B_4O_7$:Mn	7.25	270	580	1 mGy – 10 Gy	250
2	MgB_4O_7:Gd,Li	8.37	250	550	1 mGy – 10^3 Gy	20
3	ZnB_2O_4:Tm	22.45	300	535	10 mGy – 10^3 Gy	6
4	CdB_4O_7	34.83	185	515	0.1 mGy - 1 Gy	30
5	TLD - 100*	8.2	200	400	20 µGy – 10 Gy	20
6	$CaSO_4$:Dy*	15.3	230	480, 570	2 µGy – 10 Gy	2

***-** Values reported in literature for HARSHAW 2000 TL Analyser.

Minimum detection threshold was determined by computing 2.57 × σ, where σ is the standard deviation of the zero dose reading of phosphor (unirradiated phosphors) measured in dose units. This value depends on the type of reader used for the measurements. The values listed above are for RISO TL/OSL reader (Model DA-20).

3.7 Annealing and Reusability studies

Reusability is one of the most important properties that any dosimetric material should possess. In order to reuse the phosphor, the residual TL due to any previous irradiation followed by measurement should be removed. Thermal annealing is normally used to remove the residual TL before the reuse of the phosphor. This thermal annealing can change the defect distribution of the phosphor and thereby alter its sensitivity in some phosphors if annealing is not carried out at optimum temperature. For this, both the annealing temperature and the duration for which the phosphor has to be annealed should be known. This was determined by first fixing the duration of annealing and varying the temperature of annealing from 200 to 600°C in steps of 50°C. The residual TL was measured after each step and the temperature at which no residual TL was found is determined. Next the duration for which the sample is to be annealed was determined by fixing the determined annealing temperature and varying the annealing duration. By this the optimum condition of annealing the phosphor for reuse can be determined. The optimum condition of annealing for reuse of the phosphors studied is given in Table 3.2.

Table 3.2 Optimum condition for reuse of phosphors

Sl.No.	Material	Annealing temperature	Time	No. of cycles tested
1	LTB:Mn	500˚C	½ h	12
2	MTB:Gd,Li	250˚C	½ h	12
3	ZMB:Tm	400˚C	½ h	10
4	CTB	300˚C	1 h	6

In order to check the number of cycles the phosphor can be used without loss in sensitivity, freshly prepared sintered phosphor powder was irradiated to known dose (~ 1 Gy) and resultant TL was recorded. This phosphor was annealed at the optimum condition determined and was irradiated to the same dose to measure the TL intensity. This process was repeated at least for 10 cycles for each phosphor. No change in TL intensity or glow peak shape has been observed even after the specified number of cycles of annealing, irradiation and read out listed in table 3.2. The variation of TL intensity after different cycles of irradiation, anneal and read out is shown in Fig.3.26.

3.8 Fading

3.8.1 Storage stability: Post irradiation storage stability of the dosimeter is one of the important characteristics in the choice of a material for dosimetric applications. Thus, it is necessary to assess if the trapped charges in the phosphor can be lost before readout by thermal, optical or by any other anomalous fading. To check the post-irradiation storage stability the phosphors were irradiated to a known dose at different intervals of time up to a period of minimum three months and stored at ambient conditions. The TL measurements were carried out on a single day in order to avoid any fluctuations due to reader performance. The results of the measurements are shown in Fig.3.27

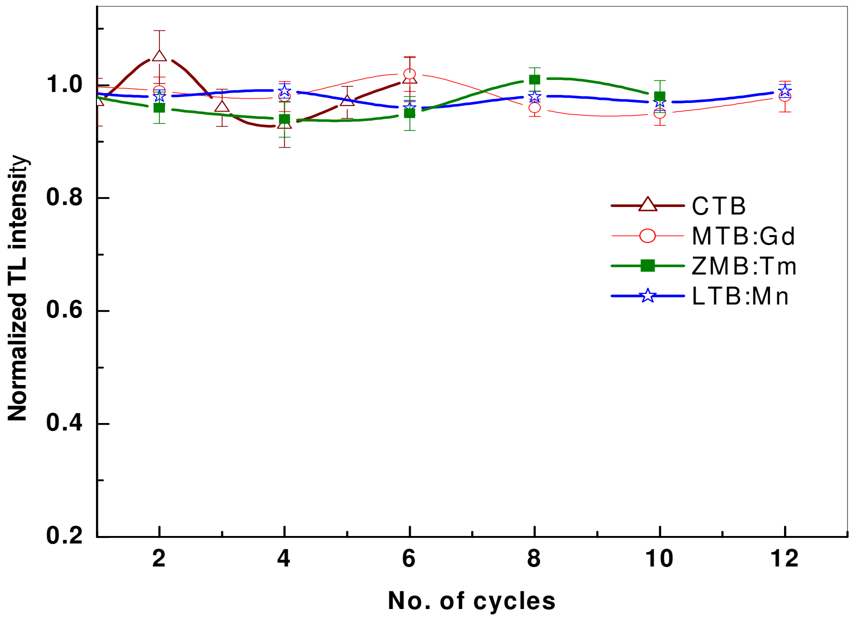

Fig. 3.26 Variation of TL sensitivity of borate based phosphors after different cycles of annealing and read out. The line across the data points is a guide to the eye.

3.8.2 Light induced Fading: Some TL phosphors when exposed to sunlight or to florescent lamps or other light sources may lose part of its signal by stimulation of the trapped charges by light photons. To study the light induced fading two sets of samples from each phosphor was irradiated to a known dose and one was packed separately in black paper and other one was kept open in room light of intensity 545 lux. Similarly to study the effect of sunlight, two sets of samples were irradiated to a known dose and one set of samples was kept open in sunlight and the other set was covered in black paper and kept along with it.

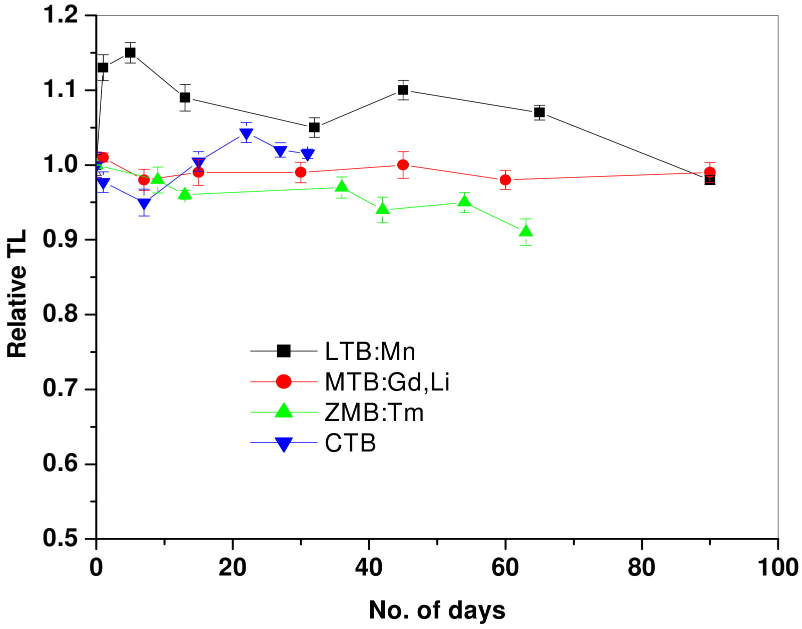

Fig. 3.27 Storage stability of borate based phosphors. The solid lines through the data points are the guide to the eye. The error bar shown is the standard deviation of the measurements carried out to generate each data point.

Table 3.3 shows the result of the TL signal lost due to storage in different conditions. Fading of TL signal can occur in TL phosphors by optical excitation of charge from the traps. Absorption of photons of energy above optical trap depth will result in the release of trapped charge and corresponding reduction in the TL signal. Opposite to the optical fading effect is the induced TL by the exposure to light. There are two models to understand the light induced TL in the TL materials which are high band gap insulators using light energy less than the energy of the band gap. In first model, photons may be absorbed by electrons in localized energy levels situated below the Fermi level. The optically freed electrons may then become trapped at other empty localized states residing above the Fermi level. From the resultant non-equilibrium state TL may result when the sample is heated. Such a process has been kinetically modeled by Chen et al. [19]. The other model is the photo transferred TL (PTTL) involves the transfer of charge from deep states into dosimetry traps during optical absorption. Since in $Li_2B_4O_7$:Mn phosphor no high temperature glow peaks are observed the possibility of PTTL can be ignored. First model may be a possible cause of TL growth in irradiated $Li_2B_4O_7$:Mn during light exposure. Further studies are needed to fully explain the phenomena and it is in progress.

Table 3.3. Loss of TL signal of gamma irradiated phosphors upon exposure to light

Material	Condition	Loss of signal		
		1 h	3 h	5 h
LTB:Mn	Black paper and kept in room light	Negligible		
	Open in room light			
	Black paper in sunlight	Negligible		
	Open in sunlight	No loss of signal but there was a slight increase of TL		
MTB:Gd, Li	Black paper and kept in room light	2%	2%	3%
	Open in room light	38%	45%	63%
	Black paper in sunlight	73%	76%	75%
	Open in sunlight	90%	100%	
ZMB:Tm	Black paper and kept in room light	Negligible (< 1%)		
	Open in room light	2%	7%	10%
	Black paper in sunlight	Shape of the glow curve changed (both the peaks merged due to PTTL)		
	Open in sunlight			
$CaSO_4$:Dy	Black paper and kept in room light	Negligible		
	Black paper in sunlight	6%	6%	7%
	Open in sunlight	16%	17%	16%

Furetta and Pellegrini [20], on storage fading studies in $Li_2B_4O_7$:Mn material reported an initial fall in TL during the first 17 days, and latter showed a sort of recovery. A growth for peak 5 is reported for the LiF:Mg,Ti phosphor for initial period of storage and showed fading for longer duration. The height of the peak 5 is shown to increase with increasing time between irradiation and readout (about 20% increase in 100 days of storage) as result of peak conversion from peak 4 to 5 in reader–annealed TLD-700 [21]. Delgado et al., [22] observed a similar increase in peak 5 and decrease peak 4 for reader-annealed TLD-100. No change was observed in the response of peak 5 for dosimeters annealed at 400°C. Fading is humidity dependent for all the forms of $Li_2B_4O_7$ studied. It is reported that in $Li_2B_4O_7$:Mn 10% fading at 0% relative humidity increasing to 40% fading at 95% relative humidity for 90 days storage at 20°C [6].

3.8.3 Effect of UV light: To study the effect of UV on shape and intensity of TL, irradiated phosphors were exposed directly to UV light of wavelength 356 nm. Table 3.4 shows the result of the exposure of irradiated phosphors to UV radiation at different time intervals.

Table 3.4 Loss of TL signal in gamma irradiated phosphors upon exposure to UV light of different duration

Material	UV of wavelength 356 nm		
	1 h	3 h	5 h
LTB:Mn	6%	9%	15%
MTB:Gd, Li	100%	No TL	
ZMB:Tm	5%	6%	5%

In the case of MTB:Gd,Li, for samples exposed directly to UV light of wavelength 356 nm, no signal was left just after one hour of storage. Thus, it can be concluded that the UV component of sunlight is responsible for the large amount of fading of TL signal upon exposure to sunlight.

3.9 Conclusions

In this chapter the dosimetric properties of various borate based TL phosphors are discussed.

(a) Lithium borate is important from the point of view of tissue equivalence. The phosphor with Mn dopant prepared by solid state sintering technique showed a dosimetric peak at 270°C, which is an important characteristic of dosimetry material. This phosphor has been found to be reusable after a simple post irradiation annealing at 500°C for 30 minutes. It has a TL sensitivity almost equal to TLD-100 (which is difficult to prepare and has a very complicated annealing procedure for re-use, compared to the simple annealing for lithium borate). $Li_2B_4O_7$: Mn has high post irradiation storage stability; negligible loss of signal has been observed when the phosphor is stored for even 90 days after irradiation. The dopant was incorporated in the form of carbonate in the matrix so that the deliquescent nature of the phosphor was avoided which was a problem reported by earlier workers. Moreover the room light sensitivity is negligible which makes it a good candidate for laboratory measurements. The loss of TL signal under UV light of 356 nm for about 3 hrs has been found to be less than 10%. Hence, this phosphor is a potential replacement for TLD-100 for dose measurement involving low energy gamma /X-rays.

(b) Magnesium borate doped with rare earths (mainly Dy and Tm) has been reported by various groups in the past. But in the present work, the detail TL characteristic of Gadolinium doped MgB_4O_7 has been carried out for the first time. The most important characteristic of this phosphor is that the TL glow peak temperature of this phosphor is at 250°C, which is high compared to other rare earth doped MgB_4O_7. Other main RE dopants studied in MgB_4O_7 (Tm and Dy) though had a better sensitivity, the peak temperatures were much less compared to Gd doped MgB_4O_7 resulting in high fading. Moreover, the TL sensitivity could be enhanced by the addition of monovalent dopants like Ag and Li which did not alter the TL emission wavelength as well as peak temperature. Yet another salient feature of this phosphor is that the emission spectra were characteristic of the host lattice though the monovalent dopants enhanced the TL sensitivity of MgB_4O_7:Gd. The TL sensitivity of MgB_4O_7:Gd is almost same as that of TLD-100 (Harshaw make), and its tissue equivalence is almost near to that of human tissue. However, MgB_4O_7:Gd,Li has a TL sensitivity almost 5 times that of TLD-100 (Harshaw make). The linearity range was up to 10^3 Gy compared to $Li_2B_4O_7$:Mn and TLD-100 (10 Gy). Though it suffers a high light induced fading, the phosphor could be used for dosimetry application where the dose measurements have to be carried out immediately after irradiation by keeping the phosphor covered in black paper. The phosphor could be reused after annealing it at 250°C for 30 min to remove the residual signal

(c) Zinc meta borate doped with different rare earth was studied for a possible enhancement of TL sensitivity as well as post irradiation storage stability. But the TL emission was characteristic of the host lattice in the case of all rare earth doped Zinc meta borate except Tb^{3+}. Out of the all rare earths studied, Tm^{3+} doped samples showed maximum TL sensitivity though its emission was characteristic of the host lattice. The TL sensitivity was found to be highest for a dopant concentration of 0.4 mol%. The phosphor ZnB_2O_4:Tm has linear dose response up to 10^3 Gy. Negligible fading of TL signal was observed when the phosphor was covered in black paper and stored in room light after irradiation. Though the post irradiation storage stability was good (less than 10% of signal only was lost in open room light when stored for 3 hrs), the two peaks of the glow curve merged when kept in sunlight due to photo transferred thermoluminescence. This phosphor could be reused by a simple post irradiation annealing of 400°C for 30 m duration.

(d) Cadmium borate (CdB_4O_7) has not been studied earlier from the point of view of thermoluminescence. The Mn activated cadmium borate ($Cd_2B_2O_5$) has been reported to exhibit four distinct peaks at 383˚C, 488˚C, 643˚C and 678˚C upon UV irradiation and low temperature measurements. Hence cadmium borate was studied to check if its TL peak temperature can be altered from the point of view of stability. Undoped cadmium borate was showing a main TL around 185°C. Hence rare earths were doped in cadmium borate to check if its sensitivity could be enhanced. Out of all rare earths Gd showed the maximum sensitivity though the TL peak was around 295°C with a decrease in TL intensity of the peak at 185°C. Hence TL glow curve was studied by codoping with monovalent dopant Ag. Similar to the case of MgB_4O_7:Gd,Ag there was an enhancement of TL of both the peaks. But the doping of rare earth and Ag gave rise to coloration to the phosphor. Hence further studies were not carried out in this direction. Solid sate diffusion reaction in inert atmosphere may improve the physical appearance of the phosphor along with enhancement of TL which is being investigated. The post-irradiation storage studies have shown that no TL signal was lost during post irradiation storage duration of 30 days. The phosphor was found to be reusable with a simple post irradiation annealing of 300°C for 1 h.

A detailed study of various borate based phosphors viz., LTB:Mn, MTB:Gd,Li, ZMB:Tm and CTB is presented in this chapter and the merits and demerits are discussed.

3.10 References

[1]. Guide to RISO TL/OSL Reader, RISO DTU, Denmark (2008)

[2]. Operation and Maintenance manual – Flourolog-3 with Datamax, Jobin Yvon-SPEX, Instruments S.A., Inc (1996)

[3]. Peter R.A., Kenneth Mccray, David Espejo,. American J of Roentgenology, 108, (1970) 197.

[4]. Holovey, V.M., Sidey, V.I., Lyamayev, V.I., Birov, M.M., J. of Phys. and Chem. of Solids, 68, 2007, 1305.

[5]. Holovey, V.M., Lyamayev, V.I., Birov, M.M., Puga, P.P, and Solomon, A.M., Func. Mater. 12, 2005, 318.

[6]. Horowitz, Y. S., 1984. Thermoluminescence and thermoluminescent dosimetry. CRC Press, Inc. Boca Raton, Florida, Vol. 1, 126-132.

[7]. Magdalyna Ignatovych, Mauro Fasoli, Andras Kelemen, Radiat. Phys. Chem 81 (2012) 1528

[8]. Gedam S.C., Dhoble S.J., and Moharil S.V., J. Lumin., (2006), 121, 450

[9]. Ellis, Rossiter,. Int. J. Appl. Radiat. Isot., 20, (1969), 201

[10]. Zhydachevskii Ya., Dyrugin A., Suchocki A., Matkovskii A., Sugak D., Bilski P., Warchol S., Nucl. Instrum. Methods Phys. Res. Sect. B 227, (2005) 545

[11]. Ignatovych, M., Holovey, V., Vidoczy, T., Baranyai, P., Kelemen, A., Radi. Phys. and Chem. 76, (2007), 1527.

[12]. Chen, W. Yang, B., Jia, S.W., J. of Synth. Cryst. 30, 2001, 79.

[13]. Srivastava, J.K., Supe, S.J., Nucl. Instrum .and methods. 160, 1979, 529.

[14]. Langmead, W.A., Walls, B.F., Phys. Med. Biol. 21, 1976, 39- 51.

[15]. Pradhan, A.S., Bhatt, R.C., Supe, S. J., Int. J. Appl. Radiat. Isot., 31, 1980, 671-674

[16]. Mirjana Prokic, Applied Radiation isotopes 52 (2000) 97

[17]. Hoogsenstraten W., Philips Res. Rep., vol -13, (1958), 515.

[18]. K.Vanheusden, C.H. Seager, W.L. Warren, D.R. Tallant and J.A. Voigt, Appl. Phys. Lett. 68 (3), 1996, 403.

[19]. Chen R., Hornyak W.F., and Mathur V.K., J. Phys. D: Appl. Phys. 23, 1990, 724

[20]. Furetta C. and Pellegrini R., Radiat. Eff. Letters 58, 1981, 17

[21]. Moscovitch, M., Szalasnczy, A., Bruml, W.W., Velbeck, K.J., Tawil, R.A.,

Radiat. Prot.Dosim. 34, 1990, 361.

[22]. Delgado, A., Gomez Ros, J.M., Muniz, J.L., Bos, A.J.J., Piters, T.M., Radiat. Prot. Dosim. 47, 1993, 231.

CHAPTER - 4

KINETIC PARAMETERS FROM TL GLOW CURVES

Chapter – 4

Kinetic parameters from TL glow curves

4.0 Preamble

The dosimetric characteristics of thermoluminescence materials mainly depend on the kinetic parameters like the trap depth, frequency factor and the order of kinetics. In this chapter the kinetic parameters of borate based phosphors were determined using different standard methods. The experimentally determined kinetic parameters were used to generate the TL glow curves by integrating the general order kinetic equations numerically using Adaptive Simpson Quadrature algorithm.

4.1 Introduction

In a TL experiment one usually obtains different glow curves under different conditions of measurements. The main goal of measuring and analyzing these TL glow curves is the extraction of the parameters that can be used to describe the TL process in the material. The dosimetric characteristic of any TL material depends mainly on these parameters responsible for TL [1]. The important parameters are the activation energy of the TL traps (E) also called the trap depth, the frequency factor (s) and the order of kinetics (b) of the TL process, the capture cross-sections for the traps and recombination centers, and the concentrations of these traps and centers. These parameters will mainly reveal the stability of the traps. If the trap depth is low, then the glow peak occurs at a relatively lower temperature and the corresponding trap is unstable. This may result in fading of TL signal at ambient temperature. If the frequency factor is high then fading may be pronounced. The order of kinetics gives information about whether the trapped charge carriers will be retrapped on heating or not. There are several methods reported in the literature for the determination of these parameters. This chapter presents the kinetic parameters of borate based TL phosphors determined by standard methods like variable heating rate method, initial rise method, peak shape methods, isothermal decay method and computerized glow curve deconvolution method. For the validation of the estimated kinetic parameters, the same parameters were used and the general order kinetic equation is integrated numerically using adaptive Simpson quadrature rule.

4.2 Kinetic analysis of thermoluminescence

The first, second and general order kinetic equations governing the thermoluminescence processes have been given by Randall – Wilkins [2], Garlick – Gibson [3] and May – Patridge [4] respectively.

4.2.1 First order kinetics: The first order kinetics is the simplest one which describes the TL process given by Randall and Wilkins [5,6]. According to them, the occurrence of a TL peak is due to the thermal release of electrons from traps and their subsequent recombination with holes trapped in the recombination centers. The assumption that the entities involved are electron traps and hole centers is for the sake of simplicity and the opposite is just as likely to occur with no further complication in the mathematical treatment. This assumes: *(i)* Only one trapping state and one recombination center are involved *(ii)* Electrons thermally released from traps recombine rather quickly with trapped holes (no retrapping into the same traps/any other trap or recombination into any other recombination center is allowed) *(iii)* Accumulation of electrons in the conduction band is assumed to be impossible. These assumptions lead to the fact that rate of recombination is equal to the rate of thermal release of electron. This rate of release should be proportional to the concentration of trapped electrons n and to the Boltzmann exponential factor $exp(-E/kT)$ at a given temperature (T). The intensity of light emission is proportional to the rate of recombination. In view of these assumptions, the basic first order kinetic equation is,

$$I = -\frac{dn}{dt} = ns\, exp[-E/kT] \tag{4.1}$$

The trap can be considered as a potential box with $'s'$ as the product of the frequency with which the electrons strike the walls of the box and the reflection coefficient. Negative sign indicates that $n(t)$ decreases with increase in time. By assuming a heating function, $T = T(t)$, we can obtain the expression for $'n'$ as a function of temperature. Considering the simple linear heating function,

$$T = T_0 + \beta t \tag{4.2}$$

Where T_0 is the initial temperature and β is the heating rate. We can solve for $n(T)$ as,

$$n(T) = n_0\, exp\left[(-s/\beta)\int_{T_0}^{T} exp(E/kT')\, dT'\right] \tag{4.3}$$

Therefore, the temperature dependence of TL intensity is given by,

$$I(T) = n_0 s\, exp(-E/kT)\, exp\left[(-s/\beta)\int_{T_0}^{T} exp(E/kT')\, dT'\right] \tag{4.4}$$

The exponential $exp(-E/kT)$ dominates when T is slightly above T_0 resulting in initial rise of the glow curve. The second exponential term dominates in the higher temperature region. Thus glow curve exhibits a peak at some temperature. The main feature of the first order kinetics is that the dosimetric peak is asymmetric; the asymmetry is such that the decrease at high temperatures above the maximum is faster than the increase at low temperatures. Also changing the initial concentration does not change the shape of the curve.

4.2.2 Second Order Kinetics: The second order kinetics was given by Garlick and Gibson [3] for one trap and one recombination center model. It is based on two assumptions. (i) The freed charge carriers have equal probability for retrapping and recombination. (ii) The concentration of electrons in traps and holes in recombination center are equal during the entire process. Consider a case where the total number of traps of the given type (free or empty) be N. The kinetic equation is given by,

$$I = -\frac{dn}{dt} = \left(\frac{s}{N}\right) n^2 exp(-E/kT) \tag{4.5}$$

where s/N has the units of m^3/s and it can be denoted by s'. Hence,

$$I = -\frac{dn}{dt} = s'n^2 exp(-E/kT) \tag{4.6}$$

Now assuming a linear heating function as in the case of first order kinetics and solving the second order differential equation we get,

$$I(T) = n_0^2 s' exp(-E/kT)\left[1 + (n_0 s'/\beta)\int_{T_0}^{T} exp(-E/kT')dT'\right]^{-2} \tag{4.7}$$

The main feature of this equation is that the glow curve is nearly symmetric with the high temperature half of the curve slightly broader than the low temperature half. Similar to the first order case the initial rise is dominated by the exponential $exp(-E/kT)$. This property is general for any order of kinetics and hence is being exploited in the *'initial rise method'* to determine the trap depth or the activation energy. At higher temperatures the second function (decreasing) dominates and hence the product function also decreases. The important difference between the first and second order kinetics is that the initial concentration is not just a multiplicative constant and hence, its change will affect the shape of the whole curve. The peak temperature remains the same with initial concentration in the case of first order kinetics, whereas the peak shifts towards higher temperatures with increase in initial concentration in the case of second order kinetics. The slight spreading of the TL emission in the high temperature side is due to the retrapping of the significant concentration of the released electrons before they recombine which causes a delay in the TL [7].

4.2.3 General order kinetics: In practical applications, most of the TL materials developed so far do not exhibit fully the first or second order kinetics, which are based on the assumptions of specific values for the retrapping and recombination probabilities. Hence, an empirical relation for the general order kinetics of TL was first suggested by May and Patridge [4] given by,

$$I = n^b s' exp(-E/kT) \tag{4.8}$$

Where s' has the dimensions of $m^{3(b-1)}s^{-1}$ and b is the order of kinetics which need not necessarily be 1 or 2. The difficulty with the empirical equation is in understanding the physical meaning of the parameter s', whose dimensions vary with the order of kinetics. This problem was addressed by Rasheedy [8] who proposed a recasting of eq. (4.8) to the form,

$$I = -\frac{dn}{dt} = \left(\frac{n^b}{N^{b-1}}\right) s\ exp(-E/kT) \tag{4.9}$$

This eq. (4.9) reduces to first order kinetic equation (eq. (4.1)) for $b = 1$ and second order kinetic equation (eq. (4.5)) for $b = 2$. Integrating eq. 4.9 gives,

$$I = n_0^b s\ exp(-E/kT) N^{1-b} \left[1 + \frac{s(b-1)(n_0/N)^{b-1}}{\beta} \int_{T_0}^{T} exp(-E/kT')dT'\right]^{-\frac{b}{b-1}} \tag{4.10}$$

Though equation 4.10 is also empirical, it removes the difficulty in understanding the meaning of s' .

The temperature corresponding to the maximum of the glow peak is obtained by setting the derivative of eqns. (4.4), (4.7), (4.10) equal to zero. If T_M is the temperature corresponding to maximum TL, we have for first, second and general order kinetics respectively the following equations,

$$\frac{\beta E}{kT_M^2} = sexp\left(-\frac{E}{kT_M}\right) \tag{4.11}$$

$$\frac{\beta E}{kT_M^2} = s exp\left(-\frac{E}{kT_M}\right)\left[1 + \left(\frac{2kT_M}{E}\right)\right] \tag{4.12}$$

$$\frac{\beta E}{kT_M^2} = s exp\left(-\frac{E}{kT_M}\right)\left[1 + (b-1)\left(\frac{2kT_M}{E}\right)\right] \tag{4.13}$$

4.3 Determination of kinetic parameters

***4.3.1 Initial rise method**:* This is one of the simplest experimental methods first suggested by Garlick and Gibson [3] to determine the trap depth of TL materials and is independent of the order of kinetics. This method is based on the assumption that, in the rising part of the TL glow curve (low temperature tail of the glow curve), the number of trapped electrons is approximately constant and the dependence of $n(T)$ on temperature T is negligible. This can be applicable for temperature below which the intensities are lesser than about 15% of the peak intensity. Based on this assumption, the TL emission in this region can be described by,

$$I(T) \propto exp\left(-\frac{E}{kT}\right) \tag{4.14}$$

Hence a plot of logarithm of intensity versus inverse temperature in the initial rise region yields a straight line with the slope proportional to $(-E/k)$, from which the trap depth E can be obtained. The intercept of the initial rise plot of general order kinetic equation [4] gives, $Intercept = \ln Csn_0\left(\frac{n_0}{N}\right)^{b-1}$, from which the frequency factor, s can be obtained using the relation, $s = antilog(Intercept - \ln(A))$, where $A = Cn_0$ is the area under the glow peak. Here $n_0 \approx N$, for saturation dose. This method is applicable only for non-overlapping and well defined isolated TL peaks.

The trap depth and frequency factors of the dosimetric peaks of all the phosphors studied were determined by initial rise method. The low temperature satellite peaks present in these phosphors were removed by the thermal cleaning technique and TL was recorded in the initial rise region at a heating rate of 5 K/s.

Table 4.1 shows the trap depth and frequency factor for the phosphors obtained by initial rise method. The dose delivered to the phosphors for recording the glow curves in the initial rise regions is also shown in the table.

Table 4.1 Trap depth and frequency factor obtained from initial rise method. The gamma dose to which the phosphors are irradiated prior to recording the glow curve in the initial rise region is shown in column 2

Material	Gamma dose (Gy)	Trap depth E (eV)	Frequency factor (s^{-1})
LTB:Mn	100	1.31±0.004	6.77×10^{11}
MTB:Gd,Li	2.41×10^{3}	1.20±0.004	2.21×10^{10}
ZMB:Tm	2.41×10^{3}	1.49±0.021	2.49×10^{11}
CTB	2	1.04±0.013	5.16×10^{10}

***4.3.2 Variable heating rate**:* Heating rate is an important parameter which affects the peak position of TL glow curves during TL readout of any order of kinetics. When the linear heating rate changes the temperature T_M corresponding to the maximum TL intensity of the peak also changes. The equation relating the heating rate and the maximum peak temperature T_M for first, second and general order kinetics is given in equations 4.11 through 4.13. Using this property of shift in the glow peak temperature with heating rate and using two different heating rates, the activation energy (E) and frequency factor (s) can be obtained by [9,10]

$$E = k\frac{T_{M1}T_{M2}}{T_{M1}-T_{M2}}ln\left[\frac{\beta_1}{\beta_2}\left(\frac{T_{M2}}{T_{M1}}\right)^2\right] \tag{4.15}$$

$$s = \frac{E}{k}exp\left\{\left[\left(T_{M2}ln\frac{T_{M2}^2}{\beta_2} - T_{M1}ln\frac{T_{M1}^2}{\beta_1}\right)/(T_{M1} - T_{M2})\right]\right\} \tag{4.16}$$

where the symbols have the usual meaning. Different pairs of heating rates and their corresponding peak temperatures were used to determine the activation energy and frequency factor. This method yields E within an accuracy of 5%, if T_M could be measured within an accuracy of ±1K.

From eq. (4.11) for different heating rates, the following linear relation first suggested by Hoogenstraaten [11] can be obtained.

$$ln\left(\frac{T_M^2}{\beta}\right) = \frac{E}{kT_M} + ln\left(\frac{E}{sk}\right) \tag{4.17}$$

A linear plot between $ln\left(\frac{T_M^2}{\beta}\right)$ and $\frac{1}{T_M}$ yields a straight line with slope $\frac{E}{k}$ and intercept $ln\left(\frac{E}{sk}\right)$ from which E and s can be calculated. Although this equation is derived from the first order kinetic equation of thermoluminescence, it can be extended to non-first order cases as suggested by Chen [12,13]. In order to determine kinetic parameters by the variable heating rate method, the phosphors were irradiated to a dose close to saturation dose and TL was recorded with different heating rates of 0.1, 0.3, 0.7, 1, 3, 7 and 10 K/s. It was observed that the glow peak shifted to higher temperatures with increasing heating rate for all the phosphors studied.

In order to determine the kinetic parameters by variable heating rate method, LTB:Mn phosphor was irradiated to a gamma dose of 2.41 kGy and the glow curves were recorded with different heating rates. Fig. 4.1 shows the TL glow curves of LTB:Mn recorded with different heating rates viz., 0.1, 0.3, 0.7, 1, 3, 7 and 10 K/s. The inset in fig. 4.1 shows the variation of peak temperature with heating rate.

It is observed that the peak temperature increases sharply at lower heating rates for all the phosphors and as the heating rate increases further there is a slow but steady increase in the peak temperature. This is because, at lower heating rates, the time spent in heating the phosphor to any particular temperature T is more and hence thermal release of electrons at that temperature is also high. But at higher heating rates, the time spent to heat the phosphor to the same temperature T is less and hence the thermal release is also less. Hence at higher heating rates, a higher temperature is required to release the same amount of trapped charges as that for lower heating rates.

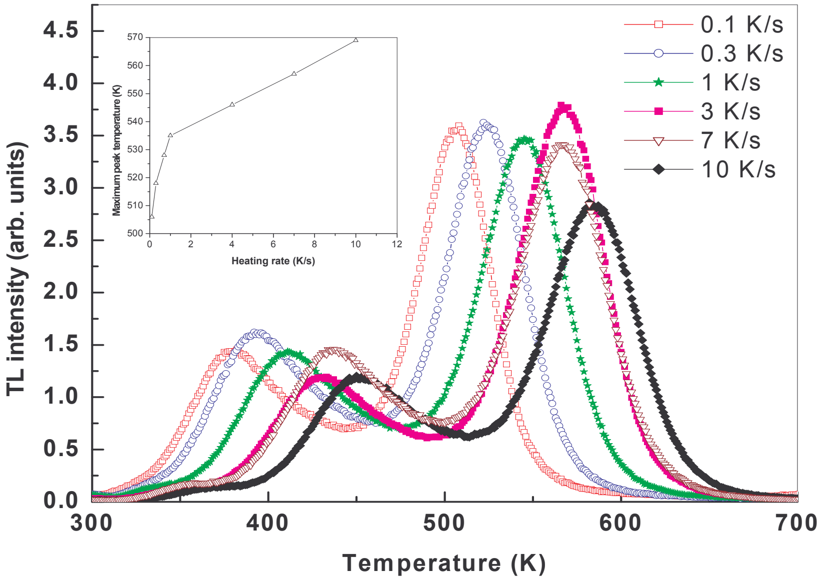

Fig.4.1 Glow curves of LTB:Mn recorded with different heating rates depicting the systematic variation of glow peak temperature T_M with heating rates. The inset shows the variation of peak temperature with heating rate.

The glow peak shifted from 506 K to 585 K when the heating rate was changed from 0.1 K/s to 10 K/s. In order to reduce the temperature lag between the heater strip and the sample, small quantities (~10 mg) of uniform grain size powder was used for the measurements. Figure 4.2 shows the plot of $ln\left(\frac{T_M^2}{\beta}\right)$ vs $\frac{1}{T_M}$ for LTB:Mn phosphor. It can be observed from the fig. 4.2 that most of the data points lie on the fitting straight line which means that, the temperature lag was less for the heating rates used in the study. The value of E and s obtained by this graphical method are 1.29 ± 0.058 eV and 2.13×10^{10} s^{-1} respectively. Further using the different sets of heating rates and their corresponding peak temperatures, the activation energy (E), and the frequency factor (s) was also be calculated by using eqns. (4.15) and (4.16.).

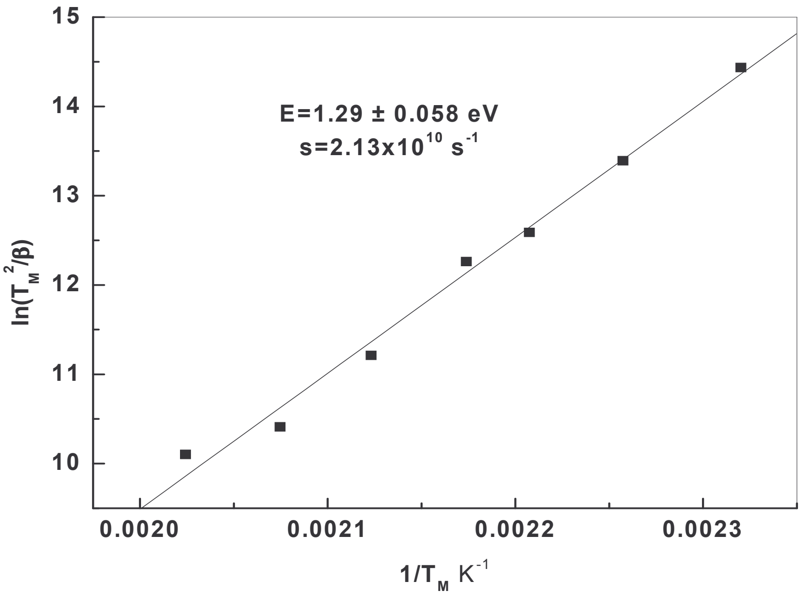

Fig. 4.2 Plot of $\ln\left(\frac{T_M^2}{\beta}\right)$ vs $\frac{1}{T_M}$ *for LTB:Mn. The solid line is a least square fit to the data points*

The average value of E and s obtained for different pairs of heating rate are 1.32 ± 0.031 eV and 5.25×10^{10} s^{-1} respectively. The trap depth and frequency factors obtained from both the graphical and theoretical methods are in good agreement with each other. In a similar way, the trap depth and frequency factor of other borate phosphors MTB:Gd,Li; ZMB:Tm and CTB phosphors were also determined by variable heating rate method. The values of the trap depth and frequency factor obtained are shown in Table 4.2.

4.3.3 Peak shape method: The shape or the geometrical properties of a glow peak depends on the order of kinetics involved in the TL process. The TL glow peaks corresponding to second order kinetics are almost symmetrical in shape whereas, those corresponding to first order kinetics are asymmetrical. Hence from the shape of the glow peak, one can get information regarding the trap depth, frequency factor and the order of kinetics utilizing peak temperature (T_M) and two temperatures corresponding to the half the peak intensity on the rising side (T_1) and falling side (T_2) of the glow curve. The total peak width at half the maximum intensity ($\omega = T_2 - T_1$), the lower temperature half width ($\tau = T_M - T_1$) and upper temperature half width $\delta = T_2 - T_M$ were calculated from which the symmetry factor $\mu_g = \delta/\omega$ was determined. Using the symmetry factor, the order of kinetics is obtained from Chen's plot [14].

Table 4.2 Trap depth and frequency factor obtained from variable heating rate method. The gamma dose to which the phosphors are irradiated prior to recording the glow curve in the initial rise region is shown in column 2

Material	Gamma dose (Gy)	Trap depth E (eV)	Frequency factor (s^{-1})
LTB:Mn	100	1.29±0.058	2.13×10^{10}
MTB:Gd,Li	2.41×10^{3}	1.20±0.054	5.80×10^{10}
ZMB:Tm	5.0×10^{3}	1.51±0.069	1.99×10^{12}
CTB	2	1.04±0.013	2.12×10^{9}

The activation energy and frequency factor were determined using the relations formulated by Chen [15] and are applicable for any order of kinetics given by,

$$E_\alpha = c_\alpha \frac{kT_M^2}{\alpha} - b_\alpha(2kT_M) \tag{4.18}$$

$$s = \frac{\beta E}{kT_M^2} exp\left(\frac{E}{kT_M}\right)[1 + (b-1)\Delta_M]^{-1} \tag{4.19}$$

where α stands for δ, τ and ω. Here,

$c_\tau = 1.51 + 3.0(\mu_g - 0.42), \qquad b_\tau = 1.58 + 4.2(\mu_g - 0.42)$

$c_\delta = 0.976 + 7.3(\mu_g - 0.42), \qquad b_\delta = 0$

$c_\omega = 2.52 + 10.2(\mu_g - 0.42), \qquad b_\omega = 1$

$\Delta_M = \dfrac{2kT_M}{E}$

Using eqns. (4.18) and (4.19), the trap depth and frequency factor were determined for all the phosphors and the mean values of $E_\delta, E_\tau, E_\omega$ and $s_\delta, s_\tau, s_\omega$ obtained are shown in Table 4.3.

Table 4.3 TL kinetic parameters obtained by peak shape method

Phosphor	Symmetry factor μ_g	Order of kinetics	Trap depth (eV)			Frequency factor (s^{-1})		
			E_δ	E_τ	E_ω	s_δ	s_τ	s_ω
LTB:Mn	0.51	1.85	1.25	1.26	1.27	1.84×10^{10}	2.47×10^{10}	2.51×10^{10}
MTB:Gd,Li	0.49	1.55	1.26	1.28	1.28	3.08×10^{10}	4.01×10^{10}	4.04×10^{10}
ZMB:Tm	0.50	1.70	1.46	1.47	1.43	9.41×10^{12}	6.23×10^{12}	5.19×10^{12}
CTB	0.506	1.80	1.07	1.09	1.10	2.89×10^{10}	5.48×10^{10}	4.54×10^{10}

It can be observed that there is not much deviation in the values of $E_\delta, E_\tau, E_\omega$ for all the phosphors. This shows that the TL peaks of the phosphors are simple and well separated from the satellite peak at the low temperature and hence are suitable for dosimetry applications. The phosphors studied shows a kinetic order varying from 1.5 to 1.85. Though the variation of $E_\delta, E_\tau, E_\omega$ is not very significant, the value of E_τ is slightly higher which reflects the asymmetric nature of the peaks due to mixed order kinetics. In the case of the non first order kinetics, instead of s, the frequency factor which has the units of inverse time, we get a quantity s'' having units $\left(cm^{-3(b-1)}s^{-1}\right)$ which depends on the concentration of the trapped charges or the absorbed dose and is termed as the pre-exponential factor. This value of pre-exponential factor is a constant for a given dose and it varies with dose. However if the measurements are carried out at the dose closer or equal to the saturation dose, the pre-exponential factor matches with the frequency factor. In order to determine the parameters by peak shape method, the phosphors are irradiated to a dose almost equivalent to that of the saturation dose. Hence, the value of the pre-exponential factor obtained is considered as frequency factor itself.

4.3.4 Isothermal decay method: This is one of the most general methods to determine kinetic parameters. This is done by recording the decay of luminescence at constant temperature on pre-irradiated phosphors. Garlick and Gibson [3] have illustrated the use of isothermal decay method to determine the kinetic parameters of first order kinetics. For the case of first order kinetics, the isothermal decay curves at a temperature T_i are exponential functions of time and is given by,

$$I = I_0 exp\left(-s\ exp\left(-\frac{E}{kT_i}\right) t\right) \tag{4.20}$$

From eq. (4.20) it is clear that a plot of $ln(I)$ versus $'t'$ will be a linear and the slope is given by,

$$slope = m_i == -s\ exp\left(-\frac{E}{kT_i}\right) \tag{4.21}$$

The slopes can be obtained for all the isothermal decay curves recorded. By taking natural logarithm to eq. (4.21), we obtain,

$$ln(|slope|) = lns - \frac{E}{kT_i} \tag{4.22}$$

Hence a plot of $ln(|slope|)$ versus $\frac{1}{T_i}$ yields a straight line with a slope of $(-E/k)$ and an intercept of $ln\, s$, from which the activation energy and the frequency factor can be estimated.

For the general order kinetics, the isothermal decay curves can be obtained by keeping temperature constant and integrating eq. (4.8) with respect to time. The isothermal decay curves for general order kinetics is given by [4,16],

$$I = I_0\left[1 + s'^{n_0^{b-1}(b-1)} texp\left(-\frac{E}{kT}\right)\right]^{\frac{b}{1-b}} \tag{4.23}$$

where

$$I_0 = s' n_0^b exp\left(-\frac{E}{kT}\right) \tag{4.24}$$

Here I_0 and n_0 are the initial TL intensity and initial concentration of trapped charges and I_t is the TL intensity at time t. By rearranging equation 4.23 we obtain,

$$\left(\frac{I_0}{I_t}\right)^{\frac{b-1}{b}} = \left[1 + s' n_0^{b-1}(b-1)t\ exp\left(-\frac{E}{kT}\right)\right] \tag{4.25}$$

$$\left(\frac{I_0}{I_t}\right)^{\frac{b-1}{b}} - 1 = s' n_0^{b-1}(b-1)t\ exp\left(-\frac{E}{kT}\right) \tag{4.26}$$

Plot of eq. (4.26) with respect to time (for a given T) results in straight lines for proper choice of order of kinetics b. The slope of the straight line plot is given by,

$$m(T) = s' n_0^{b-1}(b-1)t\ exp\left(-\frac{E}{kT}\right) \tag{4.27}$$

Finally the value of activation energy is obtained from the slope of the plot of $ln(m\{T\})$ versus $\frac{1}{T}$.

In order to determine the kinetic parameters by isothermal decay method, the phosphors was irradiated to a known dose (around 3 Gy) and decay of luminescence were recorded for five different temperatures on the rising side of the TL glow curve close to the peak temperature for each phosphor. The luminescence (phosphorescence) decay at each temperature was recorded as a function of time from a freshly irradiated phosphor. Graphs of TL intensity versus *t* at constant temperature are called isothermal decay curves. From the experimental data, $\left(\frac{I_0}{I_t}\right)^{\frac{b-1}{b}} - 1$ versus time was plotted for different temperatures for all the phosphors. The value of b (order of kinetics) was chosen in such a way that $\left(\frac{I_0}{I_t}\right)^{\frac{b-1}{b}} - 1$ versus time resulted in a straight line. The slope $m(T)$ obtained for each temperature was noted and a plot of $ln[m(T)]$ versus $1/T$ was made for each phosphor. $ln[m(T)]$ versus $1/T$ satisfies the relation $ln[m(T)] = -\frac{E}{kT} + ln[s(b-1)]$ for a general order kinetics [17] and hence using the slope and intercept of the linear fit to the data points, the activation energy and frequency factor are calculated. Fig. 4.3 shows the $\left(\frac{I_0}{I_t}\right)^{\frac{b-1}{b}} - 1$ versus time plot of LTB:Mn for $b = 1.85$ recorded for different temperatures.

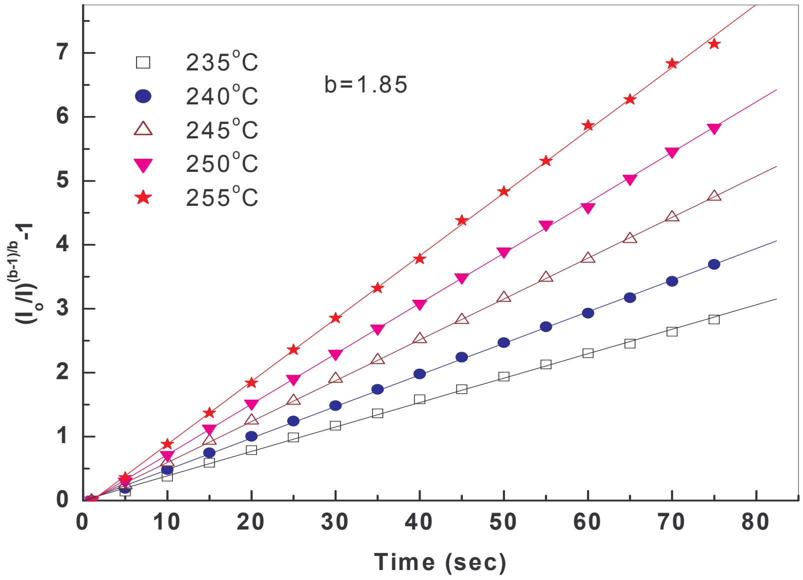

Fig. 4.3 $\left(\frac{I_0}{I_t}\right)^{\frac{b-1}{b}} - 1$ *versus time plot of LTB:Mn for* $b = 1.85$

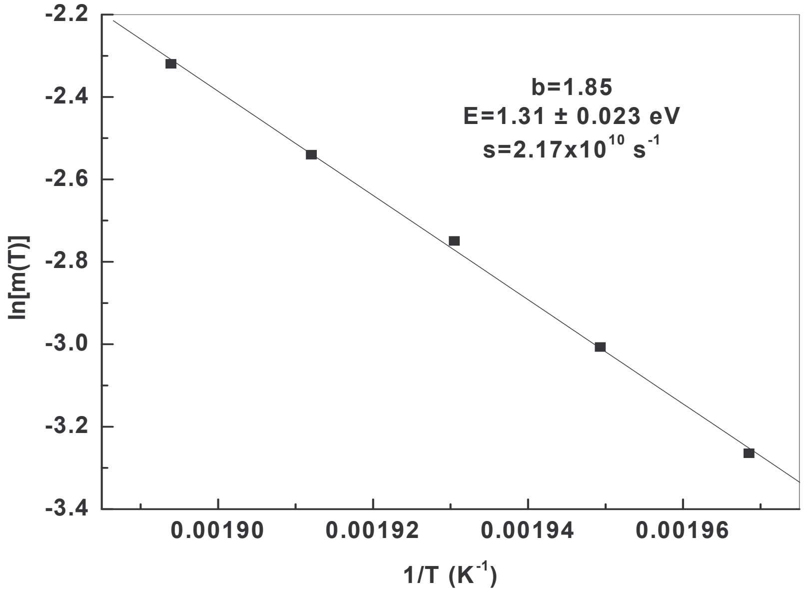

Fig. 4.4 Plot of $\ln[m(T)]$ vs $1/T$ *for LTB:Mn*

This value of b is considered as the order of kinetics. From the slopes of straight line obtained for each temperature the plot of $ln[m(T)]$ vs $1/T$ is plotted and is shown in Fig. 4.4. Using the slope and intercept, the activation energy and the frequency factor were determined. The values of E, s and b obtained by isothermal decay method are shown in table 4.4.

Fig. 4.5 shows the $\left(\frac{I_0}{I_t}\right)^{\frac{b-1}{b}}-1$ versus time plot of MTB:Gd,Li for $b=1.60$ recorded for different temperatures. Using the slopes of straight line obtained for each temperature the plot of $ln[m(T)]$ vs $1/T$ is plotted and is shown in Fig. 4.6. Using the slope and intercept, the activation energy and the frequency factor were determined.

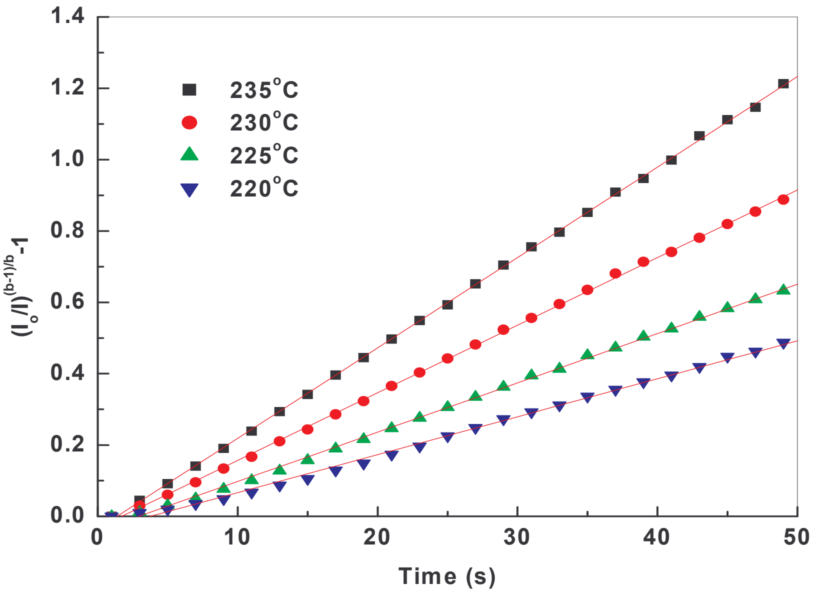

Fig. 4.5 $\left(\frac{I_0}{I_t}\right)^{\frac{b-1}{b}}-1$ *versus time plot of MTB:Gd,Li for* $b=1.6$

Fig. 4.7 shows the $\left(\frac{I_0}{I_t}\right)^{\frac{b-1}{b}}-1$ versus time plot of ZMB:Tm for $b=1.75$ recorded for different temperatures along the rising side of peak 2 of TL glow curve. The slopes of straight line obtained are noted for each temperature. The plot of $ln[m(T)]$ vs $1/T$ is shown in Fig. 4.8.

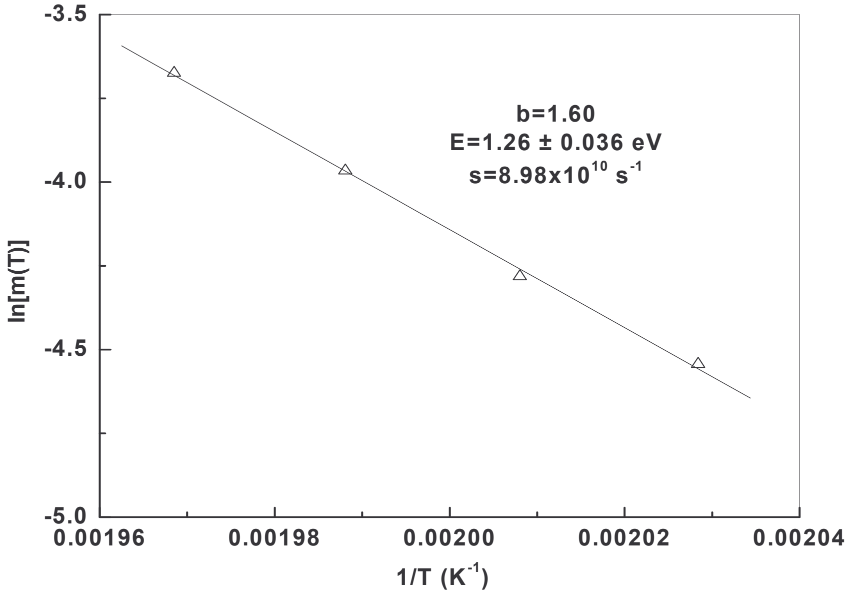

Fig. 4.6 $ln[m(T)]$ vs $1/T$ *of MTB:Gd,Li*

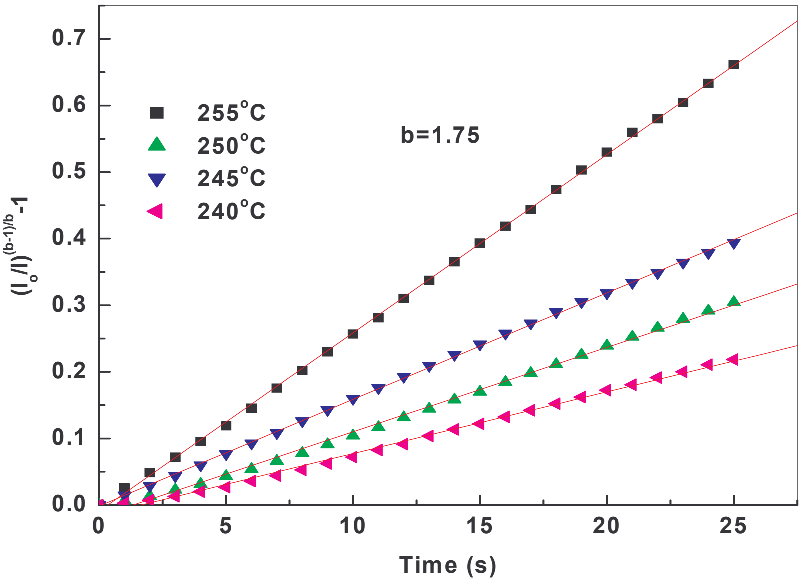

Fig. 4.7 $\left(\frac{I_0}{I_t}\right)^{\frac{b-1}{b}}-1$ *versus time plot for peak 2 of ZMB:Tm for* $b = 1.75$

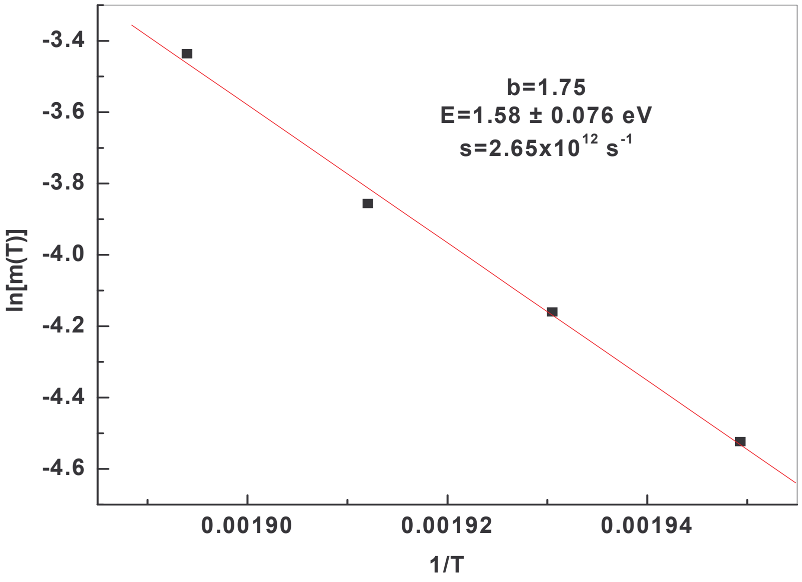

Fig. 4.8 $ln[m(T)]$ vs $1/T$ *for peak 2 of ZMB:Tm*

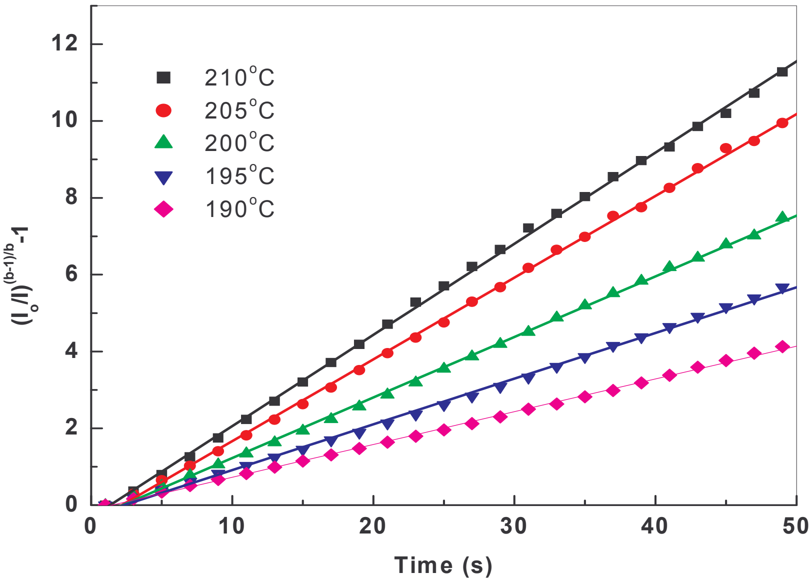

Fig. 4.9 $\left(\frac{I_0}{I_t}\right)^{\frac{b-1}{b}}-1$ *versus time plot cadmium tetraborate for* $b = 1.80$

From the slope and intercept, the activation energy and the frequency factor were determined. Fig. 4.9 and Fig. 4.10 shows similar plots for cadmium tetraborate phosphors. The values of activation energy, trap depth and order of kinetics of all the phosphors obtained by isothermal decay method is shown in Table 4.4

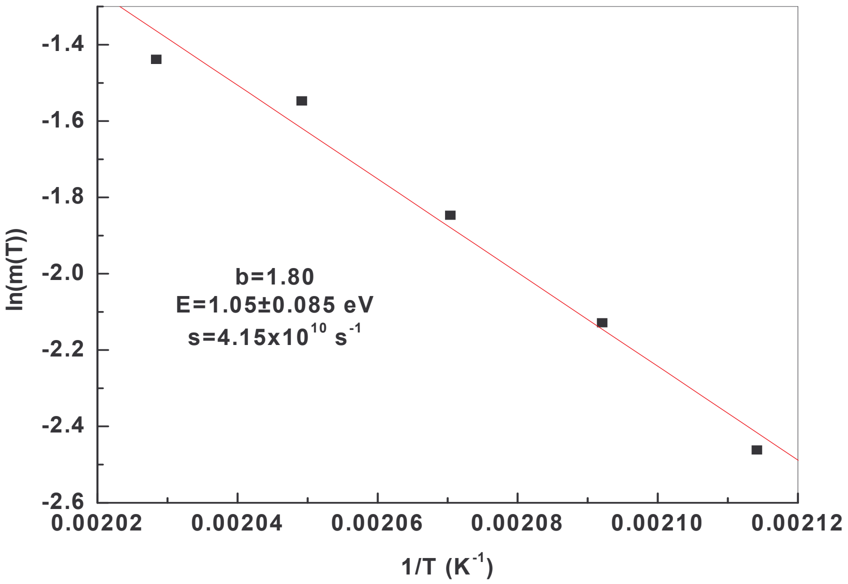

Fig. 4.10 $ln[m(T)]$ vs $1/T$ *for cadmium tetraborate*

Table 4.4 Kinetic parameters of borates obtained from isothermal decay method.

Material	Gamma dose (Gy)	Order of Kinetics	Trap depth E (eV)	Frequency factor (s^{-1})
LTB:Mn	3	1.85	1.31±0.023	2.17×10^{10}
MTB:Gd,Li		1.60	1.26±0.036	8.98×10^{10}
ZMB:Tm		1.75	1.58±0.076	2.65×10^{12}
CTB	0.5	1.80	1.05±0.085	4.15×10^{10}

***4.3.5 Computerized Glow curve deconvolution method*:** Computerized glow curve deconvolution was carried out using the Spreadsheet program. The experimental glow curve recorded for the phosphors was fitted into individual glow peaks by interfacing the solver utility of Micosoft Excel [18]. The general order kinetics (GOK) equation,

$$I(T) = I_M b^{b/(b-1)} exp\left(\frac{E}{kT}\frac{T-T_M}{T_M}\right)\left[(b-1)(1-\Delta)\frac{T^2}{T_M^2}exp\left(\frac{E}{kT}\frac{T-T_M}{T_M}\right)+Z_M\right]^{-\frac{b}{b-1}} \quad (4.28)$$

suggested by Kitis etal [19] was used for the fitting. Here $\Delta = \frac{2kT}{E}$, $\Delta_M = \frac{2kT_M}{E}$ and $Z_M = 1 + (b-1)\Delta_M$. The constraint that was used during the fitting was $1 < b < 2$. The Solver is an Excel Add-in general purpose software package [20] which minimizes the sum of squares of the residuals to perform a least square fitting. The experimentally determined quantities like glow peak intensity (I_M), glow peak temperature (T_M) and the guess values of trap depth (E) and order of kinetics (b) were used as fitting parameters. By changing the values of these parameters, the experimental glow curve was fitted such that the figure of merit (FOM%) defined as,

$$FOM(\%) = 100 \times \frac{\sum_p TL_{exp} - TL_{fit}}{\sum_p TL_{fit}} \tag{4.29}$$

is a minimum. Here TL_{exp} corresponds to the experimental data points, TL_{fit} corresponds to the fitted data points and the summation is over all data points.

Figure 4.11 shows the experimental glow curve (circles) along with calculated curve (solid line) using the GOK equation for LTB:Mn. The deconvoluted glow peaks are shown as red lines in the figure. The residual TL intensity versus temperature after curve fitting is shown in the inset. The experimental glow curve of LTB:Mn is fitted with four peaks. The figure of merit of the fitting is 0.013% which shows that the process used for deconvoultion is accurate. The values of order of kinetics, trap depth and frequency factors obtained for the dosimetric peak (high intense peak) are 1.9, 1.38 eV and 1.66×10^{10} s^{-1} respectively. Fig. 4.12 shows the experimental glow curve of gamma irradiated MTB:Gd,Li (circles) along with the fitted curve (solid line). The figure of merit was 0.63%. The lower value of FOM suggests that the analysis process was accurate. For the intense fitted peak, the value of activation energy (E) was found to be 1.14 eV and frequency factor $s = 2.07 \times 10^{10}$ s^{-1}. The order of kinetics used for the fitting was 1.73.

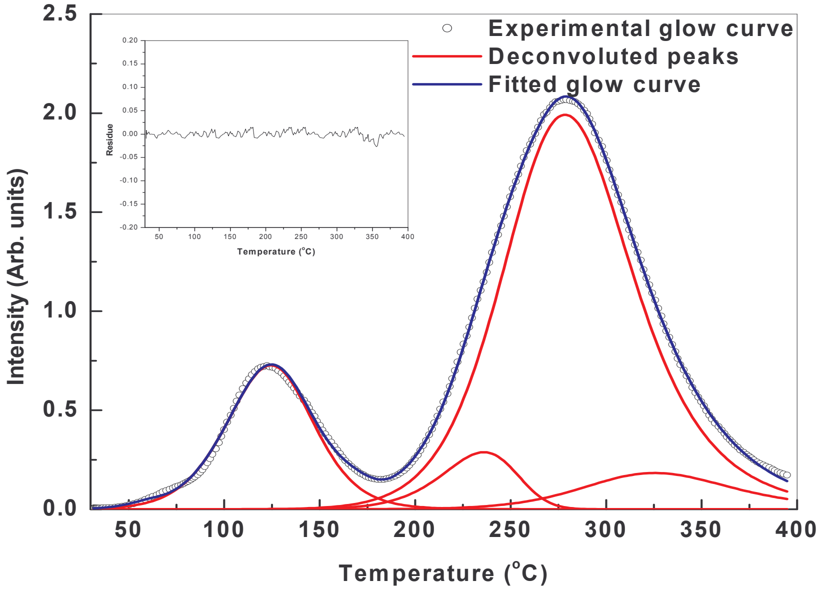

Fig. 4.11 Experimental data points along with the fitted glow curves and deconvoluted peaks of LTB:Mn

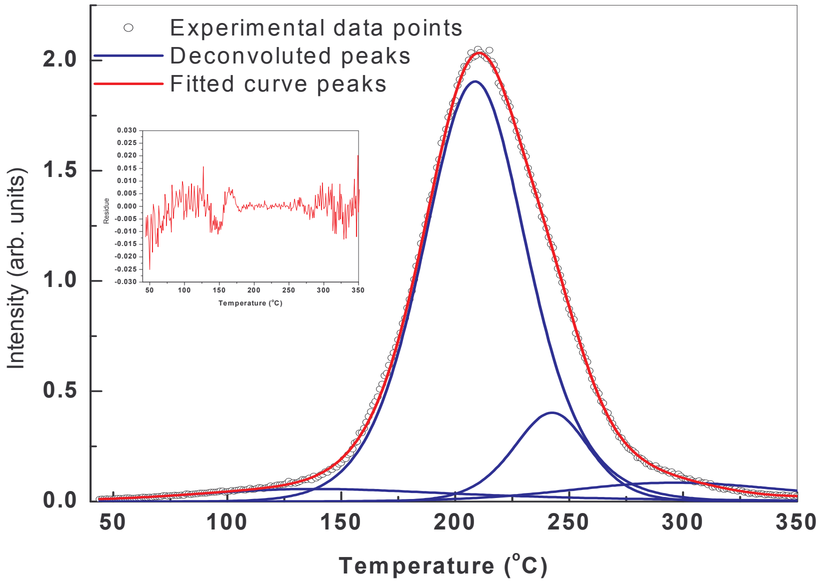

Fig. 4.12 Experimental data points along with the fitted glow curves and deconvoluted peaks of MTB:Gd, Li. The inset gives the residue of fitting.

Fig. 4.13 shows the experimental glow curve of gamma irradiated ZMB:Tm (circles) along with the fitted curve (solid line). The inset shows the residue of fitting. The figure of merit was 0.67%. The lower value of FOM suggests that the analysis process was accurate. The values of the trap depth and the order of kinetics obtained for the two dominant peaks were 0.77 eV, 1.44 eV and 1.9 and 1.75 respectively.

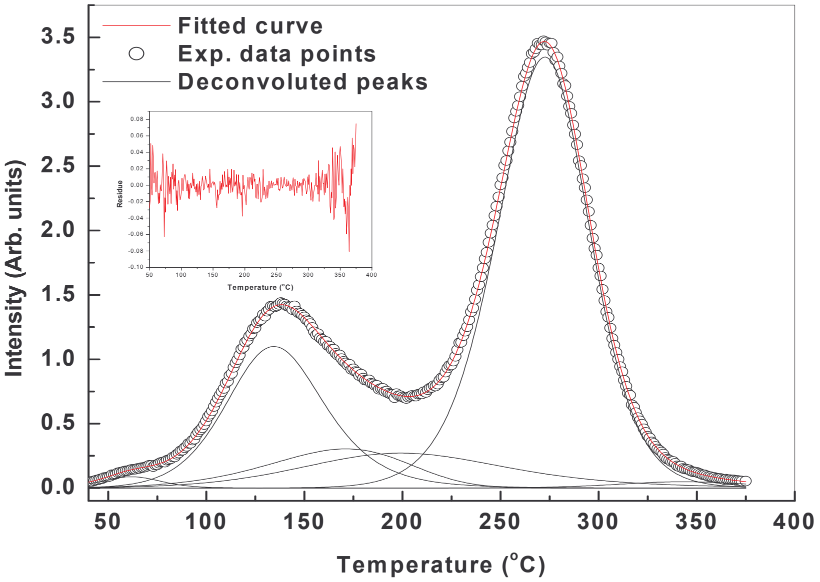

Fig. 4.13 Experimental data points along with the fitted glow curves and deconvoluted peaks of ZMB:Tm. The inset gives the residue of fitting.

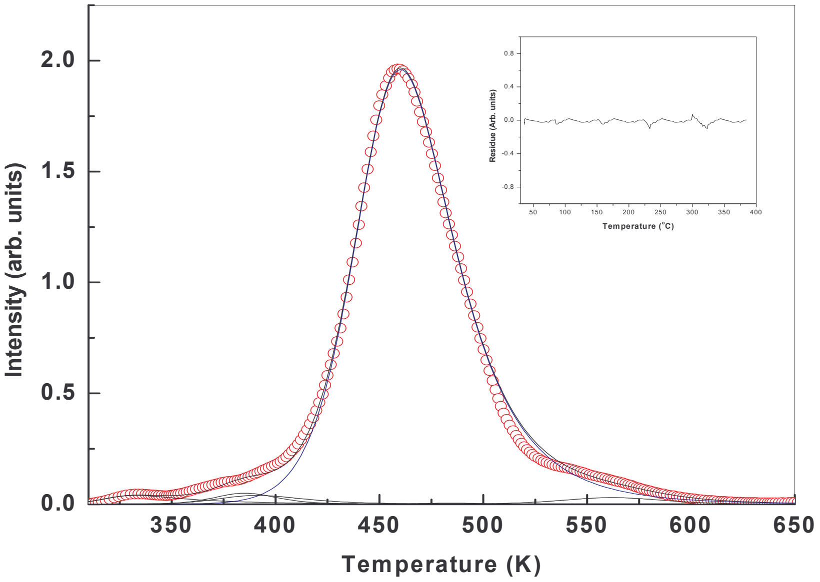

Fig. 4.14 Experimental data points(red circles) along with the fitted glow curves(black) and deconvoluted peaks(blue and low intense black) of cadmium tetraborate. The inset gives the residue of fitting.

Fig. 4.14 shows the experimental glow curve of gamma irradiated CTB phosphor (circles) along with the fitted curve (solid line). The inset shows the residue of fitting. The figure of merit was 0.43%. The values of the trap depth and the order of kinetics obtained for the dominant peak is 1.08 eV and 1.83 respectively.

4.3.6 Comparison of kinetic parameters: A comparative study was carried out with the trap depth obtained by the different methods for all the phosphors. The average values of the kinetic parameter obtained by different method are shown in Table 4.5.

Table 4.5 Kinetic parameters obtained by different methods

Material	Initial rise	Variable heating rate	Peak shape*	Isothermal decay	Glow curve deconvolution
Order of kinetics					
LTB:Mn	Could not be determined		1.85	1.85	1.9
MTB:Gd,Li			1.55	1.60	1.73
ZMB:Tm			1.70	1.75	1.75
CTB			1.80	1.80	1.83
Trap depth (eV)					
LTB:Mn	1.31±0.004	1.29±0.058	1.26	1.31±0.023	1.38
MTB:Gd,Li	1.20±0.004	1.20±0.054	1.27	1.26±0.036	1.14
ZMB:Tm	1.49±0.021	1.51±0.069	1.45	1.58±0.076	1.44
CTB	1.04±0.013	1.04±0.013	1.09	1.05±0.085	1.08
Frequency factor (s^{-1})					
LTB:Mn	6.77×10^{11}	2.13×10^{10}	2.27×10^{10}	2.17×10^{10}	1.66×10^{10}
MTB:Gd,Li	2.21×10^{10}	5.80×10^{10}	3.71×10^{10}	8.98×10^{10}	2.07×10^{10}
ZMB:Tm	2.49×10^{11}	1.99×10^{12}	6.94×10^{12}	2.65×10^{12}	2.22×10^{12}
CTB	5.16×10^{10}	2.16×10^{9}	4.30×10^{10}	4.15×10^{10}	5.48×10^{10}

*-Values of trap depth and frequency factor for peak shape method is average of $E_\delta, E_\tau, E_\omega$ and $s_\delta, s_\tau, s_\omega$

Trap depth estimated from isothermal decay method for LTB:Mn deviates from the mean (average trap depth by all methods) by twice the standard deviation. Frequency factor varies over one order of magnitude across the different methods for all the materials studied and this is consistent with what is noted in the literature [21]. Order of kinetics estimated is in good agreement. The difference in the value of trap depth in the case of LTB:Mn from that reported by Manam and Sharma [22] may be due to the difference in the synthesis procedure which has resulted in a different glow peak temperatures.

4.4 Validation of kinetic parameters*:* In order to validate the estimated kinetic parameters, the glow curves were computed using the experimentally determined kinetic parameters. A typical numerically integrated glow curve for LTB:Mn along with the experimental glow curve is shown in fig. 4.15.

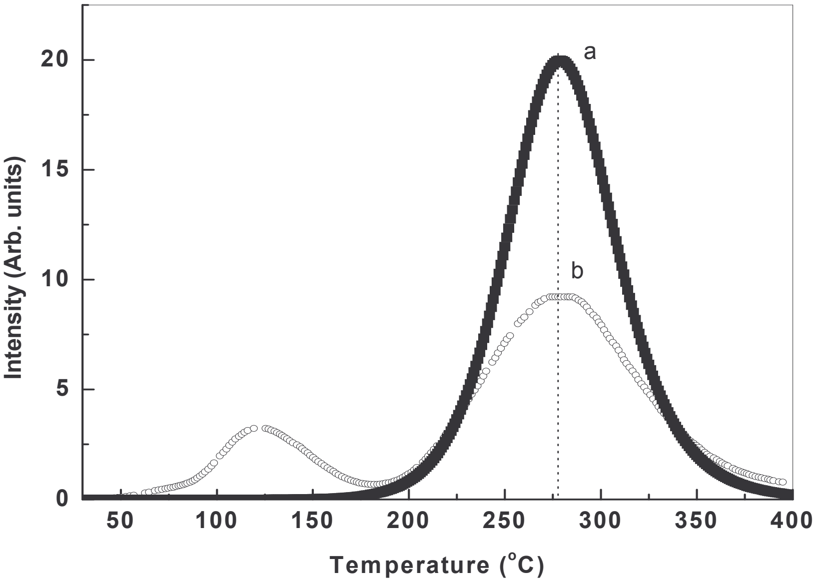

Fig. 4.15 Comparison of TL glow curves of LTB:Mn phosphor (a) Numerically integrated glow curve using experimentally determined kinetic parameters (b) Experimental glow curve

The general order kinetic equation given by Yigal and Horowitz [23],

$$I(t) = sn_0 exp(-E/kT)\left\{\frac{(b-1)s}{\beta}\int_{T_0}^{T} exp(-E/kT')\,dT' + 1\right\}^{-\frac{b}{b-1}} \qquad (4.30)$$

where the symbols have their usual meaning was numerically integrated using the adaptive Simpson Quadrature algorithm. The temperature at which peak occurs for all the phosphors studied was checked for agreement with the experimentally obtained peak temperatures. The heating rate used for the generation of glow curve is same as that used for experimental measurements.

4.5 Conclusions:

Kinetic parameters of polycrystalline powder samples of borate based phosphors viz., LTB:Mn, MTB:Gd,Li, ZMB:Tm and CTB synthesized by solid state sintering technique was determined by different standard methods. The parameters obtained by different methods are in agreement with each other. The estimated kinetic parameters are validated, by numerically generating the glow curves, from the general order kinetic equation using the experimentally determined parameters. It is found that the peak temperature for the numerically integrated and the experimental glow curves agree.

4.6 References

---

[1] Kitis G., Furetta C., Prokic M., and Prokic V., J. Phys. D: Appl. Phys. **33** (2000) 1252

[2] Randall J.T. and Wilkins M.H.F., Proc. Roy. Soc. A **184** (1945) 346

[3] Garlick G.F.J and Gibson A.F., Proc. Phys. Soc. **60** (1948) 574

[4] May C.E. and Patridge J.A., J.Chem. Soc. **40** (1964) 1401

[5]. Randall J.T. and Wilkins M.H.F., Proc. Roy. Soc. London, **184** (1945) 365

[6]. Randall J.T. and Wilkins M.H.F., Proc. Roy. Soc. London, **184** (1945) 390

[7]. Bos A.J.J. Nucl. Instr. Methods in Phys. Res. B **184** (2001) 3

[8]. Rasheedy M.S., J. Phys.: Condens. Matter **5** (1993) 633

[9]. Porfianovitch I.A., J. Exp. Theor. Phys. USSR **26** (1954) 696

[10]. Booth A.H., Canad. J. Chem. **32** (1954) 214

[11]. Hoogenstraaten, Philips Res. Rep. **13** (1958) 515

[12]. R. Chen, S.A..A. Winer, J. Appl. Phys. **41** (1970) 5227.

[13]. R. Chen, Y. Krish, Pergamon Press (1981)

[14]. Chen R and Winer S.A..A, J. Appl. Phys. **41**(1970) 5227

[15]. R. Chen, J. Electrochem. Soc. **116** (1969) 1254.

[16]. Takeuchi N., Inabe K and Nanto H., J. Mater. Sci. **10** (1975) 159

[17]. Manam J., Sharma S.K., Radiat. Phys. Chem. **72** (2005) 423.

[18]. Afouxenidis D., Polymeris G. S., Tsirliganis N. C. and Kitis G., Radiat. Prot. Dosim. **149** (2012) 363

[19]. Kitis G., Gomez-Ros J.M. and Tuyn J.W.N., J. Phys. D: Appl. Phys. **31** (1998) 2636.

[20]. Billo, E. J. Excel for Scientists and Engineers. Wiley (2007).

[21]. Jose M.T., Anishia S.R., Annalakshmi O., Ramasamy V., Radiat Meas. **46** (2011) 1026.

[22]. Manam J., Sharma S.K., Radiat. Eff. Defects Solids **163** (2008) 813.

[23]. Horowitz S.,Thermoluminescence and Thermoluminescent Dosimetry, vol.1, CRC Press Inc., 200052–84.

CHAPTER - 5

EPR - TL CORRELATION

Chapter – 5

EPR – TL correlation

5.0 Preamble

Electron paramagnetic resonance (EPR) is a technique that can be employed to investigate the presence of paramagnetic species (trapped electron or a hole). In the case of TL materials, EPR offers a non-destructive method of obtaining the information on the charge traps in the crystal lattice. The information about the charge traps though vital to explain the TL process, cannot be obtained from the TL measurements alone. The TL emission spectrum provides information on the wavelength of the emission center but cannot give information about the nature of electron and hole traps. In TL applications, the main requirement is the identification of radiation induced defects. This chapter presents a correlation between TL and EPR signals and thereby elucidates a mechanism for TL in the borate based phosphors.

5.1 Introduction

EPR spectroscopy, which deals with the splitting of the spin sub levels under the influence of an external magnetic field, can measure defect concentrations up to 10^{-9} molar concentrations. This is in contrast to the TL technique, which is sensitive to much smaller defect concentrations of the order of 10^{-15} molar concentrations. In order to make a TL-EPR correlation, one should keep in mind that all TL traps need not be paramagnetic and accordingly all EPR signal (paramagnetic radicals) from an irradiated sample need not be related to TL traps. In order to accurately correlate TL and EPR signal, isothermal decay of various TL peaks at room temperature and at elevated temperatures should be studied and also step wise annealing treatment has to be carried out at different temperatures until all the peaks are bleached. Another important point that has to be noted is that a measurable EPR signal is achieved for a radiation dose which will be close to the saturation dose of most TL phosphors, whereas TL signals is observed even at dose levels of the order of 10^8 lower than the saturation dose. It is because of this reason; EPR-TL correlation gives information only on TL traps that correspond to the near saturation kinetic behaviour of TL.

EPR experiments reported in the thesis were performed using a Bruker EMX X-band spectrometer with 100 kHz field modulation. The g-value was calibrated with standard DPPH (α, α'-diphenyl–β-picryl hydrazyl) and is used as a field marker. EPR measurements were carried out for samples which are unirradiated, irradiated and annealed at different temperatures after irradiation for identification of free radicals formed on irradiation. The microwave frequency used was ~ 9.4 GHz (power 3.196 mW).

The electromagnetic radiation source (X-band microwave region) and the detector are housed in a box called the 'microwave bridge'. The microwave source is a Klystron oscillator. Schottky barrier diode detector is used to detect the reflected microwave and to convert the microwave power to an electric current. The microwave cavity is a metal box cylindrical in shape and resonates with the microwaves like an organ pipe resonating with sound waves. Due to this resonance there will be standing wave inside the cavity. When the sample is introduced into the microwave cavity, the samples will have a non-resonant absorption of microwaves. This non-resonant absorption lowers the value of quality factor Q, because of the increased losses and the coupling changes. The cavity is no longer critically coupled and microwave will be reflected back to the bridge resulting in an EPR signal. If there is an EPR signal, the field modulation quickly sweeps through part of the signal and the microwaves reflected from the cavity are amplitude modulated at the same frequency. The signal channel produces a DC signal proportional to the amplitude of the modulated EPR signal. The modulated EPR signal is compared with a reference signal having the same frequency as the field modulation. The signal channel is sensitive to only those signals having the same frequency and phase of the field modulation. This phase sensitive detection with magnetic field modulation increases the sensitivity by several orders of magnitude if the parameters like modulation amplitude, frequency and time constant are properly chosen.

5.2 Radiation induced defects in borates

The most important information regarding the radiation induced defects in borates can be obtained from the electron paramagnetic resonance spectroscopy. In order to understand the observed EPR signal following irradiation with ionising radiation, knowledge of the possible defect forming centers is required. Figure 5.1 shows the schematic of possible defect centers in borate based system. In the borate based phosphors studied in this thesis, both BO_4 and BO_3 networks are arranged to form a three dimensional network. From the figure 5.1, it can be understood that if four oxygen atoms surround the network former (R, R' or R''), they are in tetrahedral arrangement with the network former at the center. Boron enters the lattice both in tetrahedral co-ordination and as planar triangular units. When boron (3 valence electrons) is present in tetrahedral arrangement the extra electron required for charge compensation is taken from the surrounding cations. Thus in the figure 5.1, if R" is Boron, then the complex R"O4 may act as a negative point defect as long as the complex is isolated from the charge compensating cation. Such point defects act as hole traps. This hole trap center is termed as 'Boron oxygen hole center' denoted as

BOHC. The oxygen which acts as the trap bridges R and R”. The non-bridging oxygen can be looked up as another negatively charged point defect which can trap a hole in the absence of any nearby charge compensating cations at the interstitials.

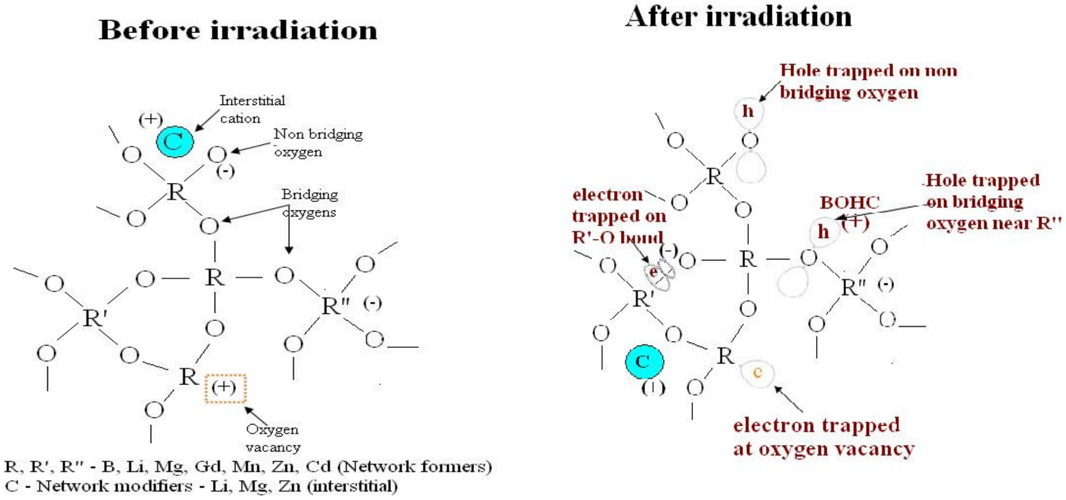

Fig. 5.1 Schematic of possible defect centers in borate based phosphor showing the different types of radiation induced paramagnetic centers and their relationship with pre-existing radiation defects in the lattice.

The possible electron trap centers that can result upon gamma irradiation are the Boron electron center (BEC) which arise when both R’ and R are of the same valency, but one has a greater electron affinity. In such cases the electron can be trapped at the antibonding orbital of R’–O bond. The stability of such defect center increases if there is nearby charge compensating interstitial ion. Also the interstitial cations can themselves serve as electron trap. Oxygen vacancies which may be formed for charge compensation due to the addition of dopants to the lattice during synthesis may act as electron trap centers.

5.3 EPR TL correlation LTB:Mn

5.3.1 EPR signal: In order to identify the defect centers responsible for thermoluminescence in manganese doped lithium tetraborate phosphors, EPR measurements were carried out on unirradiated, gamma irradiated (1 kGy) and phosphors irradiated to gamma dose and annealed at different temperatures (viz., 50, 100, 150, 200, 250 and 300°C for 1 h duration). All the samples correspond to an Mn doping of 0.3 mole% in lithium tetraborate, which was found to be the optimum dopant concentration yielding maximum TL sensitivity. Figures 5.2 shows the EPR signals recorded under different conditions. EPR signal of unirradiated LTB:Mn phosphor is shown in fig. 5.2 (1). The resonance line centered at g = 2 is due to Mn^{2+} ions in the matrix as paramagnetic species. The broad and unresolved response is characteristic of Mn–Mn interactions (dipolar or exchange coupled) [1,2]. The intensity of EPR signal is small because of low doping concentration of Mn (0.3 mol%). It has been observed in xMnO.(1-x)[Bi2O3.GeO2] glasses, the EPR intensity increases appreciably only for doping of more than 10 mol% of MnO [3]. We have also observed the increase in the intensity of EPR signal if the concentration of Mn in increased. However, we have not presented the data here, since we are interested in investigating the sample that gives highest TL sensitivity.

Gamma irradiated phosphors shows the presence of free radicals in the region around g=2.0023 corresponding to the free electron resonance region. From the B-O coordination observed in the infrared spectrum discussed in chapter 2 (Fig. 2.6), it is clear that lithium tetra borate is made up of both BO_3 and BO_4 networks. The main crystal motif of lithium tetraborate is described as consisting of boron–oxygen complex (4B+9O) arranged as two identical trigonal and two identical tetrahedral groups. Eight such boron–oxygen complexes are present in one unit cell of lithium tetraborate. The lithium ions stabilize the boron-oxygen framework being distributed in helicoidal voids spreading along the Z-axis [4]. Also the TL emission in lithium tetraborate (Fig. 3.3) is characteristic of Mn^{2+} ions.

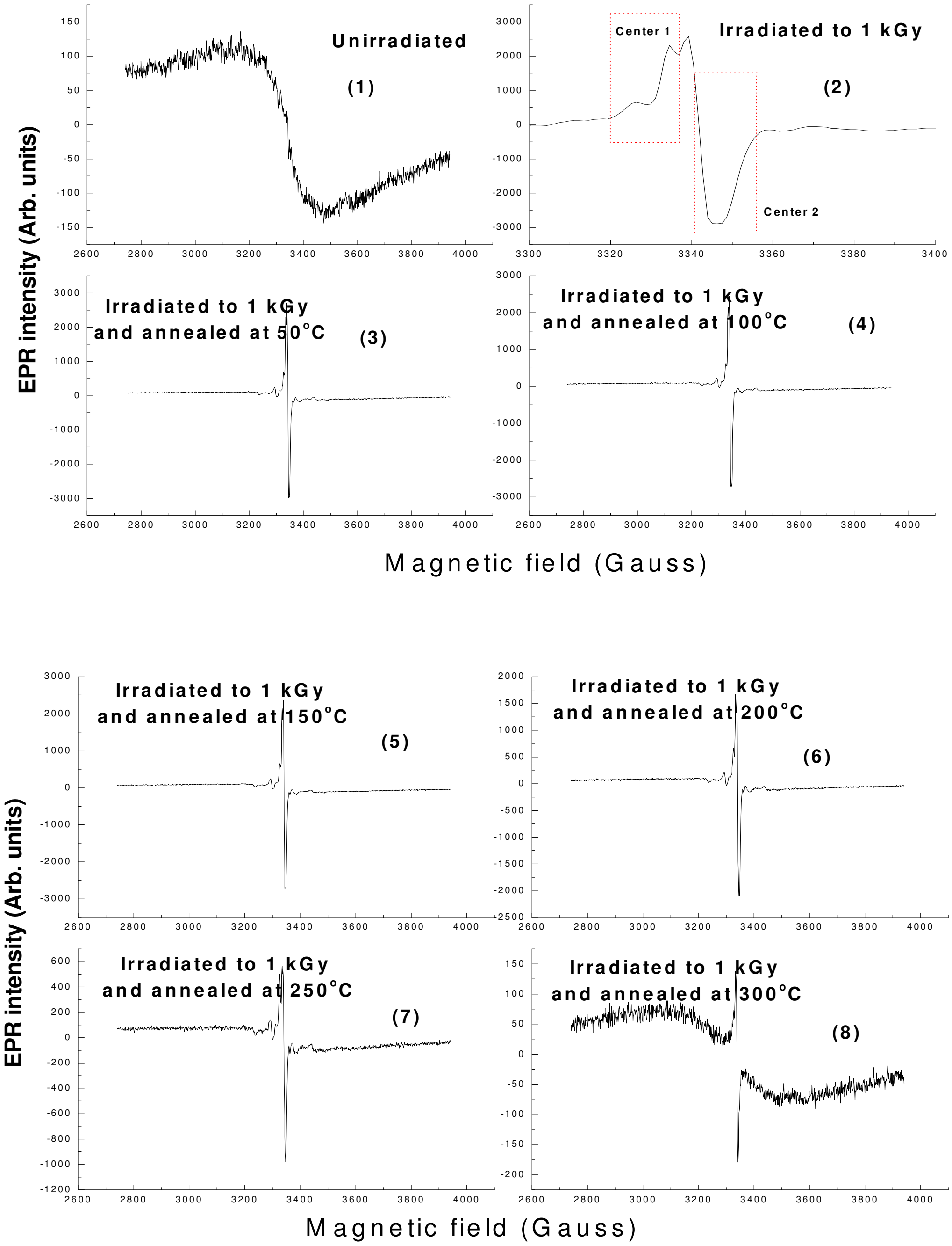

Fig. 5.2 EPR spectrum (first derivative) of $Li_2B_4O_7$:Mn phosphor under different conditions. The conditions are given in each of the plot. The figure 2 is given in enlarged scale in order to isolate and identify the paramagnetic radicals formed upon irradiation

For the case of irradiated lithium tetraborate phosphors, two paramagnetic radicals were observed. Center 1 with a g-value characterized by 2.00429 is identified as 'boron oxygen hole center' (BOHC) [5], which is a hole trapped on an oxygen ion that links two BO_4 units. This represents a hole trapped at the bridging oxygen of the two tetrahedral networks in the boron-oxygen complex [4,6] where the boron (B^{3+}) is replaced by Manganese (Mn^{2+}). Because of the lack of positive charge at boron site due to Mn substitution, the hole trapped at this center becomes more stable. This trapped hole caused the breakage of bond between the two tetrahedral networks and hole centers at broken oxygen bonds are known to exhibit high thermal stabilities [7]. Orange red luminescence band of Mn^{2+} at the position of tetrahedral B^{3+} is excited when the hole trapped at the bridging oxygen (BOHC) undergoes recombination with some electron. This is because the electronic clouds of Mn^{2+} (d-electrons) overlaps with the valence electron clouds of the oxygen ligands resulting in the decrease in the luminescence energy [8]. Thus BOHC is identified as a hole trapping center in lithium tetraborate lattice.

Center 2 with a g-value characterized by 1.9988 is identified as an electron trapped at an oxygen vacancy (O_v^-) center [4, 9]. The electron trapped at the oxygen vacancy in a BO_3 unit will be more stable and is localized to the boron ion. When manganese is doped in lithium tetraborate, from earlier studies [10] it is understood that Mn^{2+} can occupy both B^{3+} sites and also Li^+ sites. Depending on the occupancy of Mn^{2+} in the lattice, oxygen vacancies are created in the lattice for charge compensation. These oxygen vacancies act as electron trap and are stable at room temperature. Thus upon gamma irradiation the holes are trapped in the bridging oxygen atoms and the electrons are trapped at the oxygen vacancies.

5.3.2 EPR-TL correlation:

In order to understand the thermal stability of these traps and to make an analogy with the TL observed in this phosphor, EPR measurements were carried on gamma irradiated phosphors after annealing at different temperatures from 50°C to

300°C in steps of 50°C. It was observed that both the centers were stable up to around 200°C and there was a sudden drop in the signals beyond that temperature. TL glow curves were also recorded on all phosphors for which EPR measurement were carried out to measure the thermal decay of TL in LTB:Mn phosphor. Fig. 5.3 shows the relative variation of TL signal and EPR signal of the identified radicals of gamma irradiated LTB:Mn phosphor after annealing for 1 h at different temperatures. From the figure it is clear that the decrease in EPR signal matches well with the decrease of TL.

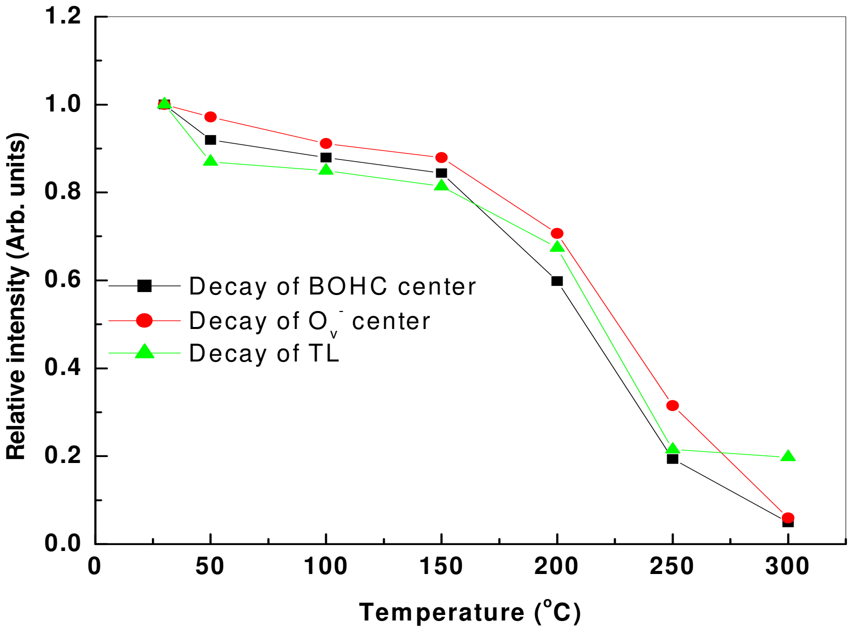

Fig. 5.3 Thermal decay of TL and EPR signal of BOHC and O_v^- *radicals formed upon irradiation in LTB:Mn phopshor.*

Further to confirm the relevance of these radicals in the TL process, the thermal activation energy of the BOHC center was determined using the relation [11],

$$ln[-ln(1-\Delta I/I)] = constant - \frac{E_a}{kT} \qquad 5.1$$

Where I is the intensity of the signal in irradiated phosphor, ΔI is the amount of decrease in EPR signal after each annealing temperature *(T)* and E_a is the thermal activation energy. The activation energy for the thermal destruction of BOHC center and O_v^- centers were found to be 1.29±0.013 eV and 1.32±0.021 eV respectively. From the kinetic analysis of TL, the trap depth was determined as 1.27±0.028 eV. This confirms that these two centers are responsible for TL in LTB:Mn phosphor. Based on the above analysis, the following model is proposed for the mechanism of thermoluminescence in LTB:Mn phosphor.

Upon irradiation,

$$Li_2B_4O_7{:}Mn \rightarrow BOHC, O_V^-$$

Upon heating,

$$BOHC \rightarrow h$$

$$O_V^- + h \rightarrow O_V^* \rightarrow (Mn^{2+})^* \rightarrow Mn^{2+} + h\boldsymbol{\nu}\ (\boldsymbol{TL})$$

That is, upon irradiation electrons are trapped at oxygen vacancies and holes are trapped at bridging oxygen of the two BO_4 tetrahedra where, the B^{3+} is replaced by Mn which causes the B-O bond of the two tetrahedral units to be much weaker. Upon heating, the holes are released from BOHC center and recombines with the electrons trapped at oxygen vacancies. This recombination energy is non-radiatively transferred to the nearby Mn^{2+} ions substituted for Li^+ ions and the excited Mn^{2+} ions gives it characteristic emission in the orange red region (580 nm).

5.4 EPR – TL correlation in MgB_4O_7:Gd,Li

EPR – TL correlation studies in MTB:Gd,Li phosphors were carried out by irradiating the phosphor to a dose of 100 Gy. EPR measurements were carried out on unirradiated, gamma irradiated and also on phosphors irradiated to gamma radiation and annealed to different temperatures viz., 50, 100, 150, 200, 250 and 300°C for 1 h duration. Figure 5.4 shows the EPR signals of unirradiated, irradiated and irradiated phosphors annealed at different temperatures. EPR spectra were recorded only to record the lines in the vicinity of free electron resonance. From fig. 5.3 it is clear that unirradiated MTB:Gd,Li phosphor did not show any EPR signal at room temperature. The EPR signal of gamma irradiated (100 Gy) phosphor recorded at room temperature at 3.196 mW power showed signatures of two radicals.

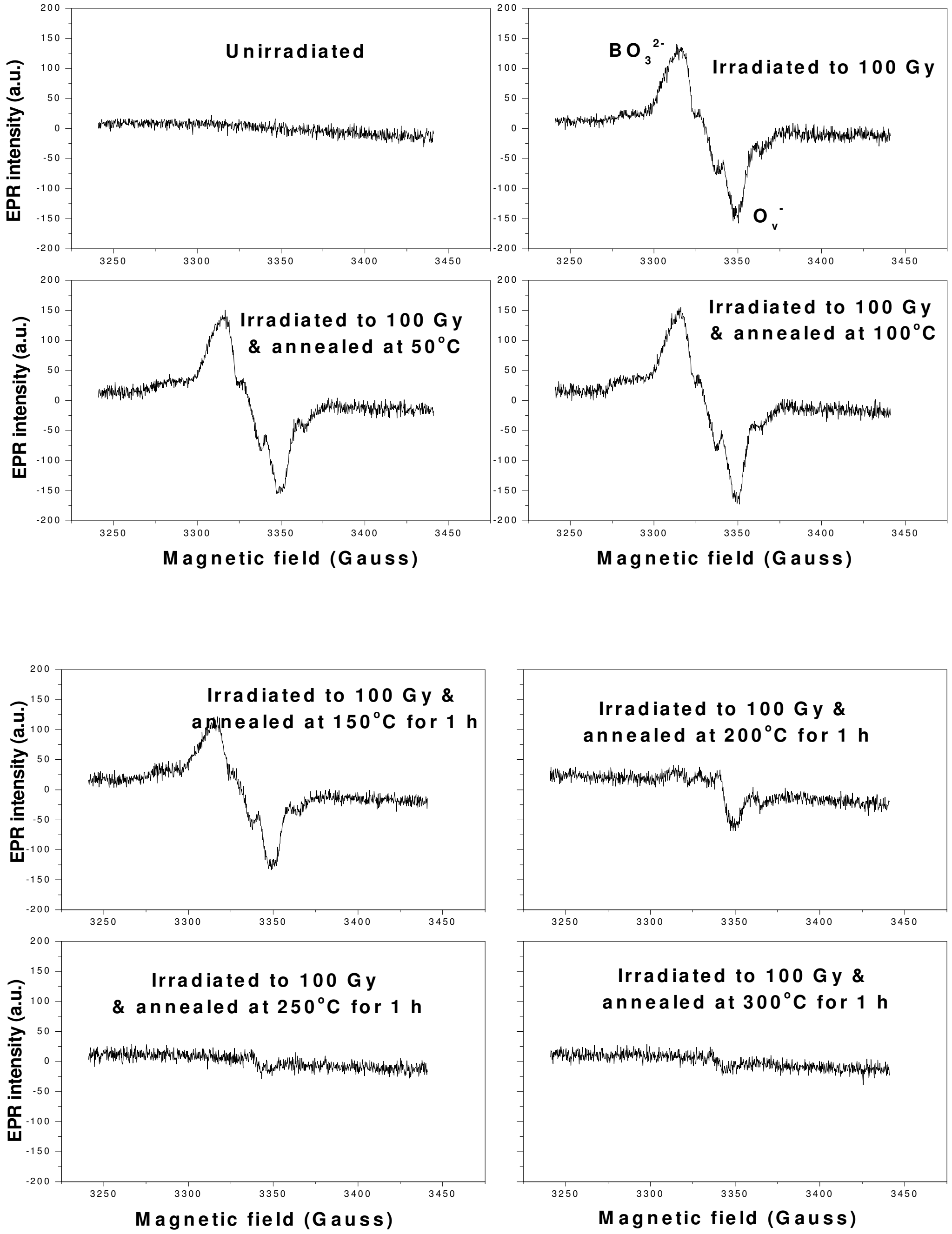

Fig. 5.4 EPR spectrum (first derivative) of MgB_4O_7:Gd,Li phosphor under different conditions. The conditions are given in each of the plot.

The EPR signal with a $g_{\perp}$ value around 2.0146 which is close to the g value reported in the literature [9] for hole trapped borate radical BO_3^{2-} formed upon irradiation. The g_{ll} and A_{ll} values were estimated to be 2.0015 and 18.31 G from the reported g_{iso} and A_{iso} for BO_3^{2-} radical [12]. The radical with g value close to free electron resonance, g=1.9981 was attributed to electron trapped at oxygen ion vacancy $\left(O_v^-\right)$ [12].

To understand the role of BO_3^{2-} and O_v^- radicals in the thermoluminescence process, EPR spectra was recorded on the irradiated phosphors after annealing for one hour at different temperatures. The signal due to BO_3^{2-} and O_v^- radical decreased with increase in annealing temperature due to the thermal destruction of the traps by the release of trapped charges. The released hole from BO_3^{2-} recombines with the electron trapped in the oxygen vacancies which results in the light emission during thermal stimulation in the greenish-yellow region (550 nm) as shown in Fig. 3.11 of chapter 3.

The emission wavelength of the oxygen vacancies are reported to be in the green region in most of the oxides [13]. Lithium which is added as a co-dopant in this lattice can enter the lattice at the interstitial positions because of the smaller ionic size. The presence of this lithium shifts the emission wavelength slightly toward the higher wavelength region [14].

Also TL intensity measurements were also carried out on phosphors annealed at different temperatures. The thermal decay of TL and the EPR signals of BO_3^{2-} and O_v^- radicals are shown in Fig. 5.5.

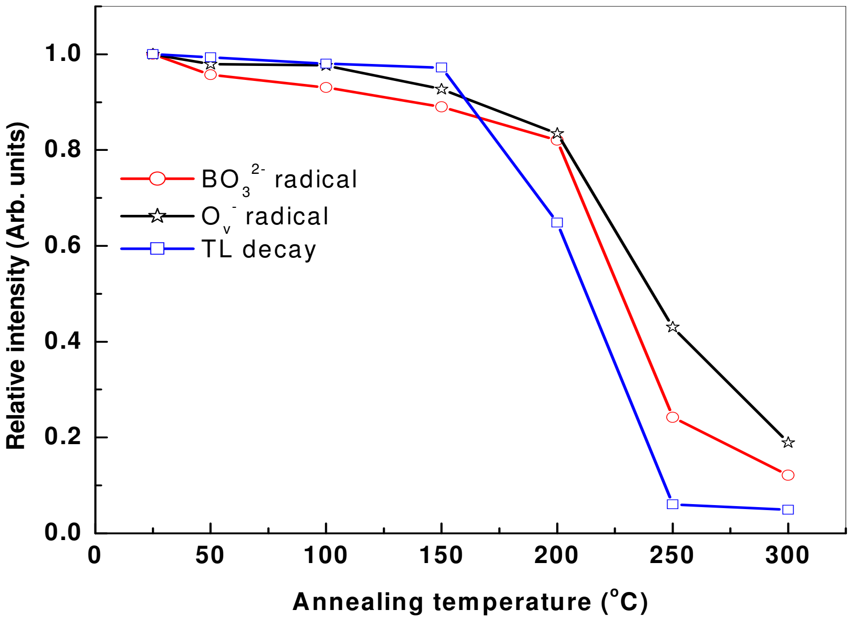

Fig. 5.5 Thermal decay of TL and EPR signal of BO_3^{2-} *and* O_v^- *radicals formed upon irradiation in MTB:Gd, Li phopshor.*

The TL intensity was found to drop suddenly beyond annealing temperature of 200°C which is same as the temperature at which the EPR signals also drops. The TL emission spectra in MTB:Gd,Li is around 550 nm (greenish yellow) characteristic of the intrinsic defects present in the lattice (oxygen vacancies stabilized by Li impurities). However it has been observed that in the case of other rare earth (Dy, Tm or Tb) doped magnesium tetraborate phosphors, the TL emission was characteristic of the rare earth dopant unlike the case of gadolinium doped magnesium tetraborate. EPR measurements on these borates did not show any difference in the basic defect centers. Hence the final emission differs based on how the recombination energy is emitted from the lattice. Thermal activation energy of BO_3^{2-} and O_v^- centers determined form the decay of EPR signal intensity by using equation 5.1 is 1.18±0.015 eV and 1.19±0.042 eV respectively. This is almost equal to the trap depth obtained by the kinetic anlaysis of thermoluminescence (1.20±0.004 eV). Hence we conclude that the centers identified are responsible for the TL process in magnesium tetraborate system.

By correlating the EPR, TL emission spectra, and PL spectra, the following mechanism is proposed for the thermoluminescence in MTB:Gd,Li phosphor.

Upon irradiation,

$$MgB_4O_7 : Gd, Li \rightarrow BO_3^{2-}, \quad [O_v]^-$$

On heating,

$$\begin{aligned} &BO_3^{2-} \rightarrow BO_3^{3-} + h \\ &[O_v]^- + h \rightarrow [O_v]^* \rightarrow [O_v] + h\nu \ (TL) \end{aligned}$$

In the case of other RE (Dy, Tm, Tb) doped MTB phosphors, the TL emission is characteristic of the RE dopant. But the EPR spectra recorded at room temperature in gamma irradiated phosphors is similar to that of Gd doped phosphors. Hence in those phosphors, the recombination energy from the oxygen vacancy related defect is transferred to the nearby rare earth ion and the TL emission is due to the de-excitation of the rare earth ion.

5.5 EPR – TL correlation in ZnB_2O_4:Tm

Zinc metaborate is a special class of borates formed of mainly tetrahedral borate networks and the tetrahedras are coupled at certain corners to form the complex 3 dimensional array [15, 16]. In the tetrahedra, one oxygen atom is connected to a zinc atom and the other 3 atoms are shared by 3 different tetrahedra. Though all B-O bonds are similar, the oxygen coupled with zinc is unique and the symmetry can be considered as trigonal instead of tetrahedral co-ordination. Hence the basic unit can be visualized as containing a central atom (Boron) bonded to two different kinds of atoms viz., oxygen bound to zinc and the other three oxygen atoms connected into the network. In order to identify the radicals/trap centers formed upon irradiation, EPR spectra was recorded for the gamma irradiated phosphor (undoped and Tm doped) with a microwave frequency of 9.404 GHz (power 3.196 mW) and is shown in Fig.5.6.

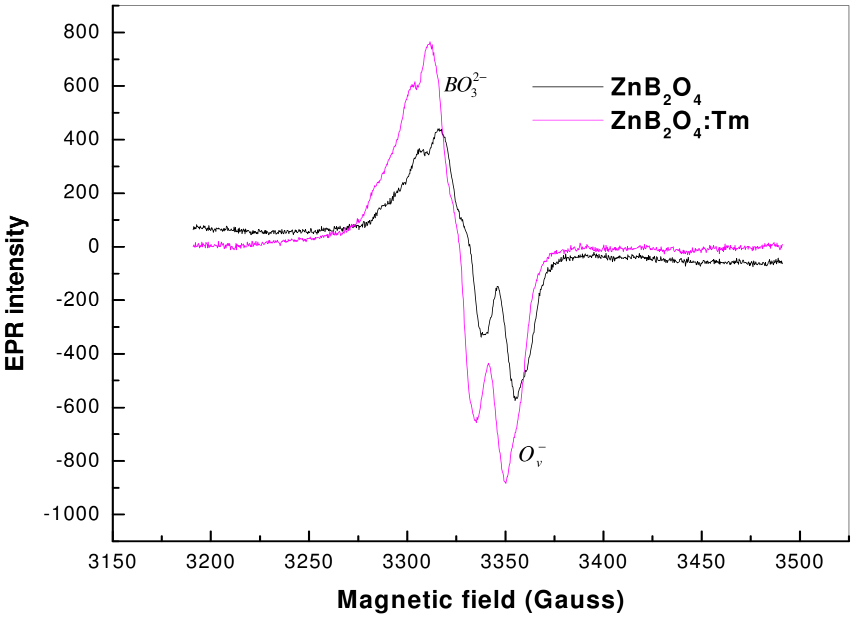

Fig. 5.6 EPR spectra of gamma irradiated (Dose 5 kGy) ZnB_2O_4 *and* ZnB_2O_4*:Tm*

Undoped and Tm doped zinc borate phosphor showed similar EPR spectra but only the intensity of the signal varied. This is similar to that observed in TL analysis where the glow peak temperature remains the same for both the cases and only the glow peak intsensity varies (Fig. 3.16). This shows that the defect centers responsible for thermoluminescence remain the same in both doped and undoped, but only the concentration of the defect increases upon doping.

To establish a relation between the observed TL and the trap centers identified by EPR, EPR measurements were also carried out on unirradiated, irradiated and irradiated and annealed powder samples of ZnB_2O_4 doped with Tm. EPR spectrum recorded under different conditions are shown in the Figures 5.7

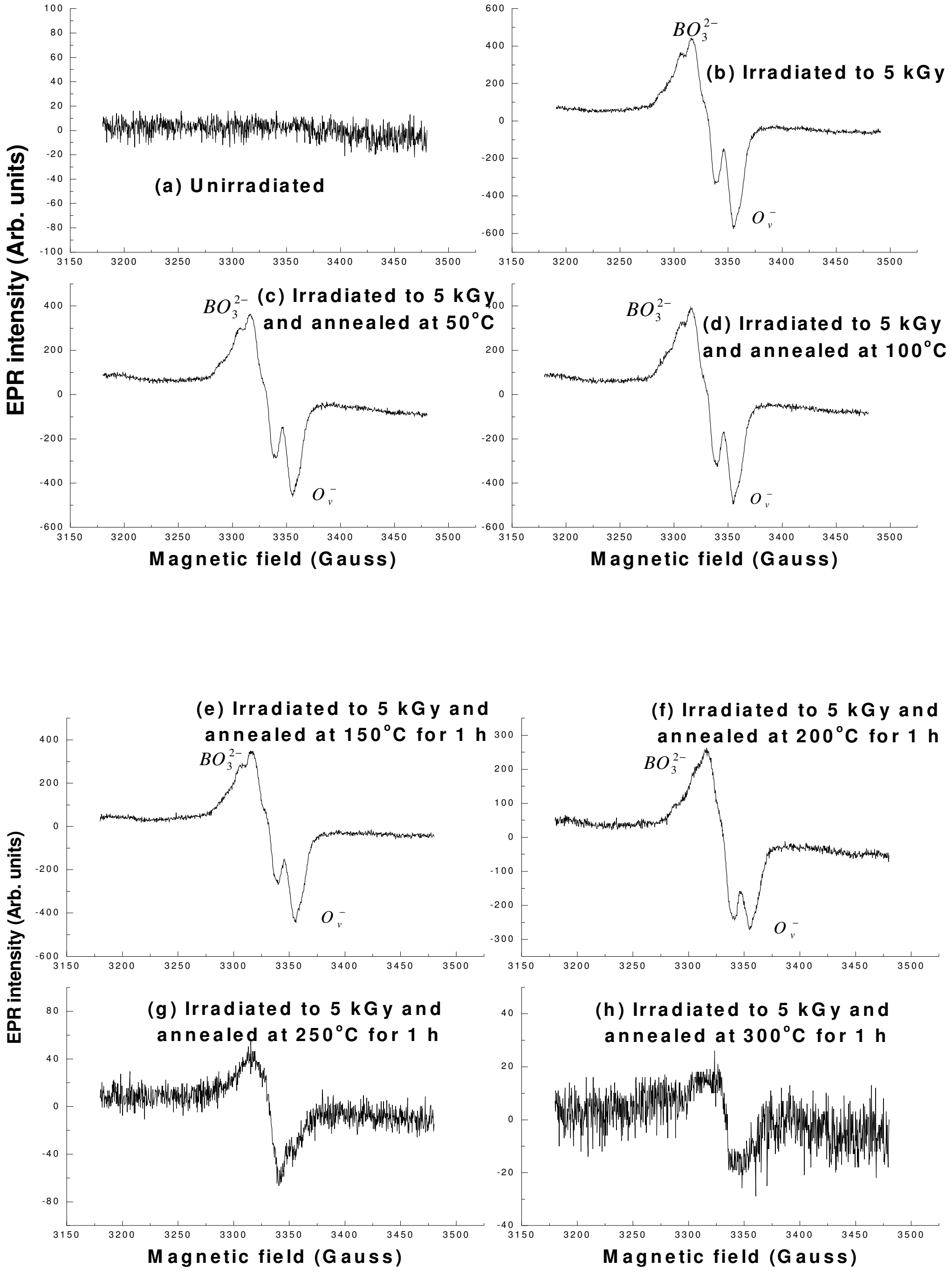

Fig. 5.7 *EPR spectrum (first derivative) of* ZnB_2O_4*:Tm phosphor under different conditions. The conditions are given in each of the plot.*

Unirradiated phosphor did not show any EPR signal at room temperature indicating the absence of any paramagnetic defect centers prior to irradiation. The EPR signal in both doped and undoped phosphor is the same but for the variation in intensity of the signal. The EPR spectrum showed a broad signal with an unresolved structure and a relatively sharp signal. The EPR signal with a $g_{\perp}$ value around 2.0168 which is close to the g value reported in the literature [9] for hole trapped borate radical can be identified as the hole trapped BO_3^{2-} radical formed upon irradiation. The g_{ll} and A_{ll} values were estimated to be 2.0027 and 14.41 G from the reported g_{iso} and A_{iso} for BO_3^{2-} radical [7]. The radical with g value less than 2, g=1.9974 was attributed to electron trapped at oxygen ion vacancy (O_v^-) [9]. The signal due to BO_3^{2-} and O_v^- radical reduces with increase in annealing temperature. The thermal decay behaviour of TL and EPR signal of the radicals formed upon irradiation is shown in Fig. 5.8.

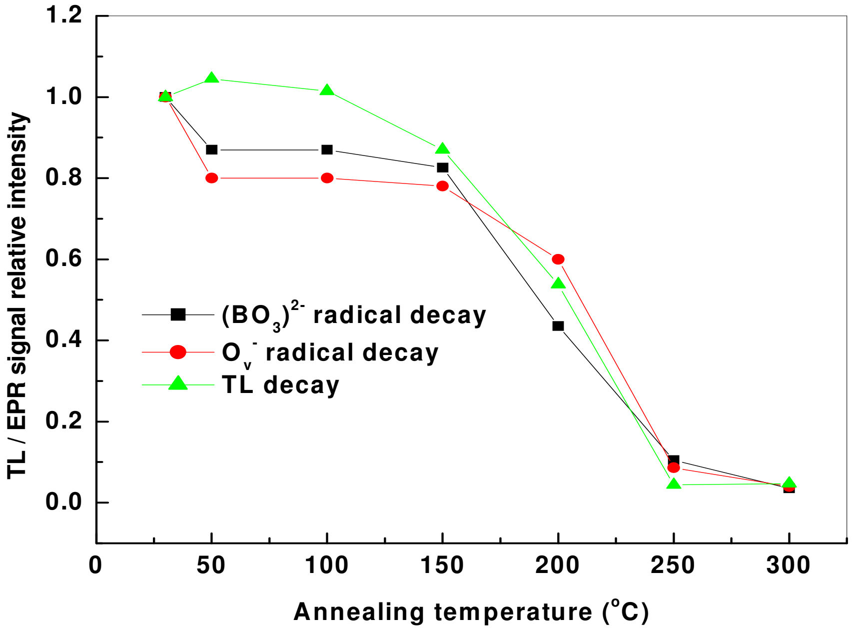

Fig. 5.8 *Thermal decay of TL and EPR signal of* BO_3^{2-} *and* O_v^- *radicals formed upon irradiation in* ZnB_2O_4*:Tm phopshor.*

The reduction in EPR signal is due to the thermal destruction of the radicals by the release of trapped charges. The hole trapped in the borate radical gets released and recombines with the electron trapped in the oxygen vacancies resulting in the light emission during thermal stimulation.

By correlating the EPR, TL emission spectra, and PL spectra, the following mechanism is proposed for the thermoluminescence in ZnB_2O_4:Tm phosphor.

Upon irradiation,

$$ZnB_2O_4 : Tm \rightarrow BO_3^{2-}, \quad [O_v]^-$$

On heating,

$$\begin{aligned} &BO_3^{2-} \rightarrow BO_3^{3-} + h \\ &[O_v]^- + h \rightarrow [O_v]^* \rightarrow [O_v] + h\nu \; (TL) \end{aligned}$$

5.6 EPR – TL correlation in Cadmium borate

In order to identify the defect centers formed upon gamma irradiation in cadmium tetraborate phosphor, EPR measurements were carried out on unirradiated and gamma irradiated cadmium tetraborate phosphors. In order to find the relation between the radicals identified using EPR and the TL recorded by the phosphors, EPR measurements were also carried out on irradiated phosphors annealed to different temperatures from 50 to 300°C in steps of 50°C for 1 hour duration and are shown in Figs. 5.9. It was found that there were no paramagnetic defect centers in unirradiated phosphor. The saturation dose in the case of cadmium tetraborate phosphor is 1 Gy and for EPR measurements the phosphor was irradiated to a dose of 10 Gy. Hence the EPR signal is not very strong as in the case of other borate phosphors studied. The EPR spectra of irradiated phosphor show the signature of two types of defect centers.

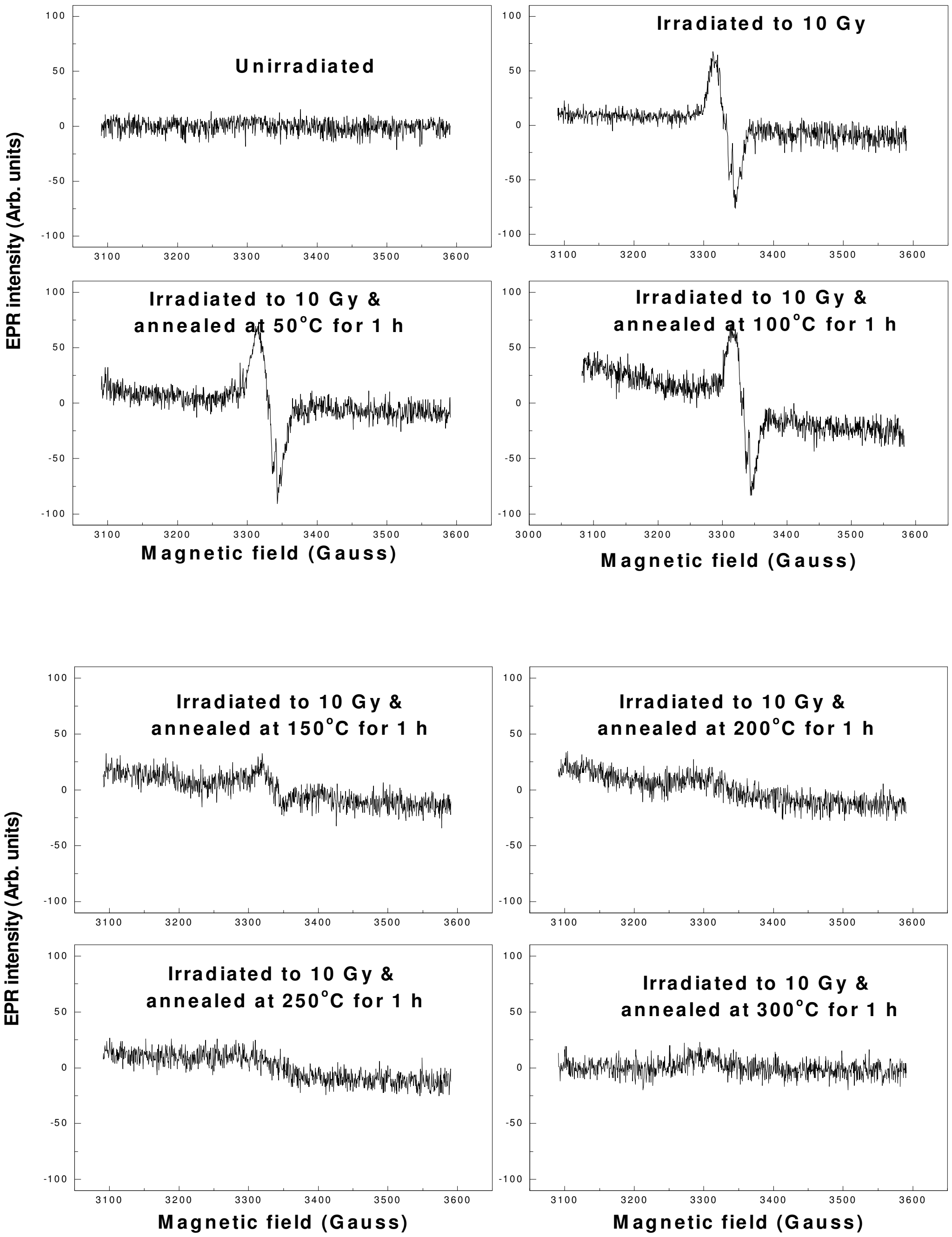

Fig. 5.9 EPR spectrum (first derivative) of CdB_4O_7 phosphor recorded under different conditions. The conditions are given in each of the plot

The paramagnetic defect center with g value 2.0127 corresponds to the BO_3^{2-}center which corresponds to the hole trapped at borate radical. From the IR spectra reported in chapter 2 (Fig. 2.8), cadmium tetraborate is formed of network of both BO_3 and BO_4 units. The other paramagnetic radical corresponds to a g-value of

2.0024. This is identified to be a Boron electron center (BEC) corresponding to the electron trapped in the dangling bond orbital at the site of the oxygen vacancy.It was observed that the EPR signal dropped drastically for samples annealed at 150°C itself. The glow peak temperature of this phosphor is around 185°C. Hence the drop of EPR signal at 150°C can be associated with the decrease in the concentration of trapped charge carriers responsible for TL. The TL intensity was also measured for all annealed phosphors.

The thermal decay of TL and EPR signal of the identified paramagnetic radicals are shown in Fig. 5.10. It is clear from Fig. 5.9 that the defect centers BO_3^{2-} and the BEC are responsible for TL.

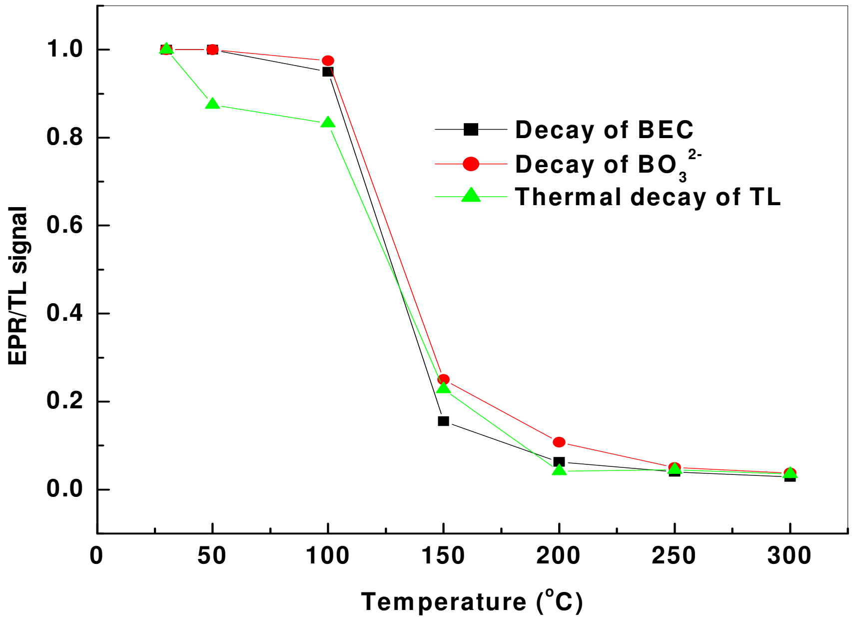

Fig. 5.10 Thermal decay of TL and EPR signal of the identified traps in cadmium tetraborate phosphor.

Based on the above observations, the following mechanism is proposed for TL in cadmium tetraborate phosphor. The electrons and holes formed as a result of gamma irradiation are trapped in the respective traps. Electrons are trapped at the dangling bond orbital of the oxygen vacancy. This oxygen vacancy can be at the site of boron which is tetrahedrally co-ordinated or it can be from a site of boron which is trigonally co-ordinated. Holes are trapped at the BO_3^{3-} radical. When the phosphor is heated holes are released from BO_3^{3-} and they recombine with the electron trapped at the dangling bond orbital of BEC. Though this recombination is similar to that of a recombination of oxygen vacancy, the emission of this is at 515 nm. This is due to the presence of cadmium and the defect center BEC is more sensitive to the type and quantity of alkali/alkaline/transition metal elements present in the lattice. Thus we can conclude that,

Upon irradiation,

$$CdB_4O_7 \rightarrow BO_3^{2-} \text{ , } O_V \text{ (BEC)}$$

On heating,

$$BO_3^{2-} \rightarrow BO_3^{3-} + h,$$

$$BEC + h \rightarrow BEC^* \rightarrow BEC + h\boldsymbol{\nu}\ (\boldsymbol{TL})$$

5.7 Conclusions

EPR measurements were carried out on all the four TL phosphors studied viz., LTB:Mn; MTB:Gd,Li; ZMB:Tm and CTB phosphors. The defect centers formed upon gamma irradiation were determined. The thermal decay of the EPR signals were determined and compared with the thermal decay of TL. From the obtained results, a mechanism for TL in these phosphors is proposed.

5.8 References

---

[1]. Xue H.T. and Zhao P.Q., J. Phys. D: Appl. Phys., **42** (2009) 015402,

[2]. Podgorska D., Kaczmarek S.M., Drozsowski W., Wabia M., Kwasny M., Warchol S. and Rizak V.M., Mol. Phys. Rep., **39** (2004) 199

[3]. Ardelean I., Peteanu M., Filip S., Simon V. and Todor I. , Sol. State Commun., **105** (1998) 339

[4]. Swinney M.W., McClory J.W., Petrosky J.C., Yang Sh., Brant A.T., Adamiv V.T., Burak Ya. V., Dowben P. A. and Halliburton, L. E. *J. Appl. Phys* **107** *(*2010) 113715

[5]. Griscom D.L., J. non-cryst. Solids, **13** (1973/74) 251

[6]. Igor N. Ogorodnikov, Victor Yu, Yakovlev, Lyudmila I. Isaenko, Radiat. Meas. **38** (2004) 659

[7]. Shkrob, I. A.; Tadjikov, B. M.; Trifunac, A. D. *J. Non-cryst. Solids*, **262** (2000) 6.

[8].Biernacki, S.; Kutrowski, M.; Karczewski, G.; Wojtowicz, T.; Kossut, J. *Semicond. Sci. Technol.*, **11** (1996) 48.

[9].Porwal N.K., Kadam R.M., Seshagiri T.K., NatarajanV., Dhobale A.R., Page A.G., Radiat. Meas. **40** *(*2005*) 69*

[10]. Sennova N., Bubnova R., Shepelev Yu., Filatov S., Yakovleva O., J. Alloy. Compd., **428** (2007) 290

[11]. Huzimura R., Asahi K., Takenaga M., Nucl. Instrum. Methods, **175** (1980) 8.

[12].Taylor P.C., Griscom D.L., Bray P.J., J. chem. Phys. **54** (1971) 748

[13].Vanheusden K., Seager C.H., Warren W.L., Tallant D.R. and Voigt J.A., Appl. Phys. Lett. **68** (1996) 403

[14]. Rauch C., Gehlhoff W., Wagner M.R., Malguth E., Callsen G., Kirste R., Salameh B., Hoffmann A., Polarz S., Aksu Y., and Driess M., J. Appl. Phys. **107**, (2010) 024311

[15]. Weir C.E., Schroeder R.A., J. Res. NBS, **68A** (1964) 465.

[16]. Krogh-Moe J., Z. Krist. **117** (1962) 166

CHAPTER - 6

SUMMARY AND FUTURE DIRECTIONS

Chapter – 6

Summary and Future Directions

6.0 Summary

Borate based phosphors have been studied in the work presented in the thesis for their application in thermoluminescence dosimetry. Lithium tetraborate and magnesium tetraborate with appropriate dopants and co-dopants studied in this work are nearly tissue equivalent materials and can be employed in clinical as well as personnel dosimetry applications. Further, zinc metaborate and cadmium tetraborate have higher effective atomic number compared to tissue. However they can be employed in environmental dosimetry and also in personnel dosimetry by using some filters. Borate based phosphors have a distinct advantage of responding to mixed neutron and gamma field with suitable doping of neutron sensitive isotopes of boron. In addition, these materials are easy to prepare, have single and simple dosimetric peak at reasonably high temperatures, exhibit linear dose response on an average over doses ranging two to three orders of magnitude, have excellent storage stability, have simple annealing procedure for reuse.

Lithium tetraborate doped with manganese, magnesium tetraborate doped with gadolinium and co-doped with monovalent lithium, zinc metaborate doped with thulium and undoped cadmium tetraborate have been considered for detailed investigations and presentation in the thesis because of their superior dosimetric properties such as temperature of the dosimetric peak, TL sensitivity etc compared to other dopants and co-dopants studied in the respective families. For each of the material, synthesis, structural and morphological characterization, TL dosimetric studies, PL studies, estimation of kinetic parameters using different methods, study of electron paramagnetic resonance – TL correlations to understand the mechanism of TL have been carried out. Important findings of the research work reported in the thesis are as follows.

6.1 Important findings of the work.

Solid state sintering is used to synthesize all the phosphors used in this work, which is simple, cost effective, and does not require high purity chemicals. This method can be used to produce the material in bulk quantities in less time.

Lithium tetraborate:

- $Li_2B_4O_7$:Mn prepared using solid state sintering method exhibits a dosimetric peak around 280˚C, which is highest temperature for this material studied in the literature. The high temperature glow curve results in no fading for three months. Further, $MnCO_3$ used as an initial material for Mn doping in the present study resulted in the material that is non hygroscopic. In the reported literature, $MnCl_2$ or manganese acetate was used for Mn doping.
- It is found that maximum TL intensity occurs for 0.3 mol% of Mn doping.
- From TL emission and PL studies, it can be concluded that the excitation wavelength of Mn partly matches with emission wavelength of host LTB lattice. The TL emission spectra are characteristic of Mn^{2+}.
- The sensitivity of $Li_2B_4O_7$:Mn is determined to be 0.9 times that of TLD 100 (Harshaw make). The low sensitivity can be attributed to incompatibility of the emission wavelength with spectral response of photomultiplier tube.
- Dose response of $Li_2B_4O_7$:Mn is linear in the dose region of 1 mGy to 10 Gy followed by supralinearity till the saturation dose of 10^3 Gy. The minimum measureable dose was 250 μGy.

- The kinetic parameters of LTB:Mn phosphor was determined and the trap depth was found to be around 1.30 eV. The frequency factor was of the order of 10^{11} s^{-1}. The order of kinetics is 1.85.
- EPR – TL correlation studies has been carried out on LTB:Mn phosphor and the paramagnetic defect centers responsible for TL were identified. The thermal decay of the EPR signal corresponding to these defects and the thermal decay of TL are in line with each other. Also the activation energy of the paramagnetic centers and the trap depth obtained by kinetic analysis are nearly equal and hence the defects identified in EPR were responsible for TL in this phosphor
- The electron trap was identified as oxygen vacancies and the hole traps are the bridging oxygen atoms. When the phosphor is heated, the electrons are released from the electron trap and recombine with the trapped holes. The excitation energy during the recombination is transferred to the nearby Mn^{2+} ions which emits at 580 nm.

Magnesium tetraborate:

- MgB_4O_7 is synthesized with different rare earth dopants, viz., Tm, Gd, Ce, Dy and Tb. Gd has been doped for the first time and MgB_4O_7:Gd has TL peak at highest temperature 250˚C compared to all other dopants studied.
- Maximum TL intensity is observed for Gd concentration of 0.2 mol%.
- MgB_4O_7:Gd codoped with monovalent elements resulted in enhancement in TL intensity. Studies have been carried out with codopants Li, Na and Ag and highest TL intensity is observed for optimal concentration of Li (0.3 mol%).
- The TL emission spectrum is around 550 nm characteristic of the host lattice and not of the dopants.
- The TL sensitivity is 5 times that of TLD 100 (Harshaw make).

- The phosphor is found to have a linear response to gamma radiations from 1 mGy to 10^3 Gy and the minimum detection threshold is 20 μGy.
- MTB:Gd,Li phosphor was found to exhibit light induced fading and hence is suitable for immediate dose measurements and should be used in black encapsulation.
- The kinetic parameters of MTB:Gd,Li phosphor was determined by different standard methods and the values of trap depth, frequency factor and order of kinetics are around 1.25 eV, 10^{10} s^{-1} and 1.60 respectively.
- The trap centers responsible for thermoluminescence were identified using EPR technique. Upon irradiation, electron is trapped in oxygen vacancy and hole is trapped forming a radical BO_3^{2-} . On heating, the released hole from BO_3^{2-} recombines with the electron trapped in the oxygen vacancies which results in the light emission during thermal stimulation in the greenish-yellow region (550 nm).

Zinc metaborate:

- Zinc metaborate doped with Tm has highest TL intensity among the dopants studied, namely, Gd, Tb, Mn, Dy and Tm. The dosimtric peak is observed at 300°C. Optimum concentration of Tm for maximum TL intensity is 0.4 mol%.
- The TL emission spectra (535 nm) of this phosphor was characteristic of the host lattice defects mainly oxygen vacancies.
- Gamma dose response was found to be linear from 10 mGy to 10^3 Gy and the minimum measurable dose was found to be 6 μGy.
- The trap depth, frequency factor and order of kinetics was found to be of the order of 1.6 eV, 10^{12} s^{-1} and 1.80. This value of trap depth matches with the activation energy determined from the thermal decay of EPR signal of the paramagnetic defect centers identified upon gamma irradiation.

- Mechanism for thermoluminescence is ZMB:Tm is similar to that MTB with trap centers responsible for TL are same.

Cadmium tetraborate:

- Cadmium tetraborate phosphor exhibits a dosimetric peak at 185°C.
- The gamma dose response of this phosphor is linear in a very narrow dose region 0.1 mGy to 1 Gy. However the minimum measurable dose is around 30 μGy.
- From the correlation between the trap depth obtained by kinetic analysis of TL glow curves and the thermal decay of EPR signal of the paramagnetic radicals observed upon gamma irradiation a possible mechanism of TL is proposed. Upon irradiation electrons are trapped at the dangling bond orbital of the oxygen vacancy, known as boron electron centre (BEC). This oxygen vacancy can be at the site of boron which is tetrahedrally co-ordinated or it can be from a site of boron which is trigonally co-ordinated. Holes are trapped at the BO_3^{2-} radical. When the phosphor is heated holes are released from BO_3^{2-} and they recombine with the electron trapped at the dangling bond orbital of BEC. Though this recombination is similar to that of a recombination of oxygen vacancy, the emission of this is at 515 nm.

6.2 Future Directions

Studying the neutron dose response of the developed borate based phosphors: Lithium (^{6}Li), Boron (^{10}B), Gadolinium (Gd) and Cadmium (Cd) have good thermal neutron absorption coefficient. Preliminary neutron irradiation studies on the borate based phosphors synthesized with natural boron and lithium showed that the phosphors can be used for the detection of thermal neutron. Detailed studies on the measurement of thermal neutron of varying flux/dose and establishing the calibration curves can be carried out. Further, the neutron sensitivity of these phosphors can be improved by using enriched boron as well as lithium during synthesis.

Energy response of the phosphors: One of the requirements for clinical or personnel dosimeter is to have a dosimeter with flat energy response at all energies. This mainly depends on the effective atomic number. Generally tissue equivalent materials have flat energy response. Of the four phosphors developed during the course of the thesis work, LTB:Mn is tissue equivalent, MTB:Gd, Li is nearly tissue equivalent whereas ZMB:Tm and CTB are not tissue equivalent. Hence, these phosphors may have over-response at lower energies. For using a material as a dosimeter, the response of the phosphor at lower energies has to be carried out and the suitable filters that can be used to flatten the energy response at all energies should be identified.

Field test of the developed borate phosphors: In order to demonstrate the use of the phosphors as personnel dosimeters as well as clinical dosimeters, field test has to be carried out under different conditions along with the presently used standard dosimeters. Once the energy response is studied and appropriate filters are designed, the performance of the present phosphor (made in the form of suitable dosimeter) has to be checked under field conditions.

Radioluminescence and optically stimulated luminescence studies: Borates based phosphors are also reported to be good optically stimulated luminescence dosimeters. An intense radioluminescence was observed in ZMB:Tm during gamma irradiation. Hence, the radioluminescence measurements and feasibility of using the phosphors as optically stimulated luminescence dosimeters is another direction of future work.

LIST OF PUBLICATIONS

List of Publications

Publications in journals

(a) Published

1. **O. Annalakshmi**, M.T. Jose and G. Amarendra, Dosimetric characteristics of manganese doped lithium tetraborate – An improved TL phosphor, *Radiation measurements, Vol – 46, (2011), 669 – 675*

2. **O. Annalakshmi**, M.T. Jose, U. Madhusoodanan, B. Venkatraman and G. Amarendra, Kinetic parameters of lithium tetraborate based TL materials, *Journal of luminescence, Vol – 141, (2013), 60 – 66*

(b) Communicated

1. **O. Annalakshmi**, M.T. Jose, U. Madhusoodanan, J. Subramanian, B. Venkatraman G. Amarendra and A.B. Mandal, Thermoluminescence dosimetric characteristics of Thulium doped ZnB_2O_4 phosphor, *Journal of luminescence*, (Submitted in April 2013, under review)

2. **O. Annalakshmi**, M.T. Jose, U. Madhusoodanan, B. Venkatraman and G. Amarendra, Synthesis and thermoluminescence characterisation of MgB_4O_7:Gd,Li, *Radiation measurements,* (Submitted in June 2013, under review)

3. **O. Annalakshmi**, M.T. Jose, B. Venkatraman and G. Amarendra, Synthesis and luminescence characteristics of cadmium borate phosphors, *Materials research Bulletin* (Submitted in July 2013, under review)

4. **O. Annalakshmi**, M.T. Jose, U. Madhusoodanan, J. Sridevi, B. Venkatraman G. Amarendra and A.B. Mandal**,** Radiation induced defect centers in manganese doped lithium tetraborate phosphor, Radiation protection dosimetry (Communicated, August 2013)

5. **O. Annalakshmi**, M.T. Jose, U. Madhusoodanan, J. Sridevi, B. Venkatraman G. Amarendra and A.B. Mandal, TL mechanism in RE doped magnesium tetraborate phosphors, Radiation effects and defects in solids, (Communicated, August 2013)

6. **O. Annalakshmi**, M.T. Jose, J. Sridevi, B. Venkatraman G. Amarendra and A.B. Mandal, Kinetic parameters and TL mechanism in cadmium tetraborate phosphors, Journal of luminescence, (Communicated, August 2013)

Publications in Conferences

1. **O. Annalakshmi**, M.T. Jose. S.R. Anishia and G. Amarendra, Dosimetric studies on tissue equivalent TL phosphor $Li_2B_4O_7$:Mn, Proceedings of NCLA -2009, Feb 18- 20, 2009, Kolkata

2. **O. Annalakshmi**, S.R. Anishia and M.T. Jose, Luminescence studies in cadmium borate TL phosphor, National conference on Luminescence and its applications on Feb 9-11, 2010 held at Gandhigram Rural Institute, Gandhigram, Tamilnadu

3. **O. Annalakshmi**, M.T. Jose, U. Madhusoodanan, B. Venkatraman and G. Amarendra, Dosimetric properties of $Zn(BO_2)_2$:Gd thermoluminescence phosphor, National Symposium on Radiation Physics (NSRP-19) during December 12 – 14, 2012 held at Radisson Blu Resort Temple Bay, Mamallapuram.

4. **O. Annalakshmi**, M.T. Jose, U. Madhusoodanan, B. Venkatraman and G. Amarendra, Synthesis and thermoluminescence dosimetric characteristics of MgB_4O_7:Gd, National Conference on Luminescence and its Applications (NCLA-13) during January 8 – 10, 2013 held at PES Institute of Technology, Bengaluru.

Publications in journals not included in the thesis

1. A. R. Lakshmanan, M. T. Jose, and **O. Annalakshmi**, High-sensitive $CaSO_4$:Dy thermoluminescent phosphor synthesis by co-precipitation technique, *Radiat Prot Dosimetry (2008) 132 (1): 42-50*

2. S.R. Anishia, M.T. Jose, **O. Annalakshmi**, V. Ponnusamy and V. Ramasamy, Dosimetric properties of rare earth doped $LiCaBO_3$ thermoluminescence phosphors, *Journal of luminescence, Vol – 130, (2010), 1834– 1840*

3. S.R. Anishia, M.T. Jose, **O. Annalakshmi**, and V. Ramasamy, Thermoluminescence properties of rare earth doped lithium magnesium borate phosphors, *Journal of luminescence, Vol – 131, (2011), 2492 -2498*

4. M.T. Jose, S.R. Anishia, **O.Annalakshmi**, V. Ramasamy, Determination of thermoluminescence kinetic parameters of thulium doped lithium calcium borate, *Journal of luminescence, Vol - 46 (2011), 1026 - 1032*

5. **O. Annalakshmi**, M. T. Jose, and U. Madhusoodanan, Synthesis and characterisation of $BaSO_4$:Eu thermoluminescence phosphor *Radiat Prot Dosimetry (2012) 150 (2): 127-133*

6. **O. Annalakshmi**, Varghese Anto Chirayath, S. Hari Babu, M. T. Jose, G. Amarendra, Positron lifetime studies of $CaSO_4$:Dy thermoluminescence phosphors, *Physica Status Solidi (C), Vol – 6, (2009) 2516 - 2518*

Publications in Conferences not included in thesis

1. S.R. Anishia, M.T. Jose, **O. Annalakshmi**, and V. Ponnusawmy, Dosimetric Characteristics of $LiCaBO_3$Thermoluminescence Phosphor, Proceeding of NCLA -2009, Feb 18- 20, 2009, Kolkata

2. **O. Annalakshmi**, M.T. Jose and G. Amarendra, Thermoluminescence and Photo luminescence Studies on $BaSO_4$:Eu Phosphor, Proceeding of NCLA -2009, Feb 18- 20, 2009, Kolkata

3. S.R. Anishia, **O. Annalakshmi** and M.T Jose, Thermo luminescence properties of lithium magnesium borate phosphor, National conference of Luminescence and its applications on Feb 9-11, 2010 held at Gandhigram Rural Institute, Gandhigram, Tamilnadu